Titre: Title:	Hydrogenation of toluene on fluidized cryogels
Auteur: Author:	Deiva Venkatesh Ramachandran
Date:	1995
Type:	Mémoire ou thèse / Dissertation or Thesis
Référence: Citation:	Ramachandran, D. V. (1995). Hydrogenation of toluene on fluidized cryogels [Master's thesis, École Polytechnique de Montréal]. PolyPublie. https://publications.polymtl.ca/31803/

UNIVERSITÉ DE MONTRÉAL

HYDROGENATION OF TOLUENE ON FLUIDIZED CRYOGELS

DEIVA VENKATESH RAMACHANDRAN

DÉPARTEMENT DE GÉNIE CHIMIQUE

ÉCOLE POLYTECHNIQUE DE MONTRÉAL

MÉMOIRE PRÉSENTÉ EN VUE DE L'OBTENTION

DU DIPLÔME DE MAÎTRISE ÈS SCIENCES APPLIQUÉES (M.Sc.A.)

(GÉNIE CHIMIQUE)

AVRIL 1995

ISBN 0-612-03677-4

UNIVERSITÉ DE MONTRÉAL

ÉCOLE POLYTECHNIQUE DE MONTRÉAL

Ce mémoire intitulé:

HYDROGENATION OF TOLUENE ON FLUIDIZED CRYOGELS

présenté par: RAMACHANDRAN Deiva Venkatesh

en vue de l'obtention du diplôme de: Maîtrise ès Sciences Appliquées

a été dûment accepté par le jury d'examen constitué de:

M. PERRIER Michel, Ph.D., président

M. KLVANA Danilo, Ph.D., membre et directeur de recherche

M. CHAOUKI Jamal, Ph.D., membre et codirecteur

M. GUY Christophe, Ph.D., membre

ACKNOWLEDGEMENTS

I express my sincere gratitude to my research directors, Professors Danilo Klvana and Jamal Chaouki whose able guidance and continuous support helped me enormously in successfully carrying out my research work.

I gratefully acknowledge the affection and support of my family in India and to the Ambroise family in Laval without whom I would not have been able to work at Ecole Polytechnique.

I cherish the opportunity of having worked with Dusan Kusohorsky who initiated me into the practical aspects of the hydrogenation process and always shared his experience in times of need. I owe my gratitude to Dr. Jitka Kirchnerova who taught me the preparation and characterization of cryogels. My special thanks to Ali Gonzalez for his friendship and the invaluable and stimulating discussions regarding my work.

I thank Mr. Carol Painchaud for his co-operation and timely construction of the fluidized bed reactor. I would also like to thank Mr. Robert Delisle and Mr. Jean Huard of the chemical engineering department and Mr. George Sarfi (Verre H et S) for their excellent work.

I sincerely thank the president Dr. Michel Perrier and the members of the jury, Dr. Christophe Guy, Dr. Jamal Chaouki and Dr. Danilo Klvana who evaluated my thesis in such short notice and for their profound words of appreciation.

Last, but not the least, I thank all my friends at the department of chemical engineering for their friendship and co-operation which make my graduate study a memorable one.

RÉSUMÉ

La crise énergétique au niveau mondial a motivé les chercheurs à développer des nouvelles technologies de stockage d'énergie. Dans l'industrie du transport, les principaux problèmes rencontrées sont la diminution des ressources pétrolières et le coût élevé d'essence. Une des solutions probable consiste à l'utilisation d'énergie hydro-électrique pour générer de l'hydrogène. Cette méthode permet le stockage du gaz employant des hydrocarbures aromatiques dans un unité d'hydrogénation. Le produit obtenu représentant un vecteur d'hydrogène est introduit dans l'intérieur d'une unité automobile. L'hydrocarbure hydrogéné est récupéré dans un réacteur de déshydrogénation. Ensuite, le gaz participe dans la réaction de combustion génèrant de l'énergie requise pour conduire le véhicule.

Pour atteindre l'objectif mentionné ci-haut, ce projet envisage l'hydrogénation industrielle du toluène sur des catalyseurs Ni/Al_2O_3 de type cryogel. Des tests d'activité et de fluidisabilité de ces cryogels ont été réalisé suivi par l'hydrogénation du toluène dans un réacteur à lit fluidisé.

La préparation et la caractérisation des cryogels ayant différents teneurs de Ni ont été faits. Les tests d'activité des cryogels Ni/Al_2O_3 ont été réalisé à deux températures de réaction (130°C et 150°C). La composition de Ni dans la gamme 4.5-14% a

augmenté l'activité du catalyseur. Pour des teneurs supérieures à 14% Ni, aucun effet sur l'activité a été observé. Les études d'activation ont montré que l'activité est améliorée par un fort débit d'hydrogène mais d'une autre part, elle est réduite par un chauffage rapide. La fluidisabilité des cryogels a été testé dans une colonne cylindrique. Les résultats ont montré une mauvaise fluidisabilité de ces poudres. Cela peut être expliquer par la présence des forces interparticulaires caractéristique des particules C, ce qui se manifeste par les phénomènes de renardage et d'agglomération des particules. La valeur de 14% a été choisi comme la teneur optimale de Ni d'après les tests d'activité et de fluidisabilité.

Une colonne conique a été construite dans le but d'améliorer la qualité de la fluidisation du cryogel. A des vitesses élevées, il était possible de fluidiser le cryogel sans agglomération. Le lit fluidisé conique a été maintenu dans un état bien mélangé. Une équation d'Ergun modifié pour prédire la perte de charge à travers le lit fixe conique et une corrélation pour estimer la vitesse minimale de fluidisation ont été développé. Pour utiliser ces équations, un modèle du lit ségrégé a été proposé. Les résultats montrent que le gaz a été bien distribué dans le lit.

L'hydrogénation du toluène sur le catalyseur 14% Ni/Al_2O_3 a été réalisée dans le réacteur à lit fluidisé conique. Les conversions expérimentales ont été adéquatement prédites par les modèles de réacteurs homogènes (piston et parfaitement mélangé).

ABSTRACT

The ever-increasing global energy crisis has demanded researchers to develop novel technologies of energy storage. Particularly, in the transport industry, depleting resources and high cost of petroleum are of major concern. One possible solution is to exploit hydroelectric power which can be used to generate hydrogen. The gas is stored using aromatic hydrocarbons in an hydrogenation plant. The resultant alicyclic compound serves as a hydrogen vector and is filled in vehicle tanks. Onboard the vehicle, hydrogen can be recovered by a dehydrogenation reactor and the released gas takes part in a combustion reaction providing sufficient energy to drive the vehicle.

To achieve the aforementioned storage objective, this project envisages the industrial hydrogenation of toluene on highly porous Ni/Al_2O_3 cryogel catalysts. Activity and fluidizability studies were carried out on these powders culminating in the hydrogenation reaction in a specifically designed fluidized bed reactor.

The cryogels used were prepared and characterized at the Chemical Engineering laboratories. Activity tests on Ni/Al_2O_3 catalysts containing varying nickel compositions at two different reaction temperatures, viz., 130°C and 150°C, as well as catalyst activation studies have been performed in a fixed bed integral reactor. Catalytic activity is negligible below 4.5% Ni, increases with increase in the nickel

composition in the range 4.5-14% while remaining constant above 14%. It was found that the catalytic activity decreases with the rate of heating but increases with the flow rate of hydrogen during the activation process. Cryogels exhibited poor fluidizability in a cylindrical fluidizer with the occurence of bed plug-rise, channelling, particle agglomeration and bed segregation as a result of the prevailing interparticular forces typical of cohesive powders belonging to Group-C of Geldart's classification. The optimum nickel composition in the catalyst was found to be 14% based on the activity and fluidizability tests.

To achieve an uniform and unsegregative fluidization of the cryogel bed, a conical fluidizer was designed and constructed. Agglomerate-free fluidization of cryogels was possible in this conical fluidizer which maintains bed solids in a well-mixed state at high gas inlet velocities. A segregated packed bed model was proposed and used to derive a modified Ergun equation which predicts well the bed pressure drop and the minimum fluidization velocity which in turn indicates that the gas is well distributed in the bed region.

The hydrogenation of toluene on the 14% Ni/Al_2O_3 cryogel was carried out in the conical fluidized bed reactor and the conversions were adequately predicted by the homogeneous PFR and CSTR models.

CONDENSÉ EN FRANÇAIS

Un des problèmes technologiques majeurs de ce siècle est le stockage d'énergie. La disponibilité hétérogène (spatiale et temporelle) de l'énergie est la cause de ce problème. Particulièrement, dans l'industrie de transport, la diminution des ressources pétrolières et l'augmentation de leur coût a motivé les chercheurs à développer des nouvelles technologies pour le remplacement des combustibles à base d'hydrocarbures.

Au Canada, la grande disponibilité de l'énergie hydroélectrique rend plus économique la production d'hydrogène par électrolyse. Le stockage d'hydrogène peut être réalisé par plusieurs méthodes telles la liquéfaction, la compression, etc.,. La méthode proposée par l'Institut de Recherche d'Hydro-Québec (IREQ) consiste à stocker l'hydrogène à l'aide d'hydrocarbures aromatiques. Les hydrocarbures aromatiques sont régénérés dans un véhicule possédant un réacteur de déshydrogénation. L'hydrogène résultant de la déshydrogénation agit comme carburant pour générer l'énergie mécanique. Les hydrocarbures aromatiques sont ensuite acheminés à l'usine pour être rehydrogénés.

Au département de génie chimique de l'École Polytechnique, après avoir exploré la déshydrogénation du méthylcyclohexane, les recherches se sont orientées vers le procédé d'hydrogénation du toluène afin de compléter le cycle de stockage.

Des catalyseurs pulvérulents Ni/Al_2O_3 de type cryogel (semblable aux aérogels) avec des porosités élevées grâce au séchage par la méthode de cryodessiccation ont été préparés dans le cadre de ce projet.

Les échantillons ont été préparés avec différentes teneurs de nickel, soit 0, 4.5, 9.13, 14 et 20%. Les mesures du diamètre moyen des particules de cryogel (entre 10 et 30 μm) ont été obtenues par l'analyse optique au laser, leur surface spécifique par la méthode de BET (250-300 m^2/g) et leur masse volumique apparente et la distribution des pores par la porosimètrie au mercure.

Pour choisir la teneur optimale de nickel dans le cryogel, des tests d'activités ont été élaborés pour chaque échantillon (0.366 g) en gardant les mêmes conditions d'activation. Ces études (réaction à 130°C et 150°C) ont montré que l'activité du catalyseur augmente avec la teneur du nickel entre 4.5% et 14% et reste constante à partir de cette dernière valeur.

D'autre part, on a utilisé une colonne de 5 cm de diamètre pour les tests de fluidisabilité. Les études hydrodynamiques dans la colonne cylindrique ont permis de constater une mauvaise qualité de fluidisation pour tous les cryogels étudiés. La présence des forces interparticulaires qui est caractéristique de ce type de particules (poudres cohésives appartenant au groupe-C de la classification de Geldart) a permis d'expliquer la formation d'agglomérats observés expérimentalement.

La vitesse minimale de fluidisation des agglomérats les plus petits a été trouvée à partir de la fluidisation dans la colonne vibrée manuellement. On a constaté que la vibration a amené une amélioration de la qualité de fluidisation.

Basé sur les résultats des études d'activité et de la fluidisabilité, le catalyseur Ni/Al_2O_3 ayant 14% de nickel a été choisi pour la suite des travaux.

En outre, les conditions opératoires optimales pour la phase d'activation ont été déterminées avec le cryogel 20% Ni/Al_2O_3 lequel a une activité quasi égale à celle du catalyseur choisi. L'étude a permis de constater que pour un taux de chauffage sous hydrogène plus grand que 1°C/1 min (entre 200 et 500°C), l'activité diminuait à cause du frittage du catalyseur. Le paramètre le plus important lors de l'activation a été le débit d'hydrogène. Quant au temps d'activation, on a constaté qu'il n'avait

pas d'effet. Les deux échantillons activés pendant 14 h et 28 h respectivement avaient la même activité.

Des tests d'activité avec le cryogel choisi (14% Ni/Al_2O_3) ont permis de valider le modèle cinétique d'hydrogénation qui avait été développé antérieurement pour la même teneur de nickel dans le catalyseur. Ce modèle a été adopté dans ce travail.

Pour améliorer la qualité de fluidisation du catalyseur choisi (14% Ni/Al_2O_3), plusieurs méthodes ont été essayées pour détruire les agglomérats qui se forment spontanément. Cela n'a produit aucun effet sur la fluidisation des cryogels qui sont très cohésifs sauf lorsqu'on utilise un lit conique.

Les caractéristiques de la colonne conique sont les suivantes: hauteur 21 cm, diamètre d'entrée 5 cm et angle du cône 28°. La hauteur de la colonne conique a été déterminée à partir du profil de vitesse axiale.

On a préparé 25 g du cryogel (14% Ni/Al_2O_3) nécessaire pour l'étude hydrodynamique et la réaction dans le lit fluidisé. L'étude hydrodynamique était menée en diminuant la vitesse du gaz fluidiseur. Pour une vitesse à l'entrée du lit conique correspondant à 44 cm/s, le cryogel était fluidisé tout en étant parfaitement mélangé. On n'a pas observé le phénomène d'agglomération pour des vitesses

supérieures à cette vitesse critique. A des vitesses inférieures à 44 cm/s, le lit était fluidisé présentant un coeur constitué d'agglomérats (taille des agglomérats = 2 mm) et une partie annulaire de particules originales.

Ainsi, les résultats expérimentaux montrent les poudres cohésives de type cryogel caractérisées par les forces interparticulaires peuvent être fluidisées dans un lit fluidisé conique. Lorsqu'on avait réduit la vitesse de gaz, le lit a été trouvé dans le regime à lit fixe toujours avec la structure de coeur-annulaire.

Une équation d'Ergun modifié pour prédire la perte de charge à travers le lit fixe conique ainsi qu'une corrélation pour estimer la vitesse minimum de fluidisation ont été développé. Étant donné que le lit fixe actuel consiste à une mélange binaire des particules, un modèle décrivant le lit a été proposé avec des hypothèses pour utiliser les équations mentionnées ci-haut.

Finalement, la colonne conique a été employée comme un réacteur à lit fluidisé pour la réaction d'hydrogénation. Les expériences ont été réalisées en variant la masse du catalyseur (24-17g) correspondant à une hauteur (10-8 cm) pour une température d'opération de 150°C et un débit de toluène de 1 cm^3/min.

La réaction d'hydrogénation dans le lit fluidisé conique a été aussi simulée en considérant les modèles homogènes des réacteurs piston et parfaitement mélangé.

Le résultat de la modélisation montre très peu de différence entre les modèles considérés ce qui s'explique par la cinétique qui correspond à une réaction lente. Les conversions expérimentales obtenues pour la réaction d'hydrogénation du toluène sont adéquatement représentées par les valeurs simulées dans toute la gamme des temps de séjour.

TABLE OF CONTENTS

LIST OF TABLES

LIST OF FIGURES

LIST OF PHOTOGRAPHS

LIST OF APPENDICES

LIST OF SYMBOLS AND ABBREVIATIONS

A	Cross-sectional area of the bed (m^2)
C	Particle collector
D	Diameter of the bed at dsitance z from the distributor (m)
d_p	Particle size (μm)
d_s	Sauter mean diameter (mm)
E	Activation energy (J/mole)
F	Force (N)
F^0	Molar flow rate at entrance conditions (mole/s)
g	Acceleration due to gravity (m/s^2)
H_0	Fixed bed height (m)
H	Bed height (mm)
ΔH	Heat of reaction (KJ/mole)
H_m	Maximum spoutable height (m)
HR	Hausner ratio (-)
m	Mass of solids (kg)
Δm	Mass of the conical volume element (kg)
P	Fluid pressure (Pa)
p	Partial pressure (Pa)
ΔP	Pressure drop (Pa)

P_{in}	Pressure regulator reading (psi)
ΔP_d	Pressure drop cross the distributor (mm H_2O)
ΔP_b	Pressure drop across the bed (mm H_2O)
ΔP_A	Mercury manometer in A
ΔP_R	Mercury manometer in R
ΔP_s	Water manometer in sampling box
Q	Volumetric flow rate of the fluid (m^3/s)
r	Rate of reaction (mole/g.min)
R	Universal gas constant (J/mole/K)
S	Solids stirrer in reactor A
T	Temperature (°C)
T_A, T_R	Thermocouple in reactors A and R
T_{tol}	Thermocouple in toluene conduit
U	Velocity of the fluid (m/s)
U	Height averaged velocity (m/s)
V	Volume (ml)
ΔV	Elemental volume of the conical bed (m^3)
V_{hc1}, V_{hc2}, V_{hc3}	H_2 cylinder valves
V_{nc}	N_2 cylinder valve
V_{d2} (UP/DOWN)	Flow direction valve
V_i	Main inlet valve

V_{iA}	Inlet valve of reactor A
V_{oA}	Oultet valve of reactor A
V_{iR}	Inlet valve of reactor R
V_{oR}	Outlet valve of reactor R
V_{sd}	Solids downflow ball valve between A & R
V_{bp}	Valve used for hydrogen exit from R during activation
V_t	Toluene valve
V_o	Main outlet valve
V_s	Sampling valve
W	Catalyst bed weight (g)
X	Conversion (-)
z	Height from the distributor (mm)

Greek symbols

α	Tangent of the half angle of the cone (-)
ρ	Density (kg/m^3)
Θ	Apex angle of the conical bed (degrees)
ϵ	Porosity (-)

Suffix

atm, ambient	Room conditions
a	Annular zone
b	Bulk property of the cryogel bed
be	External bed property
bl	Loose bulk property
bt	Tapped bulk property
C	Critical point value of the solvent
c	Core zone
f	Fluid
g	Gas
mb	Minimum bubbling conditions
mch	Methylcyclohexane
mf	Minimum fluidizing conditions
0_{mf}	Minimum fluidizing conditions at z=0
S	Solid
sa	Solids in annular zone
sc	Solids in core
pm	perfect-mixing condition
tol	Toluene
theo	Theoretical value

Chapter 1

INTRODUCTION

1.1 Context

Novel methods of storage and conversion techniques are vital for the efficient use of energy especially to avoid large fluctuations in demand and supply. Presently, we depend on oil as the principal source of energy, mainly due to its ease of storage and transportation in liquid form. However, the ever-increasing demand of petroleum and the environmental pollution involving its application oblige us to seek other sources of energy. Electricity is expected to form a large portion of our future energy (Alderson *et al.*, 1985). Owing to the major impediment of storage problems, direct application of this option seems bleak. In such a case, utilization of electricity in times of abundant availability for the electrolysis of water produces hydrogen. The low-cost generation of electricity and the vast hydro-resources in Canada facilitate hydrogen production in an immense scale.

On the other hand, researchers have been trying to replace petroleum by a suitable and very economical automobile fuel. Some have proposed hydrogen, which as a fuel has a specific heat 160% higher than that of gasoline. An engine using hydrogen would thereby enormously minimize environmental pollution. In its turn, hydrogen poses the problem of storage in the vehicle. To this effect, methods such as

compression at 200 atmospheres, liquefaction at -253°C or storage by heavy metallic hydrides are inefficacious or undeveloped.

The '*Institut de Recherche d'Hydro-Québec*' (IREQ) proposed an indigenous technique of saturating aromatic hydrocarbons, whereby hydrogen can be stored. Figure 1.1 pictorially explains the proposed scheme of operation.

The proposed method consists of four distinct stages:

1. Hydrogen generation.
2. Hydrogenation of an aromatic hydrocarbon in a plant to produce an alicyclic compound.
3. Dehydrogenation of the alicyclic compound in a reactor onboard the vehicle to release hydrogen.
4. Combustion of the released gas in a combustion engine also aboard the vehicle.

Hydrogen generated by the electrolysis of water is used to hydrogenate an aromatic hydrocarbon. The product from the plant is discharged at various gas stations. These stations are bi-functional, i.e., they do both refill the automobiles with the hydrogen vector as well as receive the spent liquid. The saturated hydrocarbon which is easily storable would then be dehydrogenated by a catalytic reactor onboard the vehicle liberating hydrogen which would subsequently take part in a combustion reaction. The dehydrogenated hydrocarbon is also stored in another tank. The collected spent-

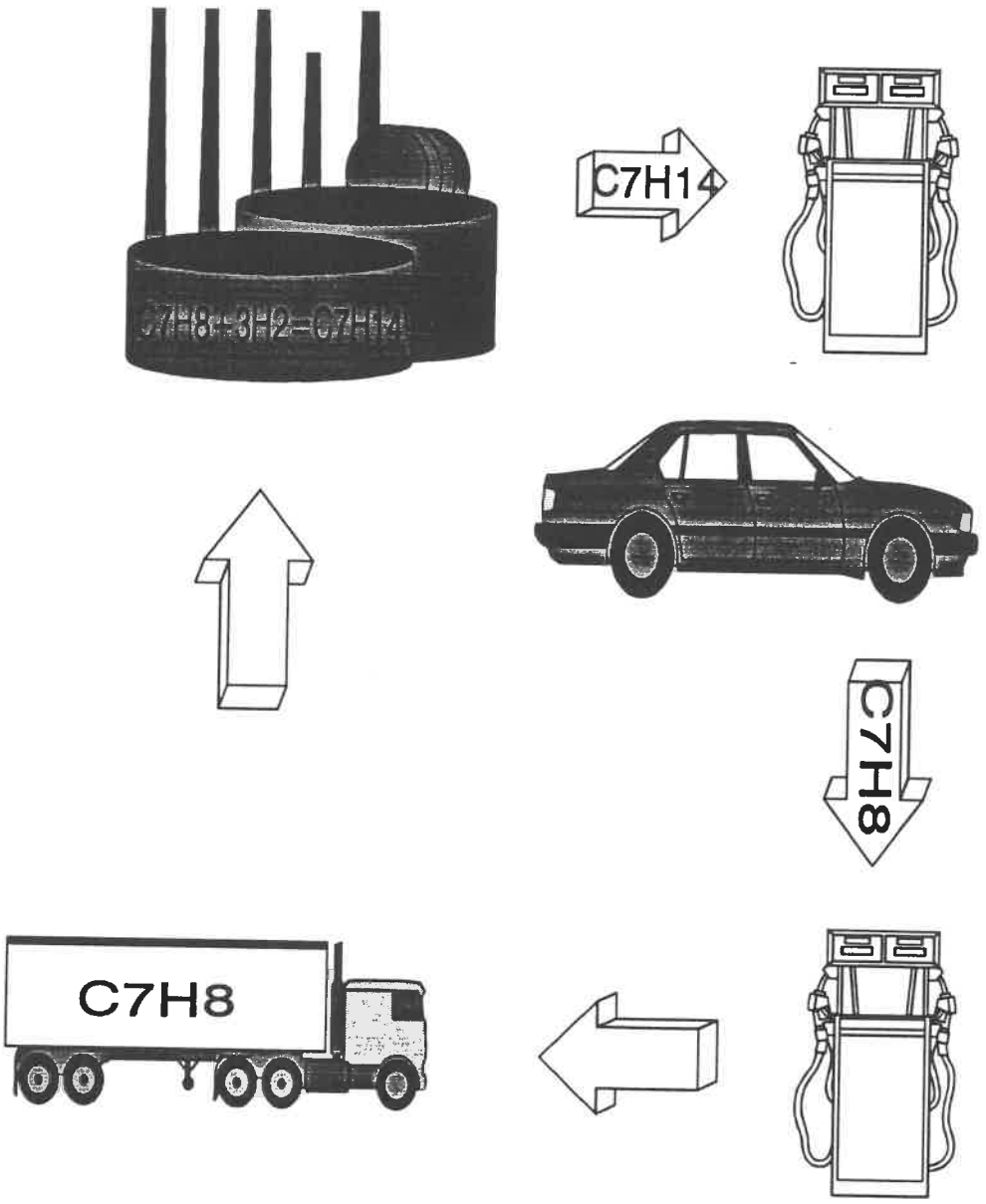

Figure 1.1 STORAGE AND USE OF HYDROGEN AS MOTOR FUEL

liquid is returned to the hydrogenation plant for recyling.

For each of the above mentioned stages, the research works and existing industrial processes wherever applicable are discussed below:

(A) Generation of hydrogen

Electrolysis of water is by far the most suitable method of generating hydrogen. Other sources are fossil-fuels, thermochemical method in places where electricity is not cheap, etc.,. Three full scale 100 kA electrolysis cells are operated at the Hydro Quebec Research centre, Varennes.

(B) Hydrogenation of the aromatic hydrocarbon

The major application of this reaction is in the manufacture of the starting material in the Synthesis of Nylon 6 and 66 and the removal of carcinogenic aromatic hydrocarbons. Nylon 6 is manufactured from caprolactum and Nylon 66 from HMDA and adipic acid. Adipic acid is produced by a two-stage oxidation of cyclohexane. The Stamicarbon and Scientific Design processes are some examples. The simplest and most commonly used aromatic hydrocarbon employed by existing industrial applications is benzene.

The conversion process is feasible either in the *gas* or in the *liquid* phase:

A summary of existing industrial processes for the hydrogenation of aromatics were dealt by LePage (1978), Alderson *et al* (1985) and Chauvel *et al* (1985). The Hydrar, Houdry, Sinclair-Engelhard, I.F.P., Arosat and the B.P. processes correspond to liquid phase hydrogenation, whereas, the Bexane and the Hytoray processes are vapor-phase processes.

Among the **liquid phase hydrogenation** processes, the *Hydrar Process* of the *U.O.P.* uses a platinum-based catalyst. Two or three fixed bed reactors in series operating at temperatures of 200-300°C and 3 MPa pressure were used. This process obviously involves high pressure and reaction temperatures besides the expensive catalyst. The exothermic heat of reaction was the sole source of heat input to steam generation in the *U.O.P.* process (Alderson *et al*, 1985). The *Sinclair-Engelhard* process involves a single fixed-bed reactor. Here the heat recovery is possible by internal tubing in which steam is produced. Unlike the Hydrar process, recycle of cyclohexane is not required, but a high hydrogen flow rate is expected to avoid uncontrollable reaction conditions. Another process using nickel in a fixed bed is the *Arosat Process* developed by Lummus. Recycling of liquid and gas is possible in this case and low pressure steam is also produced at the bulk of the reaction system. On the other hand, the *B.P. Process* is a two-stage hydrogenation process, the stream fed to the second reactor consists of 95% cyclohexane. The *Toray Industries Inc.* have also developed a process for benzene hydrogenation in multi-tubular reactors. The *Houdry*

process involves three fixed bed reactors in series functioning in the temperature ranges 140-190°C and 220-250°C. The reactor designed by the '*Institut Français du Petrole (I.F.P.)*' operates at 200°C and 4.1 MPa containing a Raney nickel suspension circulated externally. A portion of the heat of reaction leaves the system along with the saturated product in the vapor phase. The remaining heat is recovered by a heat exchanger located at the external circulation stream. Such heat energy is used to produce low pressure steam. The effluent is further treated in a downstream reactor in case of any sulphur poisoning in the initial stage.

Considering the above processes involving tubular reactors, the operational costs and security factors related to the enormous bed pressure drops are disadvantages.

An illustration of the **gas phase hydrogenation** is the *Bexane Process* developed by Stamicarbon specially uses a multi-tubular reactor with a platinum-based catalyst operating at 3 MPa and an initial temperature of 370°C. The heat is however recovered by a fluid. Another instance of the aromatic hydrogenation process is that of *Hytoray* using the T-61 noble metal catalyst.

The *Phillips Petroleum* process refers to the adiabatic hydrogenation of benzene (feed temperature=330°F) in the presence of a cyclohexane diluent using a Ni/Kieselguhr catalyst. In order to increase the benzene concentration in the feed over the value

meant for the desired effluent purity, the effluent stream is passed through a molecular sieve to meet the required standards. Worth mentioning here is the *Texaco Inc.* hydrogenation process which offers high product selectivity in the presence a volatile basic nitrogen compound (10-1000 ppm) and the catalyst, a Group-VIII metal on a refractory oxide support. Another special note on this process is the use of a two-stage reactor, the first stage having a Fe-group catalyst more efficient at low temperatures while the second has a noble metal catalyst and operates more efficiently at high temperatures. Thus the process can very well be undertaken at extreme temperatures even with sulphurous feed. The gas phase hydrogenation of benzene to cyclohexane being exothermic, the heat of reaction is partially transferred to a liquid stream (benzene and cyclohexane) which in contact with molecular hydrogen yields a vaporized reaction charge mixture. The temperature in the reaction zone is thus controlled. The major defect is that no formation of a liquid phase can be allowed in the reaction zone, since this leads to wetting of the catalyst indirectly ceasing the reaction. The unreacted liquid benzene would pass to a hotter zone and release enormous heat causing hot spots.

In all the above processes involving either the gas or the liquid phase, the major factor involving reactor design has been the transfer of the heat of reaction. It can also be observed that the control of high exothermic heat release in fixed bed reactors is achieved either by a series of adiabatic reactors with intermediate cooling or by a

multi-tubular reactor with a heat carrier fluid circulated in between the tubes. The former solution is tedious while the latter poses irregularities in pressure drop, flow rates and conversions and high investment costs. The problems of heat transfer and high pressure drop in fixed bed reactors have obliged technologists to employ an alternative reactor. *Fluidized bed reactors* have the uniqueness of efficient heat transfer. They are also best suited for industrial scale production (Chaouki,1984).

With the above practical problems in mind, an overview of the process development at the chemical engineering department of Ecole Polytechnique is presented below:

The choice of the *aromatic hydrocarbon* and the selection of a suitable *active agent* and *support* for the catalyst had to be studied. The maximum selectivity and the low melting point and low toxicity of toluene compared to benzene makes it highly suitable for the purpose (Lauga, 1989). The generally used active agents in catalysts for hydrogenation of aromatics were Pt, Pd, Ni, Co, Ru and Rh (Kusohorsky D., 1989). Platinum besides its very high cost is sensitive to impurities while Pd is normally used for partial hydrogenations. Rhodium and Ruthenium are specifically used when hydrogenolysis is to be avoided. The order of activity of these normally used metals are as follows (LePage, 1978):

Pt > Ni > Pd and specifically the hydrogenating activity per metal atom is given by

$$K_{Pt} : K_{Ni} : K_{Pd} = 18 : 7 : 1$$

While the activity of platinum is more than that of nickel, the cost of the latter is thousand times less than that of platinum. Under these considerations, nickel which has nominal costs and an acceptable activity seemed to be the best option. The support has to be inactive with respect to the reaction concerned, possess high porosity conducive to maximum diffusion rates of reactants and products and also possess a high mechanical strength. In the case of nickel as the active agent, the support mostly used is SiO_2 or Al_2O_3 (Kusohorsky, 1989).

The nickel catalysts used for the hydrogenation of toluene at the department were highly porous powders belonging to Group-C or Group-AC of Geldart's classification (Geldart, 1973; Chaouki, 1984). They are termed aerogels or cryogels depending on the method of drying the gel precursor during catalyst preparation. Aerogels are obtained by removing the solvent under hypercritical conditions, i.e., pressure and temperature exceeding the values corresponding to the critical point of the solvent. On the contrary, cryogels are prepared by drying under vacuum and cryogenic conditions. In both cases, the formation of a liquid-vapour interphase (which destroys the pore structure) is avoided.

A first study on the kinetics of hydrogenation of toluene on a Ni/SiO_2 aerogel catalyst was carried out by Pépin (1986). Kusohorsky (1989) performed kinetic studies on

Ni/SiO_2 aerogels in a tubular integral reactor and also studied the reaction in a cylindrical fluidized bed reactor. Subsequent studies by Lauga (1989) on the modelling of the above reaction in the fluidized bed developed the domain of hydrogenation of toluene on fluidized aerogels. It was noted that the cohesive forces in the case of SiO_2 support was much larger than those of Al_2O_3 support. So the support was chosen to be alumina in the subsequent studies.

Recently, experiments by Perras (1992) on the kinetics of the reaction on a Ni/Al_2O_3 cryogel prepared in the chemical engineering laboratories indicated the catalyst to be economically and functionally viable for the process. This study briefly explains the degree of fluidizability of aerogels, cryogels with inorganic precursors and cryogels with organic precursors. The cryogel catalyst, and in particular the aerogel catalysts, were very active and notably had very large specific surface areas, macro- and meso-pore volumes. The aerogels had specific surface areas in the range 600-800 m^2/g, whereas those of cryogel samples were between 300 and 400 m^2/g. Attempts to fluidize the cryogel samples led to channelling followed by particle agglomeration due to the high interparticle forces characteristic of fine cohesive powders.

As discussed earlier, the method of drying involved in the preparation of aerogels is not only highly expensive but also unsafe due to the high operating pressure and temperature. Based on economic and safety considerations, the **Ni/Al_2O_3 cryogel was**

chosen as the catalyst suitable for the hydrogenation of toluene in fluidized bed reactors (Perras, 1992).

(C) Dehydrogenation of the alicyclic compound to regenerate hydrogen

Once the hydrogenated product (methylcyclohexane) is manufactured in the plant, it is distributed at various regional gas filling stations. The hydrogen vector is then filled in vehicles (figure 1.1) and the spent liquid (toluene) is recuperated. It is now necessary to dehydrogenate methylcyclohexane to regenerate the stored hydrogen. This is possible in a dehydrogenation reactor containing a Ni/Al_2O_3 or a Pt/Al_2O_3 catalyst. Chavarie (1969) and Lakshmanan (1970) have extensively studied the dehydrogenation of cyclohexane in a continuous stirred tank reactor using these catalysts. The surface reaction between the adsorbed cyclohexane and adsorbed hydrogen is supposed to be rate limiting. The problem of concern here is one of catalyst deactivation during the dehydrogenation. Deactivation due to coke formation by catalytic cracking was quantified and simulated by a CSTR model (Pontier, 1991). It was found that deactivation could be minimized by judiciously selecting the operating conditions.

Feasibility studies on the operation of an hydrogen engine in automobiles was conducted by Touzani (1984). The dehydrogenation of methylcyclohexane in a tubular reactor at 450°C was modelled for a $Pt\text{-}Sn/Al_2O_3$ catalyst.

For the *reactor design*, the axial gas dispersion at the reactor inlet and wall heat transfer were taken into account. The packed bed dimensions were : 3 cm diameter and 80 cm length. The wall heat transfer coefficient was found to be the most important design parameter. Simulation results describe interesting features of the project. The dehydrogenation reaction being endothermic ($\Delta H = +204.57$ kJ/mol), for an hydrogen consumption of 3.55 kg/hr (equivalent to 11.91 l/100 km of gasoline), the required energy was 33.7 kW. The given gas flow rate corresponds to 41.9 kW heat loss since 35% of the produced energy of combustion is dissipated. This dissipated heat itself was to be recovered by a system of heat pipes to provide for the reactor. In all 29 tubes (Al-Si alloy, 1 mm thick) were required to be uniformly packed with 11.8 kg of pure catalyst making an overall reactor weight of 15.5 kg. Dilution of the catalyst with inerts increased bed volumes but lowered temperature gradients and therefore increased catalyst life.

However, in most hydrocarbon dehydrogenation reactions, the conversion is limited thermodynamically. The problems encountered are shift in the equilibrium or reduction in the operating temperature caused by hydrogen extraction. An effecacious method is to employ membrane reactors (palladium is the most efficient membrane for hydrogen extraction due to its maximum selectivity). Simulations by Gaches (1993) showed that use of a palladium membrane fixed catalytic tubular reactor for the dehydrogenation of cyclohexane resulted in 99% conversion even at a temperature

of 250°C. Also in this case, gas permeability is improved by reducing the thickness of the membrane. The state-of-the-art applications of membrane reactors and their extremely high potential in the petroleum and petrochemical industries have been reviewed by Guy (1992).

(D) Combustion reaction for the release of energy

The hydrogen produced by the dehydrogenation reactor is then injected into a combustion chamber where the gas mixes with a sufficient quantity of oxygen to cause an explosion when ignited. The technique is similar to that of the internal combustion engine currently used in automobiles. An hydrogen engine ensures high thermal efficiency and has the advantage of a minimum ignition energy compared to other fuels. However, the problems encountered are ineffective pre-ignition and the production of NO_x. It is reported that for a direct injection of hydrogen, the NO_x emission can be limited to a minimum by reducing the temperature of the exhaust (Touzani, 1984).

The above discussion gives an overall idea of the global objectives as well as a preview of processes involving the hydrogenation of aromatics in general and hydrogenation of toluene in particular regarding the storage of energy.

The current work concerns itself with the hydrogenation of toluene on fluidized

Ni/Al_2O_3 cryogels. As mentioned already, a recent study had suggested the use of this catalyst for the reaction.

1.2 Objectives

The main objectives of this work were the following:

1. To fluidize Ni/Al_2O_3 cryogels which belong to the Group-C of Geldart's classification (Geldart, 1973) and have very low densities.

2. To conduct and model the reaction, hydrogenation of toluene on a Ni/Al_2O_3 cryogel in a fluidized bed reactor.

The methodology proposed initially in order to reach these objectives is dictated in the following section.

1.3 Methodology

The following steps were proposed to achieve the objectives of the research work :

1. Prepare a set of four NiO/Al_2O_3 cryogels having different nickel compositions.
2. Establish a relation between the activity and the fluidizability of the catalysts.
3. Choose the optimum nickel concentration in the catalyst based on the above studies on activity and fluidizability.
4. Determine suitable conditions for the activation of the cryogel catalysts.
5. Conduct kinetic studies of the hydrogenation of toluene on the chosen cryogel.
6. Characterize the hydrodynamic behaviour of the chosen catalyst.

7. Develop a simple technique to improve the fluidizability of cryogels.
8. Conduct hydrodynamic studies of the final catalyst using the above technique.
9. Effect the hydrogenation reaction on the fluidized cryogel under improved fluidizability conditions.

1.4 Contribution to Science and technology

The current work has helped to expose the potentiality of the Ni/Al_2O_3 cryogel catalyst for use in the toluene hydrogenation process.

During the past studies, the effect of Ni on the activity and fluidizability of these catalysts were not as obvious as it is shown by this work. Characterization of Ni/Al_2O_3 cryogels were found to be explanatory tools to understand the results of the hydrodynamic studies.

Activation studies have validated the operating conditions used in previous experiments such as activity tests and kinetic studies on Ni/Al_2O_3 cryogels.

Experiments on the fluidizability of the cryogels have revealed the typical cohesive nature of these powders and also the qualitative influence of mechanical vibration of the bed on the hydrodynamics.

As a major contribution, the possibility of effectively fluidizing cryogels in conical fluidized beds has been explored. It is worth stating the uniqueness of this pioneering fluidization of Group-C particles of very low densities in a conical fluidizer. This thesis also presents the first hydrogenation study of aromatic hydrocarbons in a conical fluidized bed reactor.

Chapter 2

HYDROGENATION OF TOLUENE ON AEROGEL AND CRYOGEL CATALYSTS

2.1 Introduction

At the department of chemical engineering, Ecole Polytechnique de Montreal, during the past few years attention was focussed on the hydrogenation of toluene, vis-à-vis the hydrogenation process.

Pépin (1986) elaborated the operating conditions for the kinetic studies of toluene hydrogenation on a Ni/SiO_2 aerogel. This includes the optimal range of temperature and contact times. The selectivity was found to be 100% and the catalyst showed no deactivation.

Kusohorsky (1989) continued the development process, whose work describes the Ni/SiO_2 aerogel catalyzed reaction, both in a fixed bed as well as in a fluidized bed reactor. Kinetic studies were performed in a tubular integral reactor in the temperature range of 90-150°C and conversions between 0-98 % were obtained.

Lauga (1989) had conducted the reaction in a fluidized Ni/SiO_2 aerogel bed. The initial work of this project involving the improvement of the fluidizability of the

catalyst are dealt with in section 3.3. A model using averages of temperatures was developed and was found to be satisfactory.

Perras (1992) has modelled the reaction in a fluidized bed of 14% Ni/Al_2O_3 cryogel. The PFR and CSTR models were used for the purpose.

In another work (Klvana, 1992) the catalytic activity of an aerogel and two cryogels, one prepared from organo-metallic compounds and the other prepared from nitrates were studied. The activity of the different catalysts were found to be of the same order of magnitude. Based on economical and safety considerations, the nitrate-based cryogel catalyst was chosen for the kinetic studies (90-150°C) in a lab-scale tubular integral reactor. The fluidizability of these catalysts is discussed in the present work.

2.2 CRYOGELS

In the manufacture of fine powders, monoliths, etc., the sol-gel technique is quite common. Such solids have highly developed surface areas and porous volumes and thus are used in the fabrication of glasses, catalysts, ceramics and adsorbents (Pajonk, 1989).

A gel is a semi-solid with the solvent trapped in the capillaries. The factors affecting the texture of the final dried product are the nature of the solvent, the method of evacuation of the liquid, drying time and the final temperature (Pajonk, 1989).

During the conventional drying process which takes place at atmospheric pressure and temperatures varying between 20-200°C, the liquid evaporating from the capillaries causes a liquid meniscus (and consequently a liquid vapour-interphase). The meniscus is drawn inside the capillary during the drying process. This leads to a large increase in the surface tension forces whose magnitude increases with a decrease in the size of the capillaries. For example, if the pore width was of the order of 1.5 nm, the compression in the capillary was of the order of 10^4 psi (Pajonk G.M., 1989). An analogy to this process is the closing-together of the hairs of a brush when removed from water. The effect of this compression is a large shrinkage and thereby a reduction in the surface area and pore volumes of the final product, termed Xerogel.

The two methods of conserving the porous texture of the gel during drying are as follows (Figure 2.1):

1. Removal of the solvent above Hypercritical conditions ($T > T_c$, $P > P_c$) leading to a highly porous product termed Aerogel.
2. Removal of the solvent by sublimation leading to a highly porous product termed Cryogel. This process is termed Freeze-drying.

The term Aerogel is so, due to its physical property of a dense gas or 'air' and the term Cryogel originating from the 'Cryodessication' process. Similar to aerogels catalysts, cryogels exhibit large specific surface areas (Pajonk, 1991). The advantages of the cryogel over the aerogel are the cheap cost and safety of the freeze-drying process. During supercritical drying, the extremely high operating temperatures and pressures pose hazards. In the case of cryogels, even water, the most cheaply available solvent can be used. Nevertheless, the drying time under cryogenic conditions (48 h) is longer than that required (3-4 h) for the aerogels.

2.2.1 Textural and structural properties

Like the aerogels, the cryogels are also macroporous and amorphous as discovered from mercury porosimetry and XRD patterns respectively (Klvana *et al*, 1989). However, the texture of a cryogel was found to be less developed than that of a comparable aerogel. This is probably due to a partial destruction of the porous

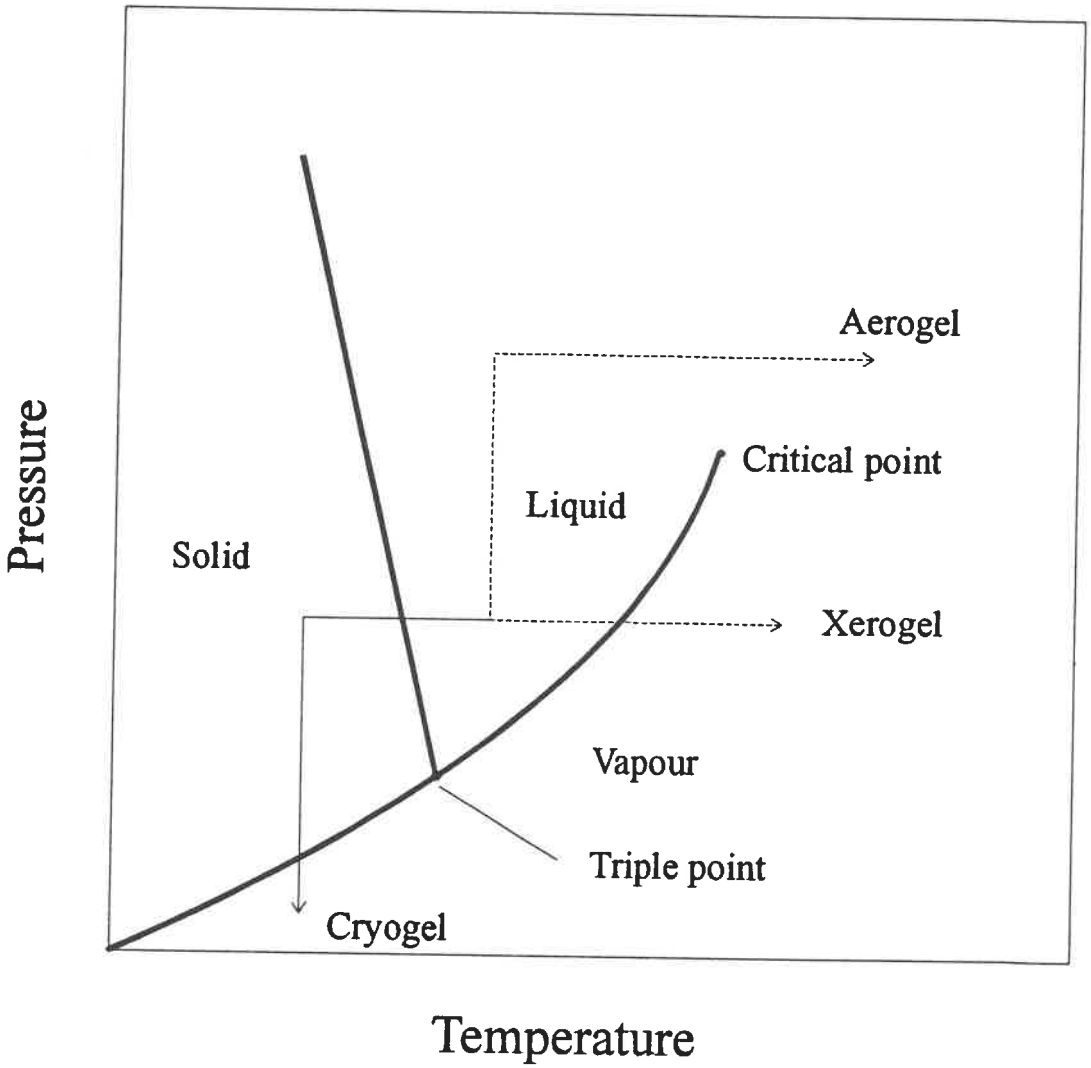

Figure 2.1 Three-phase diagram for water

texture of the cryogels during the freezing step.

Also, it was found out that while the textural properties of a cryogel (silica) remain unchanged when the age of the gel varied from 4 to 20 hours, a gel, 520 hours old had a fairly reduced specific surface area but an increased pore volume. Emphasis is made on the mechanical resistance of the gel which increases with its age. The mechanical resistance is also said to increase with the pH, whereas at pH=8.5 there was an abrupt fall in the specific surface area.

2.2.2 Preparation of Ni/Al_2O_3 cryogels

For the purpose of this work a batch of cryogels was prepared containing 0, 4.5, 9.13, 14 and 20 % Ni by weight, in a rather limited quantity for the activity and fluidizability tests. A half-litre lot was finally prepared for the reaction in the fluidized bed.

The following is the protocol adopted for preparing all cryogel samples and the entire procedure is explained schematically in Figure 2.2.:

The required quantity of nickel nitrate hexahydrate [$Ni(NO_3)_2$. $6H_2O$] is dissolved in the corresponding portion of a 1 M aluminium nitrate nonahydrate [$Al(NO_3)_3.9H_2O$] solution in a large beaker (say 1000 ml for 5 g of the final catalyst) to result in the necessary nickel composition in the catalyst.

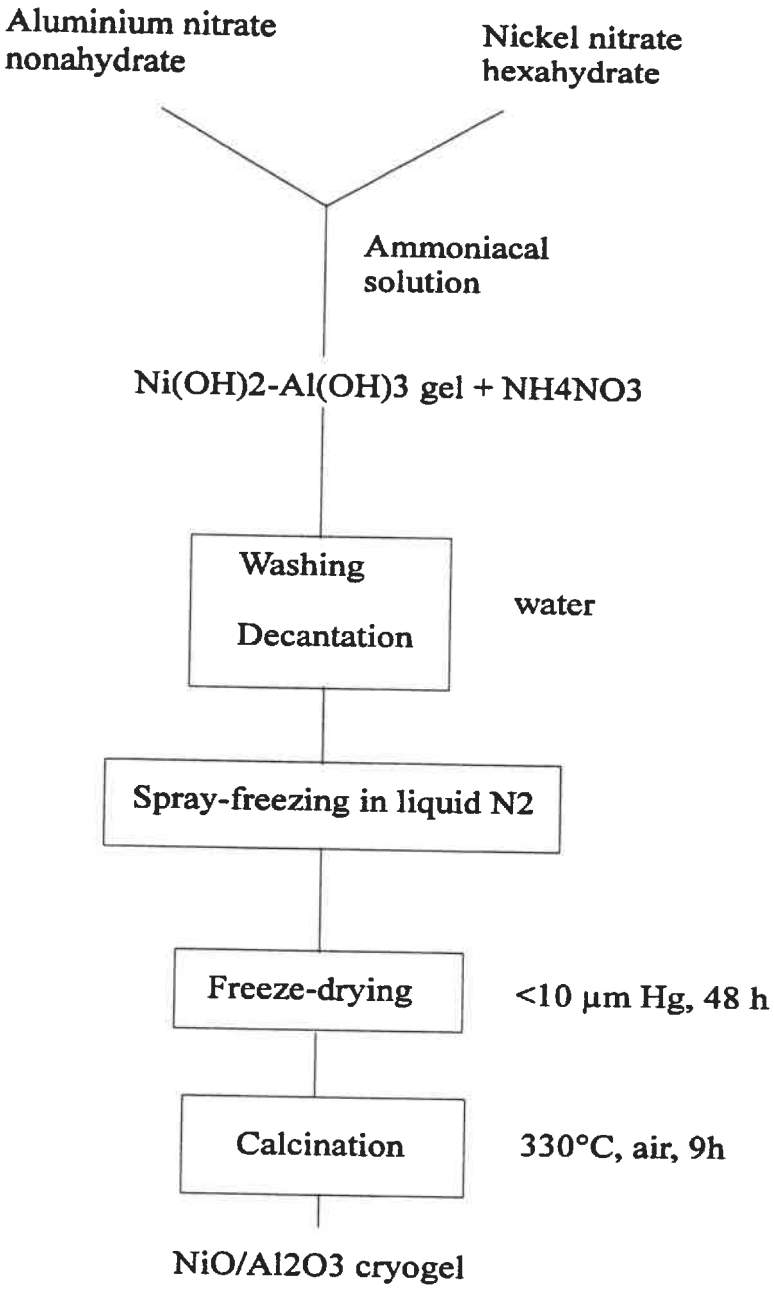

Figure 2.2 Preparation of NiO/Al2O3 cryogels

About 100 ml of distilled water is added to the mixture which is then stirred using a magnetic stirrer. About 20 ml of 2:3 NH_4OH solution is slowly added. The appearance and the subsequent disappearance of a blue colour is clearly observable. This is then followed by slow additions of a 1:9 NH_4OH solution from a burette. The pH of the mixture is monitored using an Accumet pH meter 915 (Fisher Scientific). At pH=4, the viscosity of the mixture abruptly shoots up. This is due to the formation of aluminium hydroxide. At this moment, stirring is done manually with the help of a glass rod while continuing to add the dilute ammoniacal solution. The pH is monitored till it reaches a value of 8 when the gel receives a blue tinge depending on the amount of the nickel salt added. At this pH value, all nickel forms the hydroxide $Ni(OH)_2$. The resultant NH_4NO_3 salt would be dissolved in the water present.

The beaker containing the gel is then filled with distilled water and stirred for nearly an hour. The homogeneously-stirred mixture is left to be decanted for three hours. At the end of decantation, the beaker would contain a settled bed of gel [$Ni(OH)_2$ - $Al(OH)_3$] with a clear supernatent liquid on top containing the dissolved NH_4NO_3. The time of stirring and decantation may be increased for large quantities of the gel. The supernatent liquid is then drawn out through a small tube, without disturbing the gel. Fresh distilled water of an amount equal to that of the removed liquid is added.

The above cycle is repeated three times to remove all dissolved NH_4NO_3. The supernatent liquid in the final cycle is removed carefully as much as possible. The aqueous gel is stirred for nearly thirty minutes. The homogeneous gel is then transferred into a smaller beaker for ease of handling.

A spray gun whose suction stem is kept immersed in the gel, is used to spray the gel into a bath containing liquid nitrogen at -196°C*. For safety reasons, the insulated bath is covered with a lid, though provided with a hole on one of the sides so as to introduce the spray nozzle into the chamber while spraying. A fine spray of the gel was deftly carried out at regular intervals by a constant pulsed-trigger on the spray-gun. The frozen gel should quickly be showeled into one of the special insulated glass containers**. Meanwhile, the freeze-drier Labconco Freeze-Dry system is powered, starting with the refrigeration system which reaches a temperature of -75°C, followed by the vacuum pump which reduces the pressure in the vacuum chamber to about 5-10 μm Hg#.

---

* Liquid nitrogen available at Ecole Polytechnique

** The glass vessel fixed to a flexible rubber lid with an outlet pipe, the neck housing a filter to avoid cryogel entrainment.

\# Initially, care should be taken that all exit ports of the vacuum chamber isolate it from the surroundings.

The glass vessel containing the frozen gel is temporarily (5-10 minutes) connected to a vacuum line so as to remove the vaporizing excess liquid nitrogen trapped in the gel. This is done to safeguard the vacuum system of the freeze-drier. The nitrogen-free frozen gel is then connected to one of the ports of the cryogenic vacuum chamber.

After about 48 h of freeze-drying the cryogel obtains a bluish-white tinge and its characteristic fluffy and light bulk structure. The gel is finally placed in a crucible and calcined in the presence of air at 330°C for nearly 9 hours in a furnace. The ultimate NiO/Al_2O_3 cryogel sample possess a green colour.

2.2.3 Characterization of cryogels

Batch 1 consisted of cryogels containing 4.5, 9.13, 14 and 20% Ni supported on alumina and Batch 2 consisted of a large amount of fresh 14% Ni sample prepared for the hydrogenation reaction in the fluidized bed reactor. All samples were subjected to the following tests of powder characterization after being calcined.

1. Particle size analysis was carried out using a Brinkmann particle size analyzer 2010.
2. Mercury porosimetry studies were effected in a Micromeritics Poresizer 9320.
3. Specific surface area (Microporous range) of the cryogels were measured according to the BET method in a Micromeritics Flowsorb II 2300 apparatus.
4. The same equipment helped conduct gas porosimetry studies to calculate the mesopore area and volumes.
5. Tapped and loose bulk densities were measured following standard procedures (Ham, 1994).

The results are shown in Tables 2.1 through 2.4. The effects of variation in the nickel content in the cryogel on its physical properties are discussed below:

Table 2.1 CHARACTERISTICS OF CRYOGELS (Batch 1)

Property % Nickel	Sauter* mean diameter μm	Specific Surface Area** m^2/g	Pore*** Volume cm^3/g	Average pore*** diameter μm	Density*** Bulk kg/m^3	Skeletal kg/m^3
9.13	13	247	6.85	2.29	92	248
14(batch1)	15	232	6.88	0.99	127	981
20	29	237	4.47	1.52	141	384

Table 2.2 CHARACTERISTICS OF CRYOGELS (Batch 2)

Property % Nickel	Sauter* mean diameter μm	Specific Surface Area** m^2/g	Pore Volume*** cm^3/g	Average pore*** diameter μm	Density*** Bulk kg/m^3	Skeletal kg/m^3
14(batch2)	16	268	5.13	2.23	145	566

Table 2.3 DENSITY MEASUREMENTS

% Ni in cryogel Densities#	0	9.13	14	20
Loose bulk density (ρ_{bl}),kg/m^3	29	54	111	90
Tap bulk density (ρ_{bt}), kg/m^3	36	79	169	146
Hausner ratio (ρ_{bt}/ρ_{bl})	1.2	1.45	1.53	1.61

* Brinkmann Particle Size Analyzer 2010 measurement
** Micromeritics Flowsorb II measurement
*** Micromeritics PoreSizer measurement
# Standard measurement procedure (Ham R., 1994)

Table 2.4 SURFACE AREA COMPARISON

% Nickel in cryogel Specific Surface Area(m^2/g)	0	9.13	14	20
BET method	-	247	232	237
Mercury Porosimetry	-	12	28	12

Effect of Ni content on pore volume:

According to Table 2.1, the macroporous volume as measured by the mercury porosimetry method remains unchanged with the nickel content in the cryogel sample.

Effect of Ni content on pore area:

The above mentioned studies also indicate that the macropore area thus measured appears to be constant. Moreover, BET analysis (Table 2.4) showed that the surface area also remains unaffected by the presence of nickel.

Effect of Ni content on bulk and skeletal densities:

As per the mercury intrusion results (Table 2.1), the bulk and skeletal densities (considering the detectable macropores) of the catalyst samples were found to be independent of the Ni content.

Loose and tapped density measurements were also made using a 10 ml. calibrated cylinder following the standard measurement procedure (Ham, 1994). The

observations (refer to Table 2.3) confirm the above mentioned conclusions.

Interestingly, the Hausner ratio (HR = tapped bulk density/loose bulk density) also increases with the amount of nickel. A closer look shows that alumina cryogel belongs to the Group AC particles (Chaouki, 1984). The HR values of the catalysts are certainly above 1.4, the lower limit of Group C particles and are therefore characterized by strong interparticle forces. The fluidizability of these cryogel samples can thus be predicted to be affected by the presence of nickel.

Effect of Ni content on average pore diameter:

The average pore diameter is found to be independent of the nickel content in the sample as is the pore volume.

Effect of Ni on the particle size:

Particle size analysis of the powders by the Brinkmann Lazer Analyzer prove that there is a fixed range of the sauter mean diameter of the particles (Table 2.1). The diameter of the 14% Ni sample (Batch 1) was nearly the same as that of the final catalyst sample (Batch 2).

Shape analysis on the 14% Ni/Al_2O_3 sample:

Using the same apparatus, a shape analysis of several frozen images of catalyst

particles was performed. Observations were such that the individually existing structures were flaky and the results quantified that the shape factor of these structures vary from 0.25 to 0.85 (an average of 87 scanned objects).

Gas Porosimetry studies:

Several investigators have argued that the enormous intrusion pressure applied on mercury during the high pressure run could cause the destruction of the stucture of the samples (Ternan & Mysak, 1987). This would definitely present a distorted picture of the intrusion volumes and pore areas and consequently the densities of the sample. Gas porosimetry technique is a non-destructive method of analysis. Different nitrogen-helium gas compositions were used to be desorbed/adsorbed on a weighed sample (14% Ni, final catalyst) saturated with pure nitrogen. The corresponding volumes were recorded and plotted in Figure 2.3. The experiment was conducted in the Micromeritics Flowsorb II apparatus.

Using the method of Orr and Dalla Valle (1959), the pore volume (Figure 2.3) and pore area (Figure 2.4) distributions were estimated in the pore diameter range of 32-174 Å (partial mesoporous range). A total pore volume of 0.155 ml/g and a total pore area of 120 m^2/g were evaluated.

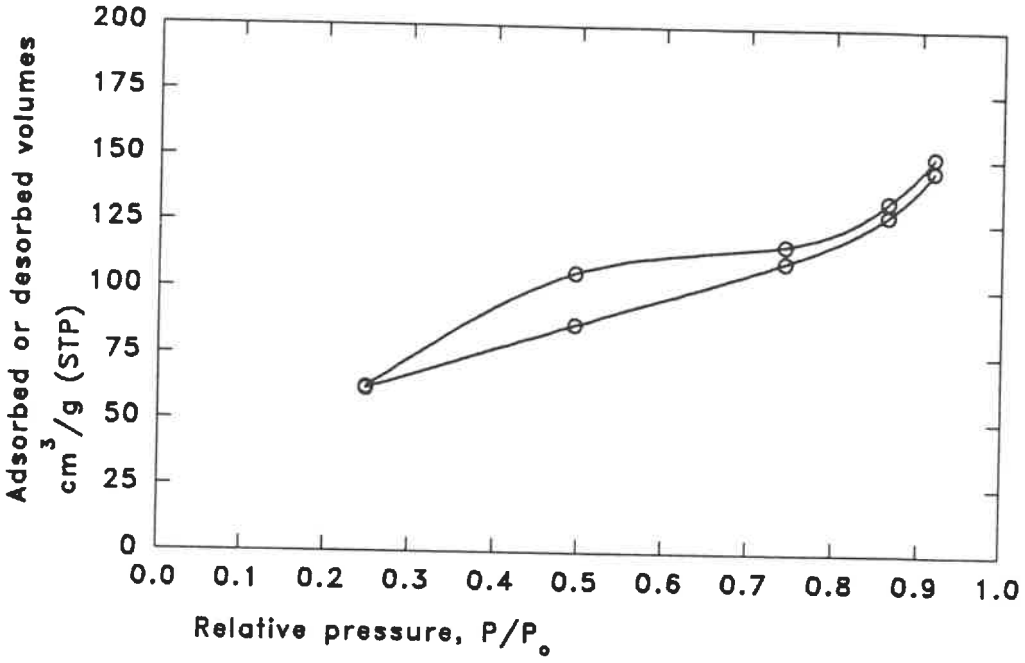

Figure 2.3 Gas porosimetry
N_2 adsorption/desorption isotherms of 14% Ni cryogel

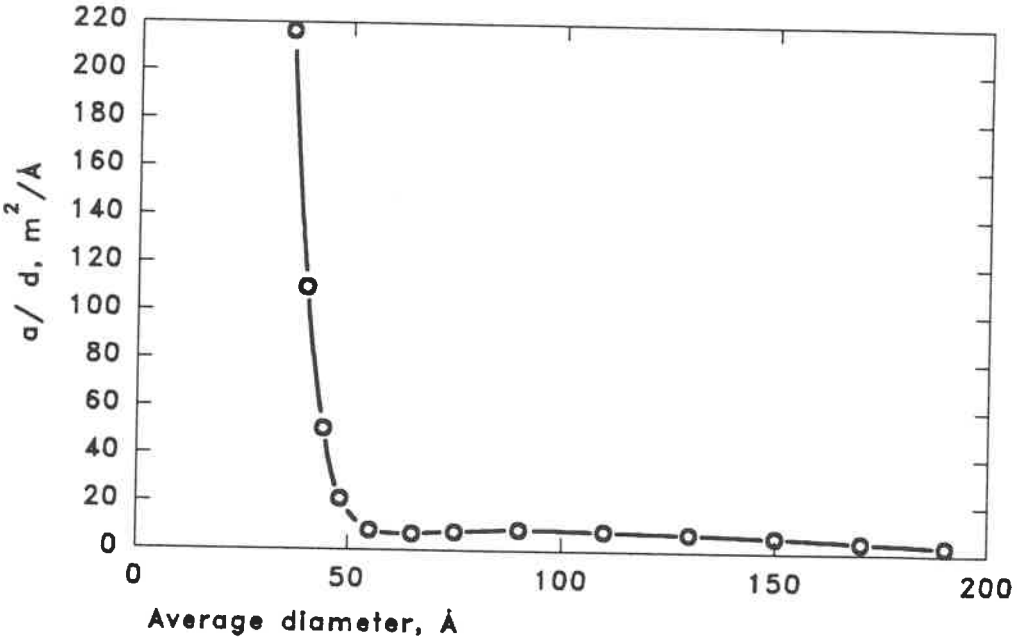

Figure 2.4 Gas porosimetry
Pore area distribution of 14% Ni cryogel

Values of 268 m^2/g by the BET method (microporous range) and 9 m^2/g by the mercury porosimetry method (macroporous range) were found for cryogels. It is worthwhile mentioning here that the measured specific surface areas of the 20% Ni catalyst prepared by modified methods of removal of the supernatent liquid viz., (a) decantation and (b) filtration showed no appreciable difference in magnitude. The values are 237 and 245 m^2/g respectively.

In short, the characterization of all the prepared cryogel samples with varying nickel compositions indicate that there is no appreciable difference in the properties. But the Hausner ratio of the NiO/Al_2O_3 cryogels clearly indicate that they belong to the Group-C of powder classification (Geldart, 1973). The alumina cryogel alone belongs to the Group-AC and is likely to exhibit hydrodynamic characteristics common to both groups A and C (Geldart & Wong, 1987).

2.3 ACTIVITY OF Ni/Al_2O_3 CRYOGEL CATALYSTS

2.3.1 Experimental set-up

The experimental arrangement used for the activity tests discussed in this chapter and also for the kinetic studies consists of the following components (Figure 2.5):

1. Hydrogen and toluene feed
2. Tubular integral reactor
3. Sampling system
4. Gas Chromatograph

1. Hydrogen and toluene feed

Hydrogen for both activation and reaction is supplied from commercially available storage cylinders, at 40 psi. The flow of the gas is measured by a rotameter.

Pure toluene is contained in two serial cylinders forming the saturator system. The regulated gas flows through the first of the cylinders and then through the other, the second cylinder avoiding any possible entrainment of the liquid. The gas can however bypass the saturator. Both the cylinders are housed in an insulated glass vessel containing distilled water, stirred and heated by an electric heater. A temperature of 50°C is maintained in the bath as indicated by a thermocouple. A mercury manometer

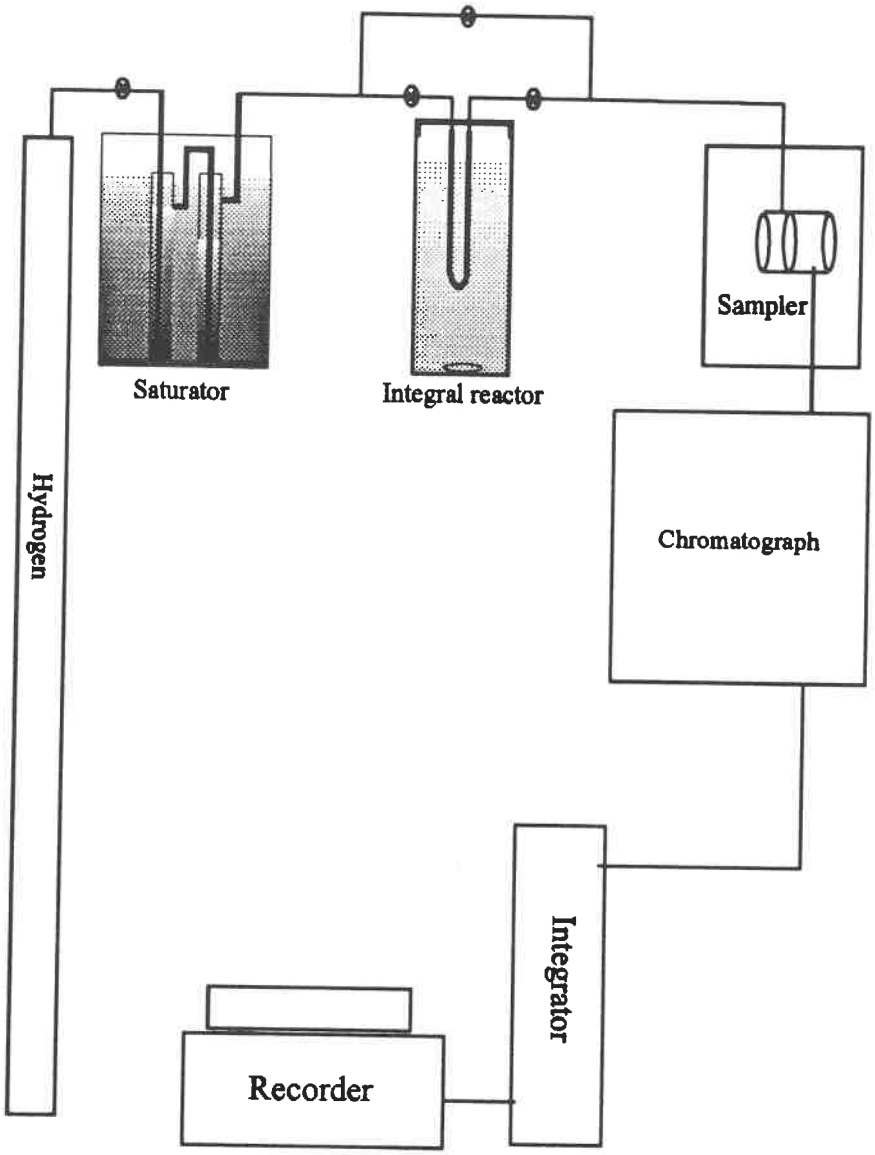

Figure 2.5 Reaction system for hydrogenation of toluene (Integral reactor studies)

measures the pressure of the gas leaving the saturator.

2. Tubular integral reactor

The reactor used was a U-shaped stainless steel tube, 31.3 cm long and 0.8 cm in diameter. To avoid compression effects of the gas flow through a catalyst bed (Kusohorsky, 1989) of low density, the catalyst is first thoroughly mixed with tiny shreds of steel wool and carefully and uniformly packed inside the reactor. This also helps in a more uniform distribution of heat, especially in this case of a highly exothermic reaction. Steel-wool studded at the two ends of the catalyst bed prevent solid entrainment as well. The gas can also bypass the reactor tube and directly leave the reaction system. The gas pressure is indicated by a mercury manometer located at the downstream end of the reactor. A thermocouple is inserted into the bed at this very end to measure the temperature inside the reactor.

During activation, the reactor is surrounded by an asbestos furnace, whereas while the reaction proceeds, the U-tube is immersed in a THERMINOL bath heated electrically and simultaneously stirred using a magnetic stirrer assembly. In either case, another thermocouple is always placed external to the reactor. However, the thermocouple inside the reactor alone is used as the input signal of the temperature controller.

3. Sampling system

Hydrogen gas carrying the hydrocarbons out of the integral reactor passes through an auto-sampler, which injects a constant (0.516 ml) volume of the product stream into a helium carrier gas flow. This is effected by a relay switch and compressed air. An ON time of 3 min and an OFF time of 2 min is used. The reaction products are thus analyzed by the Analysis section. The sampler is housed in a wooden box. The box is heated by a pair of heater coils present at the base, while the air is well-mixed by a small fan. A separate ON-OFF controller maintains the temperature in the box at 130°C measured by a thermocouple.

4. Gas Chromatograph

The gas chromatograph is equiped with both a Flame Ionization Detector (FID) and Thermal Conductivity Detector (TCD). The helium carrier gas containing the sample to be analyzed passes through a CARBOWAX 2M packed column, 140 cm in length which separates the methylcyclohexane and toluene in this serial order. The detected signal is amplified and fed to an integrator and subsequently to a chart recorder. Recordings of a mixture of methylcyclohexane and toluene show distinct peaks. The integrator calculates the area under each of the peaks and records it on a paper strip. The oven containing the packed column is also maintained at a temperature of 130°C.

Besides, the entire tubing arrangement between the saturator and the sampling system

is heated to 130°C by a ethylene glycol stream flowing in the annulus of concentric pipes. Ethylene glycol is circulated by a Micropump, from a reservoir heated electrically. The exit gas from the sampler is bubbled through water in a conical flask, connected to the central evacuation system of Ecole Polytechnique.

2.3.2 General operating conditions

Exactly 0.366 g of the catalyst is mixed with small shreds of steel wool as described earlier in section 2.3.1 . A uniform packing of the mixture is to be made inside the U-tube reactor. The ends of the catalyst bed are then made immobile by placing a pair of steel-wool studs. The reactor is bolted to its position in the reaction system after applying some thermal grease to the screws.

2.3.2.1 Activation

The asbestos furnace is then placed enclosing the reactor. Sufficient glass wool is placed over the exposed parts of the interior to prevent excess heat loss. The flow rate of hydrogen (measured downstream using a Bubble flowmeter) is fixed at 140 cc/min. The ambient conditions are noted. The set point (temperature) of the Proportional controller is then gradually raised from the ambient value to 200°C at a rate of 10°C/15 min (the required temperature is definitely reached before the next change). After the temperature of 200°C is reached, the rate of 10°/20 min. is

adopted till the final temperature of 500°C is obtained. The temperature is maintained at this maximum value for nearly 14 hours. The catalyst is then said to be activated.

2.3.2.2 Reaction

The exothermic reaction of hydrogenation of toluene can be expressed as follows:

$C_7H_8 + 3\ H_2 \xrightarrow{Ni/Al2O3} C_7H_{14}$

Based on thermodynamic considerations (Kusohorsky, 1989), the reaction temperature is fixed at 130°C and 150°C. The commencement of the reaction is preceded by the steps listed below:

1. Firstly, the THERMINOL bath is preheated to about 100°C. Then the asbestos furnace is carefully removed and the reactor immediately immersed in the stirred oil bath. The set point temperature is gradually increased to 130°C.
2. The ambient pressure and temperature are noted down.
3. The saturator heater, the ethylene glycol micropump and the sampler box heat control system are powered. The gas chromatograph is also powered.
4. When the entire system is in stable operation (stable at the required conditions, say after about an hour), the downstream valve of the reactor is closed so as to temporarily seal hydrogen in the U-tube. When a pressure drop of about 15-20 cm Hg across the reactor is indicated by the manometer, the upstream

valve is also shut while simultaneously opening the bypass valve.

5. Hydrogen gas flow is now set at the required value (say, 10-50 ml/min) and the stabilized gas stream is allowed to pass through the twin saturators. After about half an hour of continuous passage, the reactor upstream valve is opened slowly, while closing the bypass valve. Gradually, the downstream valve is also opened. The reaction is thus initiated.
6. Allowing another half hour for the process, the auto-sampler is powered and supplied with compressed air. The integrator and recorder are also powered. Twin peaks of methylcyclohexane and toluene are recorded. The integrator values for each of the peaks are noted down.
7. After the analysis (nearly constant integrator recordings), the operator returns to a new value of the hydrogen flow rate and steps 4 through 7 are repeated.
8. When sufficient points are obtained, the temperature set value is gradually increased to 150°C. The entire procedure (steps 4 through 7) are adopted for the higher temperature also.

2.3.3 Experimental results and analysis

A model calculation of the experimental results is shown in Appendix I . Activity tests were performed at the two reaction temperatures viz., 130°C and 150°C for each of the four catalysts containing 4.5%, 9.13%, 14% and 20% Ni respectively. Figure 2.6 summarizes the four pairs of curves plotted as % conversion of toluene

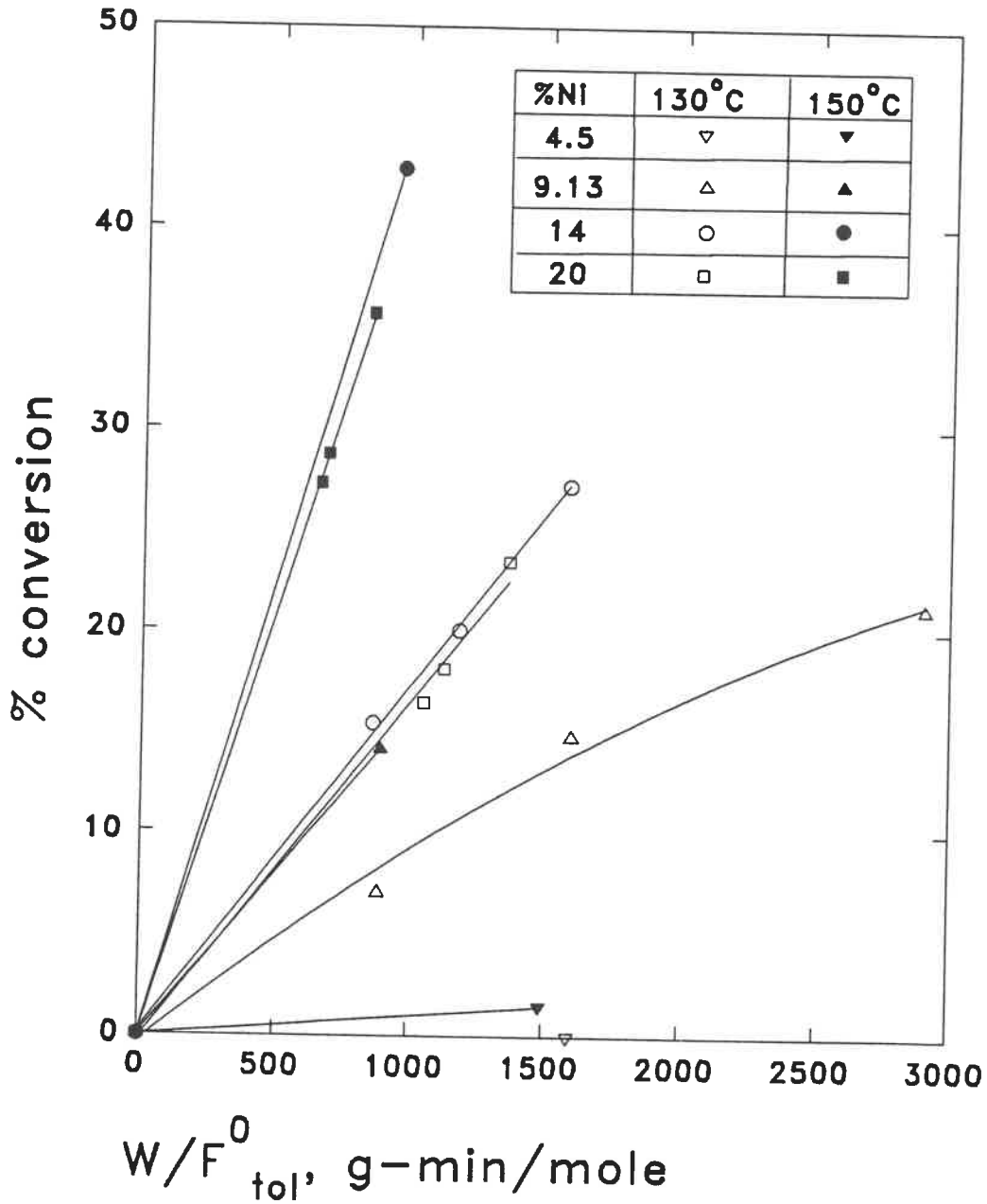

Figure 2.6 Activity of Ni/Al_2O_3 cryogels

versus the residence time (W/F_{tol}, g-min/mole). From the activity test results, the conversions of the catalysts at a specific residence time (W/F_{tol}=500 g-min/mole) is shown in figure 2.7 for the purpose of comparison. It can be observed that below a nickel composition of 4.5%, the catalyst is hardly active, the activity increasing proportionally with the metal content upto 14% Ni.

Beyond this composition, the catalyst activity is constant. It can be concluded that the minimum nickel composition required for the maximum activity of the catalyst is 14%. This catalyst is therefore best suited for the process from the point of view of activity. Coincidentally, kinetic studies in a previous work at the department (Perras, 1992) was also conducted using the very same cryogel catalyst.

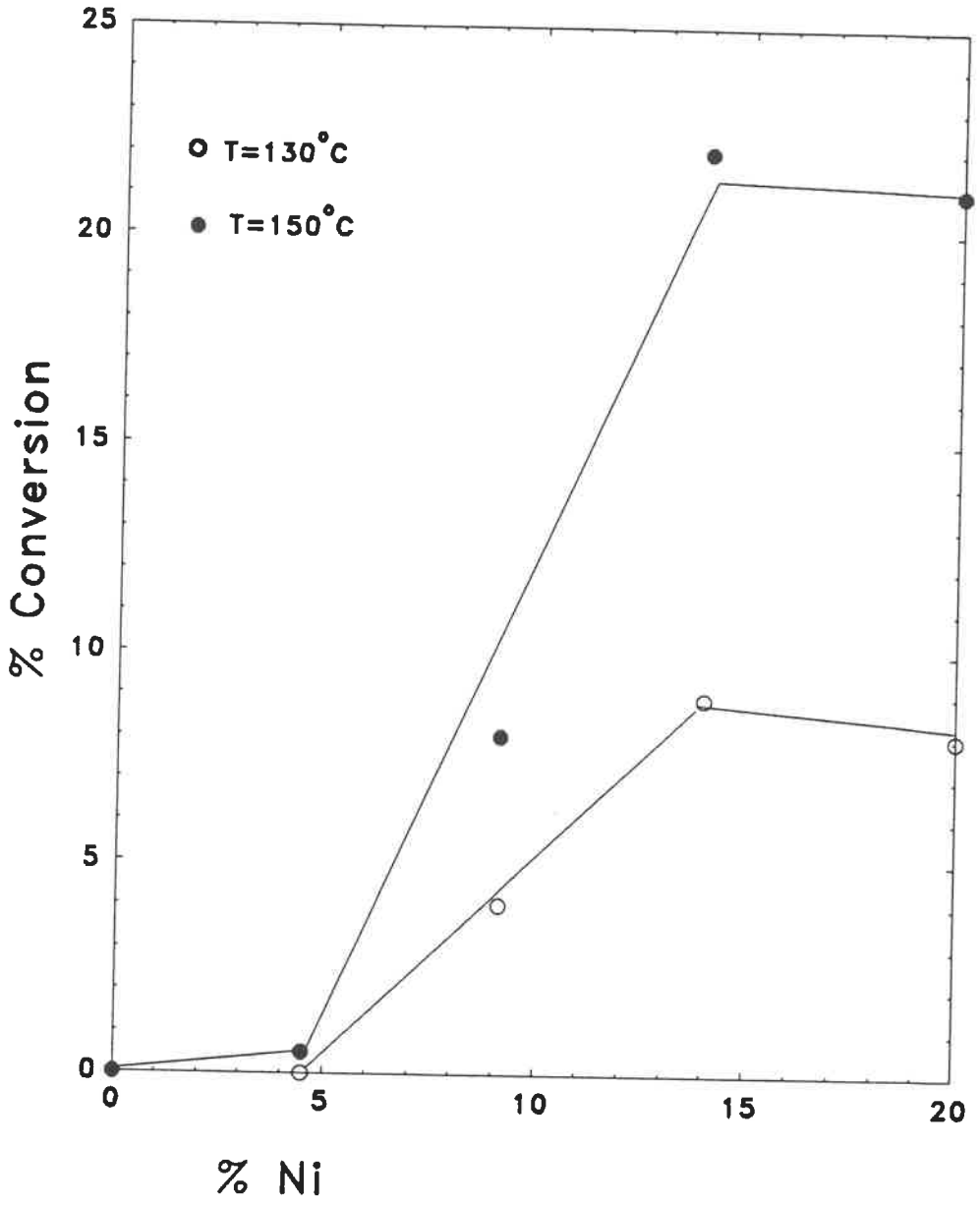

Figure 2.7 Effect of nickel composition on catalytic activity

[W/F^{0}_{tol}= 500 g-min/mole]

2.4 STUDIES ON CATALYST ACTIVATION

The four major parameters of the catalyst activation (reduction of NiO) process under consideration are the following:

1. Maximum temperature of activation
2. Rate of heating
3. Hydrogen flow rate and
4. Activation time at the maximum temperature

Table 2.5 General operating conditions of catalyst activation

Parameter	Value
Maximum temperature of activation	500°C
Rate of heating	10°C/15 min (25-200°C) 10°C/20 min (200-500°C)
Hydrogen flow rate	140 ml/min
Activation time at the maximum temperature	14 hours

Table 2.5 indicates the general operating conditions followed in previous works (Kusohorsky, 1989; Pepin, 1986; Lauga, 1989; Klvana, 1992) during catalyst activation, regarding Hydrogenation of toluene. This is also the case in section 2.3 of this chapter.

The current section explains how the four process variables were varied. It also presents the activity tests based on catalyst 20% Ni under different conditions. This particular catalyst was used since the fluidizability tests were not yet carried out before this series of experiments. It is to be recalled from section 2.3 that the activity of this catalyst is similar to that of the 14% Ni cryogel. As a result, the conclusions of the activation studies on the 20% Ni cryogel also apply to the 14% Ni catalyst. The conversions of toluene at reaction temperatures of 130°C and 150°C for the catalyst used here at the general operating conditions are taken from figure 2.6.

The objective of this section is to find suitable operating conditions of Ni/Al_2O_3 cryogel activation. Thus, only one of the process variables were altered at a time. For each of the following studies, a fresh sample (0.366 g of Catalyst 20% Ni) was used.

2.4.1 Maximum temperature

The maximum temperature of activation in the past studies was 500°C. As an extreme condition, the catalyst was activated at a minimum temperature of 200°C, at which free NiO can be reduced (Zielinski, 1982). The sample activated at 200°C was found to be practically ineffective. It was inferred that the activation temperature suited for the process was 500°C. Above this temperature, there is the possibility of the formation of nickel-aluminium spinel (Clause, 1992) caused by a chemical

interaction between the nickel and aluminium oxides, which is detrimental to further activation of the catalyst.

2.4.2 Rate of heating

The reader would recall the rate of heating used in section 2.3, viz., 10°C/15 min from $T_{ambient}$ to 200°C followed by a rate of 10°C/20 min from 200°C to 500°C.

A rapid activation rate was defined as follows:

a) Heating time of 30 min. from ambient temperature to 200°C.

b) Heating at the rate of 10°C/10 min. from 200°C to 500°C.

Care should be taken that a very high rate of heating might result in catalyst sintering, a phenomenon resulting from the agglomeration of metal atoms or crystallites in the case of supported metals, causing a reduction in the surface area of the catalyst. Figure 2.8 clearly shows that the conversion (at the reaction temperature of 150°C) is higher in the case of the normal heating rate. The lower conversions in the case of the fast activation process is explained by probable 'sintering' of the catalyst due to the high heat flux. The sample assumed a much darker colour than that resulting after a normal activation process. Also, the specific surface area of the catalyst sample recovered at the end of the reaction was 100 m^2/g. The normal activation rate will be retained for future activation of the cryogel catalyst.

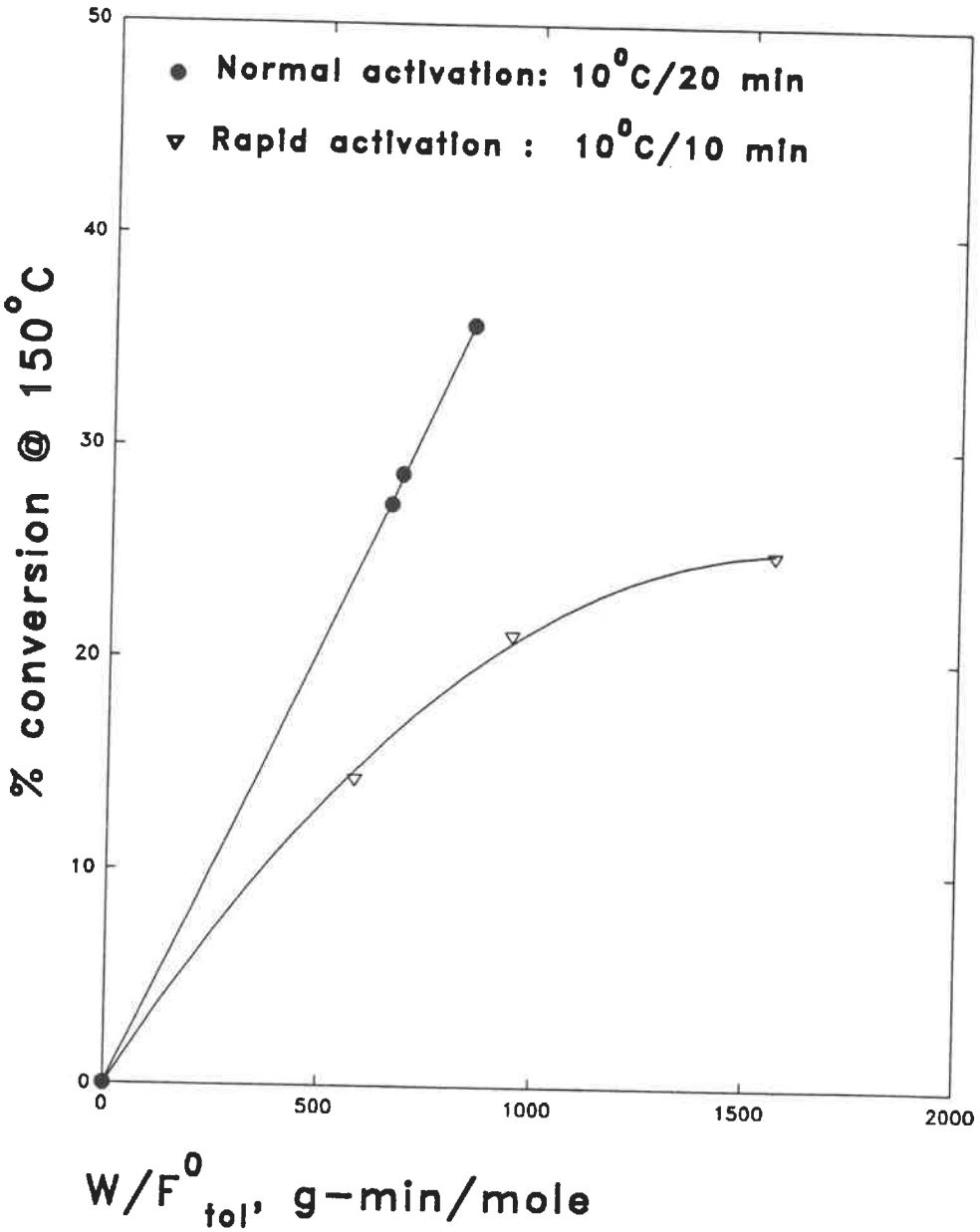

Figure 2.8 Effect of rate of heating during activation

2.4.3 Hydrogen flow rate

The normal flow rate of hydrogen during the entire activation stage is 140 cc/min. Figure 2.9 presents the conversion results (at the reaction temperature of 130°C) at three different flow rates of hydrogen, viz., 86, 142 and 381 cc/min.

At a residence time of 1000 g-min/mole, figure 2.10 clearly shows that catalytic activity increases with the hydrogen flow rate. This is due to the activation process which principally constitutes reduction of NiO via hydrogen chemisorption. Water molecules resulting from NiO reduction inhibit further reduction by being adsorbed on the surface. At higher flow rates of hydrogen, these water molecules are easily desorbed causing increase in the catalytic activity. Considering the high value of 380 cc/min, any further increase in the flow rate could cause disturbance of the powder in the reactor.

2.4.4 Activation time

As mentioned in Table 2.5, the normal time of activation (hold-up time) of the catalyst at the maximum temperature of activation (500°C) was 14 hours.

In this particular study, the activation time was doubled and the reaction was carried out both at 130°C as well as 150°C. Results of these tests can be seen in figure 2.11.

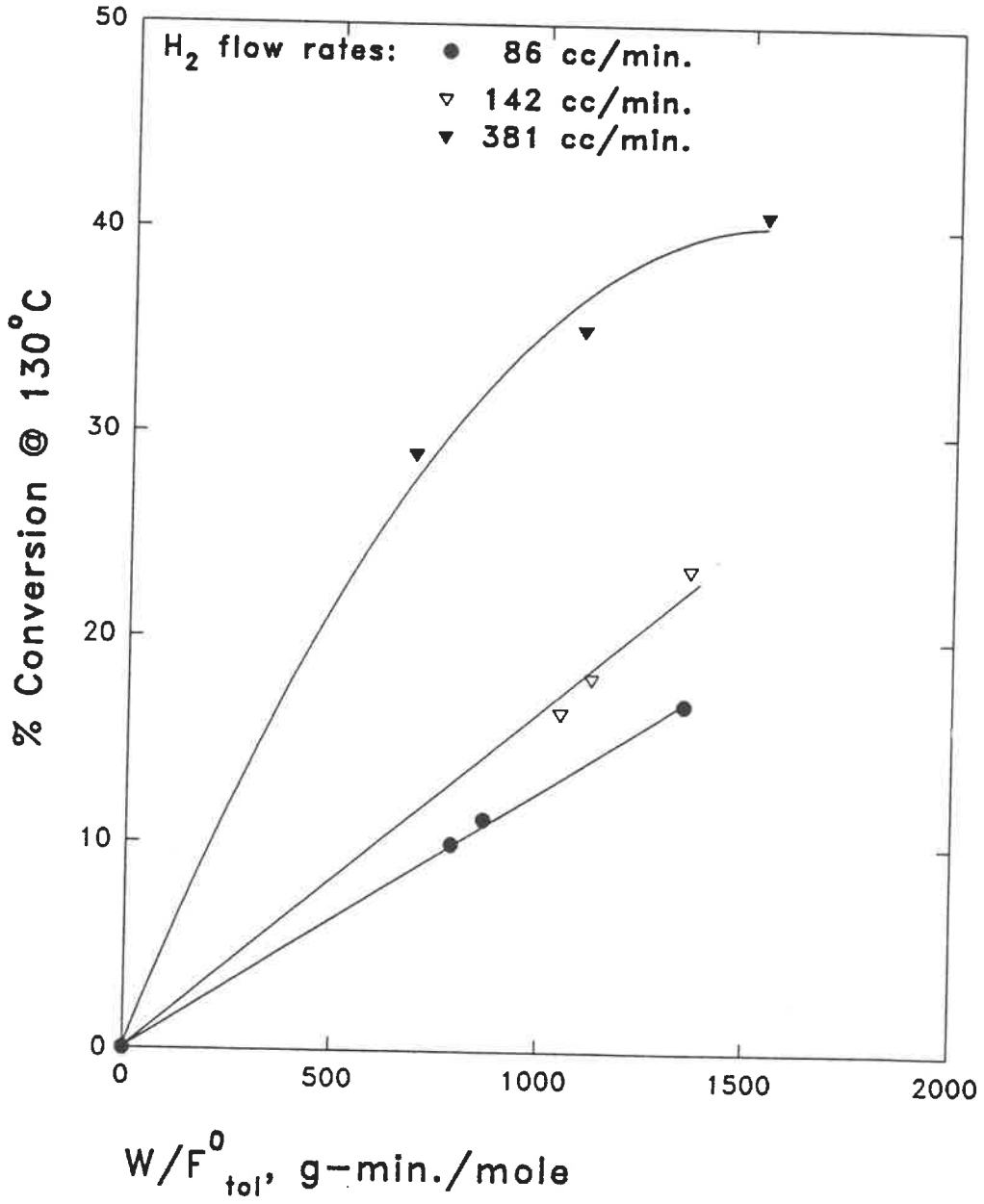

Figure 2.9 Activity at various H_2 flow rates during activation

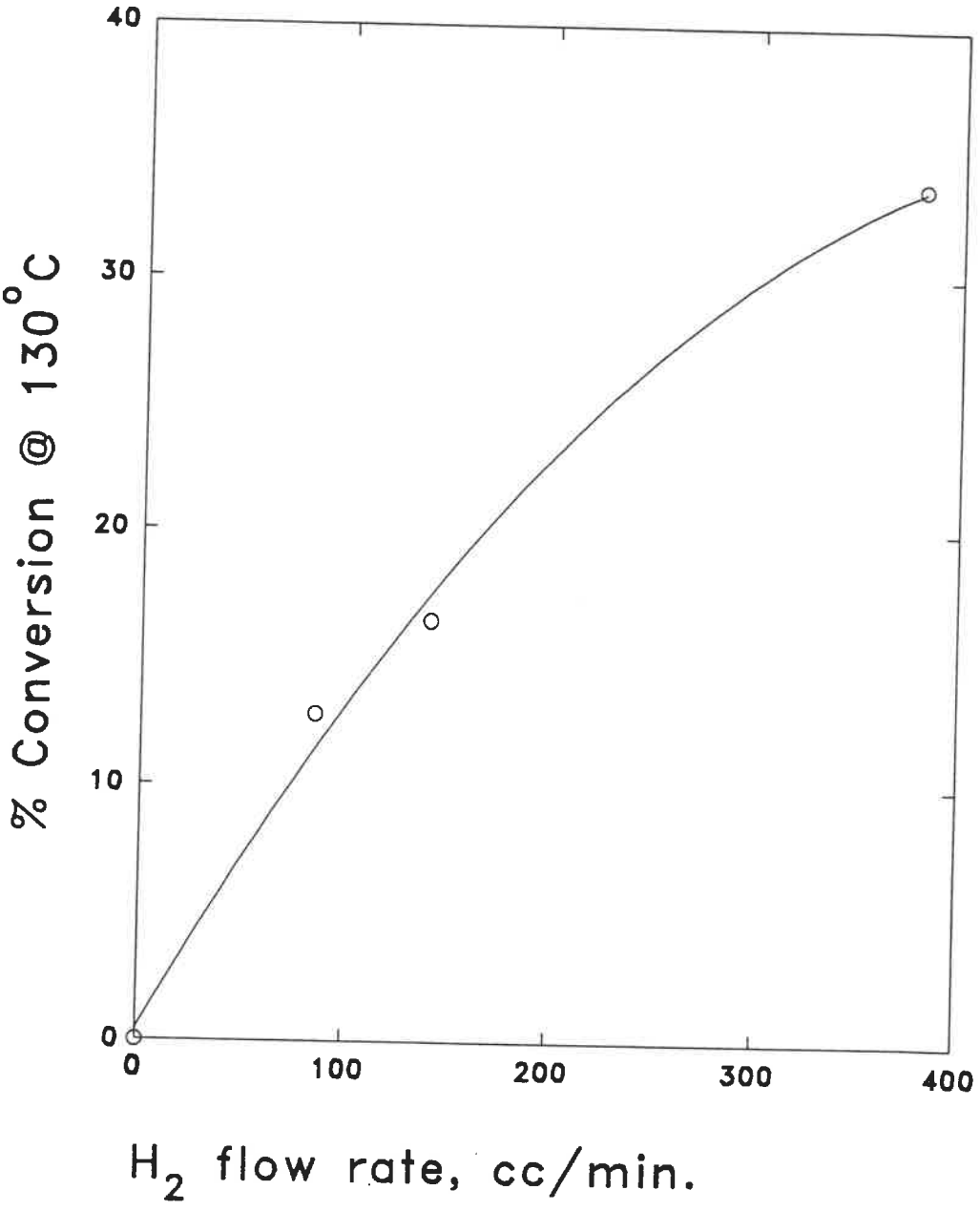

Figure 2.10 Effect of H_2 flow rate during activation on catalyst activity

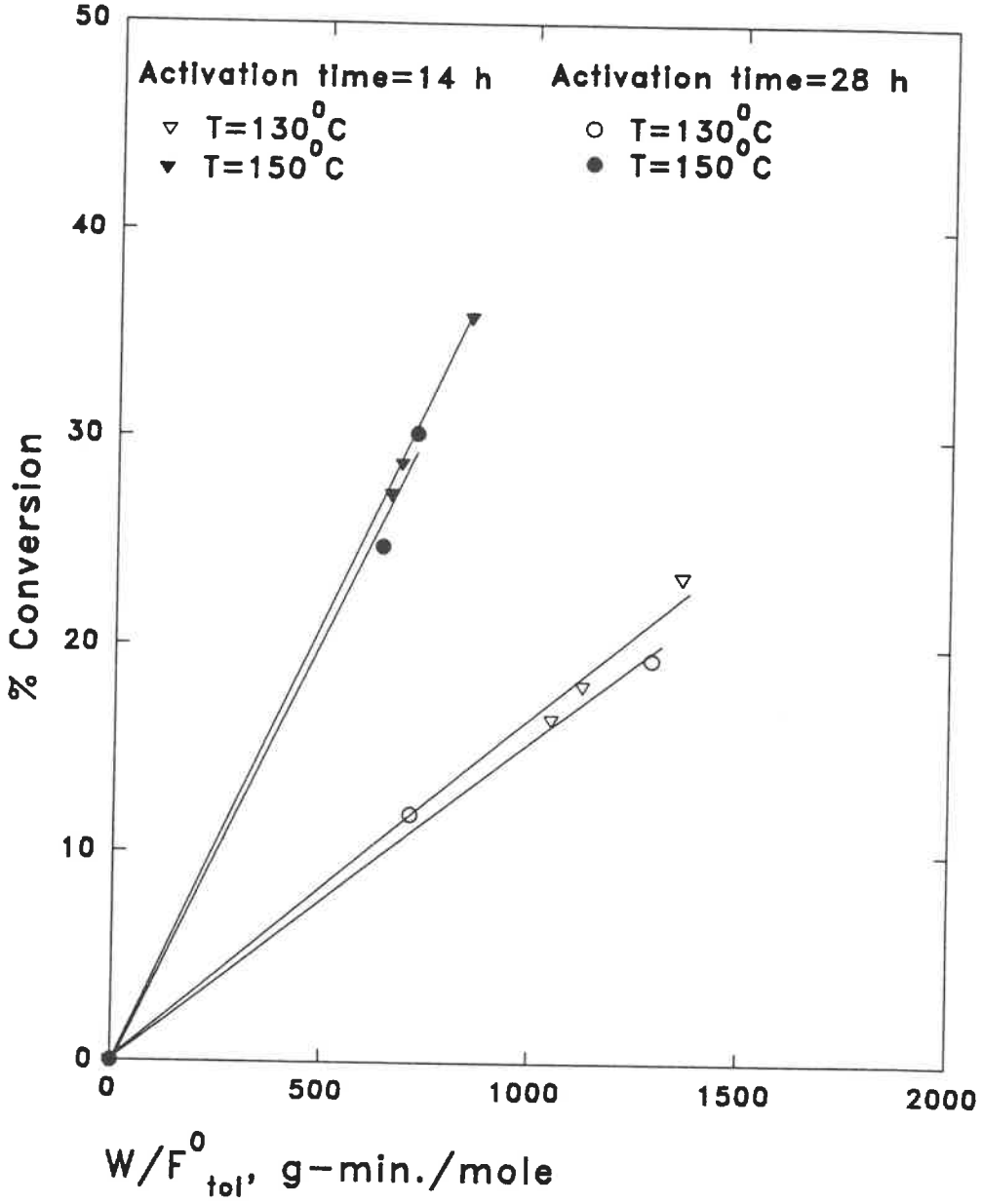

Figure 2.11 Activity at two different activation time periods

Prolongation of activation beyond 14 hours does not seem to have any appreciable effect on the activity of the catalyst. The activation time of 14 hours itself is therefore considered suitable.

It is well understood from the above mentioned studies that activation has to be conducted during 14 h at the maximum temperature of 500°C, achieved by heating rate of 10°C/20 min above 200°C. The rate of heating below this temperature was found to be superfluous. The most important factor governing the activity of the cryogel is found to be the hydrogen flow rate during the activation. All values of the activation process variables which have been used in section 2.3 and all other works mentioned earlier regarding the hydrogenation of toluene are quite suitable for the process.

2.5 Kinetic studies on the chosen catalyst

The current section briefly describes the kinetic studies of hydrogenation of toluene conducted at the department preceding this work. Both studies were performed using the same reaction system described in section 2.3.1 and procedure described in section 2.3.2.

As mentioned earlier, Kusohorsky (1989) carried out the kinetic studies on a Ni/SiO_2 aerogel catalyst (mixed with steel wool) at 90, 110, 130 and 150 °C. Studies were also conducted on the aerogel catalyst under compacted conditions. Conversion of toluene with respect to W/F^0_{tol} was found out in each case at different temperatures. In the first case, the power law model and the Eley-Rideal mechanistic model were both found to fit the kinetic data well. According to the power law model, the reaction was of zero order with respect to hydrogen. The mechanistic model fitted the experimental data satisfactorily with values of activation energy and heat of adsorption of toluene as 50.2 kJ/mol and 40 kJ/mol respectively.

Klvana (1992) deals with the kinetic studies of the hydrogenation of toluene on a 14% Ni/Al_2O_3 cryogel catalyst. Considering the fact that the catalyst chosen in section 3.3 of this work has the same nickel composition, it was decided to verify the kinetic model of the previous study. The model proposed is described as follows:

$$r = 1.4.10^5 e^{-71610/RT} p_{tol}^{0.08}$$

for $58 \leq p_{tol} \leq 12132$ and $1.4 \leq p_{tol}^{0.08} \leq 2.05$.

Experimental data from the activity test of the 14% Ni/Al_2O_3 catalyst provided in section 2.3.3 was used to test the validity of the model. Figure 2.12 shows the experimental conversions of this work versus the corresponding calculated conversions. From both these plots, it can be concluded that the kinetic model fits well the experimental data of the two independent studies. Consequently, the power law model and its parametric values of Perras (1992) have been retained for this work.

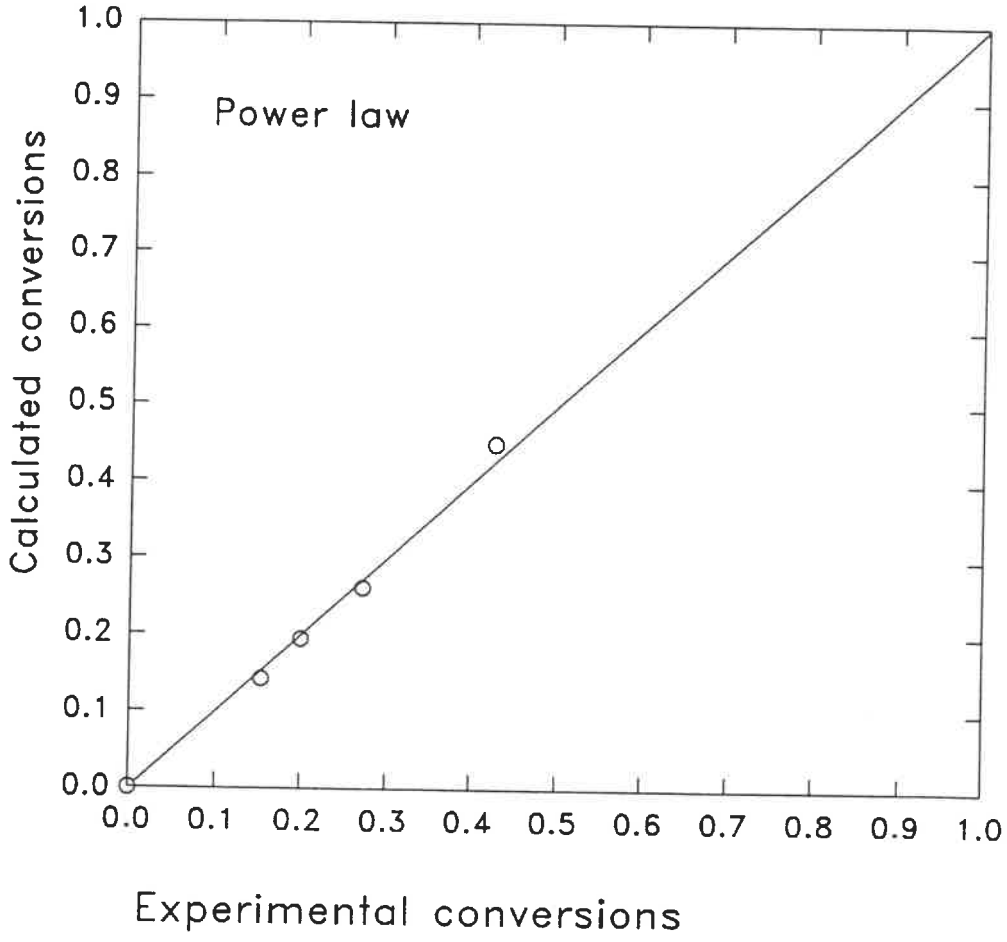

Figure 2.12 Validation of the kinetic model
Experimental conversions of this work

Chapter 3

FLUIDIZATION OF Ni/Al_2O_3 CRYOGELS

3.1 Introduction

As commonly agreed upon, particles belonging to the Group-C of Geldart's classification (Geldart, 1973) are extremely difficult to be gas-fluidized. They are characterized by particles of micron-size, low density and thereby strong interparticle forces (Chaouki, 1984). Since the mass of the individual particle is small, the interparticle forces may even be greater than the gravitational forces. The order of magnitude of these forces may reach many multiples of the weight of the particles. Consequently, a fluidizing gas being unable to overcome these forces due to its insufficient kinetic energy, spontaneously forms channels which extend all along the height of the bed. However, no theory on channelling has yet been reported. It has been shown that for C-type particles, neither the measured bed pressure drop was reproducible nor was it proper to characterize them in terms of U_{mf} and U_{mb} (Mahfoud, 1993).

The types of interparticle forces being (i) Electrostatic (ii) van der Waals and (iii) Capillary forces, their nature depends on the size, shape, roughness, hardness, chemical structure of the particles and the gas properties.

The *molecular forces of adhesion* are due to van der Waals' interactive forces dependent on the properties, size and roughness of the contacting bodies and also on the area of such contact.

Capillary forces are caused by water vapour condensation in the pores of loosely packed solids. This type of adhesive forces may however be reduced by surface-hydrophobing, say, by the introduction of a surfactant.

Electrical forces are produced by the collision (direct contact) of particles among themselves or on dissimilar surfaces whilst creating a potential drop between the rubbed surfaces resulting in particle cohesion.

On the other hand, *Coulomb's forces of adhesion* are generated by the approach of charged particles on to a surface which creates an equal but opposite charge on the other side of it (Cheremisinoff & Cheremisinoff, 1984).

Consequent to the effect of the interparticle forces, fine particles are attracted towards one another forming groups of individual particles called 'agglomerates'. However, in this thesis, the smaller agglomerates of size less than 1 mm are referred to as 'clusters', which are easily and homogeneously fluidizable. There exist powders which have the characteristics of both Group-A as well as Group-C particles termed

powders of Group-AC exhibitibing agglomeration besides a homogeneous fluidization (Geldart & Wong, 1984).

The identification of the sub-division of Group-C powders, viz., Group-C' of much lower density (ρ_p < 500 kg/m^3) was made by Chaouki (1984). They are characterized by spontaneous agglomeration during gas fluidization.

The expansion of a fluidized agglomerate bed is said to be inexpressible by the exponent 'n' of the Richardson-Zaki correlation. Chaouki *et al* (1994) predicted bed expansion taking into account the role of interparticle forces therein. Additionally, a stability criterion for homogeneous fluidization and a correlation between the elasticity modulus and the elastic wave velocity were developed. The cohesiveness of powders was expressed as a ratio of the cohesive and the gravitational forces.

The increasing industrial application of these fine particles however necessitates a satisfactory fluidization. Some of the existing and serious problems caused by powders are discussed in the literature. Some of them are particle attrition in the cyclone, size and temperature scale-up, entrainment of fines and the related density profile, solids recycle and conversion in the freeboard. In sections 3.2 and 3.4, the fluidization of cryogels and aerogels (tested for toluene hydrogenation) in particular and Group-C particles in general will be discussed.

3.2 Fluidization of cryogels in a columnar bed

The fluidization apparatus consists of a glass column 5 cm in diameter and 70 cm in height. Compressed air from the central air supply of Ecole Polytechnique passes through an air filter. The air pressure (20 psi) is fixed by a pressure regulator. Air then passes through one of the two rotameters R_1 and R_2 (R_1 used for higher flow rates and R_2 for lower flow rates) to a gas flow meter before entering the conical gas inlet of the fluidizer (figure 3.1). Between the gas inlet and the glass column is situated a gas distributor. For effective gas distribution, a fixed bed of lead shots (412μm in diameter) is present upto a height of 5 cm. A 1/8 inch steel tube extends from the surface of the packed bed to one port of a FCO 14 micromanometer (Furness Controls Ltd.) which would indicate the pressure drop across the cryogel bed in mm H_2O. The other port is open to the atmosphere.

The top end of the glass column is connected vertically to a particle disengagement zone which is in turn connected to a cyclone separator. A conical flask is connected to the bottom end of the cyclone by means of a valve collects any entrained solids.

The cryogel samples containing 0, 9.13%, 14% and 20% Ni respectively were tested for their respective fluidizabilities in the above described cylindrical fluidizer using air. The experiment was carried out following the procedure prescribed here:

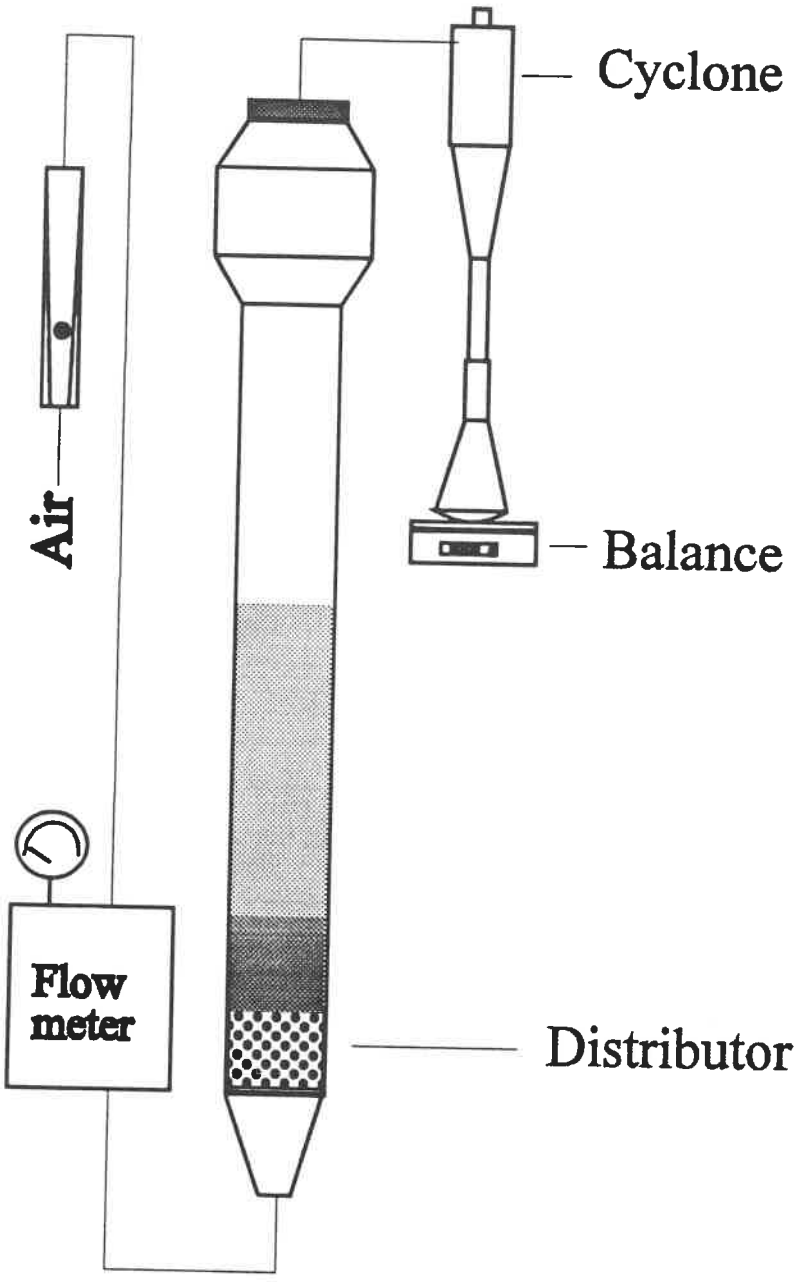

Figure 3.1 Apparatus for columnar fluidization

1. Sufficient quantity (5 g) of the cryogel to be studied is weighed.
2. The sample is slowly poured from the top of the column at an uniform rate. The initial height of the fixed bed is noted.
3. The gas flow main valve is opened, the inlet pressure fixed and the rotameter R_1 opened to its minimum calibrated value.
4. The gas flow rate is now measured. The pressure in excess of the atmospheric pressure in the gas flow meter is noted as P_{in}. After sufficient time of stabilization (20-30 min., verified by the constant value of a chart recorder connected to the micromanometer) the pressure drop across the bed is noted down.
5. The gas velocity is slowly increased to higher values and each time the stabilized velocity and pressure readings are noted down. Steps 4 and 5 are repeated for every increment in the air velocity.
6. Similarly, after reaching an air velocity of nearly twice the 'minimum clustering velocity' (ephemeral bed behaviour while increasing the air flow), the fluidizing air flow is reduced step-wise until the rotameter reads zero. Each time the steady pressure and velocity values are noted.

A tabulation of these readings is presented in Appendix II.

A) Fluidization of Alumina cryogel

Tests demonstrated the random behaviour of the alumina cryogel bed at very low air velocities, starting with a piston-like rise of the entire bed. Subsequently, the air-

lifted bed collapses and the gas is found to create channels for ease of passage. Observations show that the formation of channels is chaotic, the probability of formation depending on the local porosity in the initial agglomerate layer adjacent to the gas distributor.

The rise and fall of the pressure drop (Appendix III) during increasing air velocity in the fixed bed region is only due to the destruction and formation of the channels, respectively. At about 0.16 m/s, the entire bed fluidized (as was observed visually) forming clusters. While reducing the air velocity, the fixed bed region was more vividly defined than in the case of increasing flow. A U_{mf} value of 0.15 m/s was found out.

It is noteworthy that at 0.17 m/s (while increasing the flow), the bed exhibited a homogeneous fluidization characterized by a bed expansion ratio (H/H_0) of five. This observation is supported by the Hausner ratio of the alumina cryogel (HR=1.24) discussed in section 2.2.3 which belongs to Group AC of powder classification (Geldart *et al*, 1987). These powders are both cohesive as well as undergo an homogeneous fluidization (Chaouki, 1984). However, when the velocity was increased further the fluidization was no more homogeneous due to the spontaneous formation of larger agglomerates.

The following steps summarize the progress of fluidization of this sample:

0.02 m/s : The fixed bed rises as a piston and subsequently collapses to form the effective initial bed porosity.

0.03 m/s : Formation of channels all along the bed height. Channels are mostly concentrated at the walls.

0.06 m/s : Early agglomeration in the channels.

0.17 m/s : Break-down of stagnant zones to form spherical agglomerates and a smoothly fluidized bed of clusters above.

>0.17 m/s: Continuity in the dilute phase above the agglomerate bed.

B) Fluidization of 9.13% Ni cryogel

The fluidizing behaviour of this sample was similar to that of pure alumina cryogel. One can find in figure 3.2 the piston-like rise and the random changes in bed pressure drop during increasing gas velocity. At 0.12-0.13 m/s, there was certainly a slight bed expansion much less pronounced than that observed in alumina. Sufficient time (nearly an hour) was allowed before recording these points when the bed was mostly fluidized. Further increase in the velocity resulted in considerable agglomeration of the entire bed, whence partial fluidization occurred. The flow was then reduced to produce a classical trace of a partially fluidized bed.

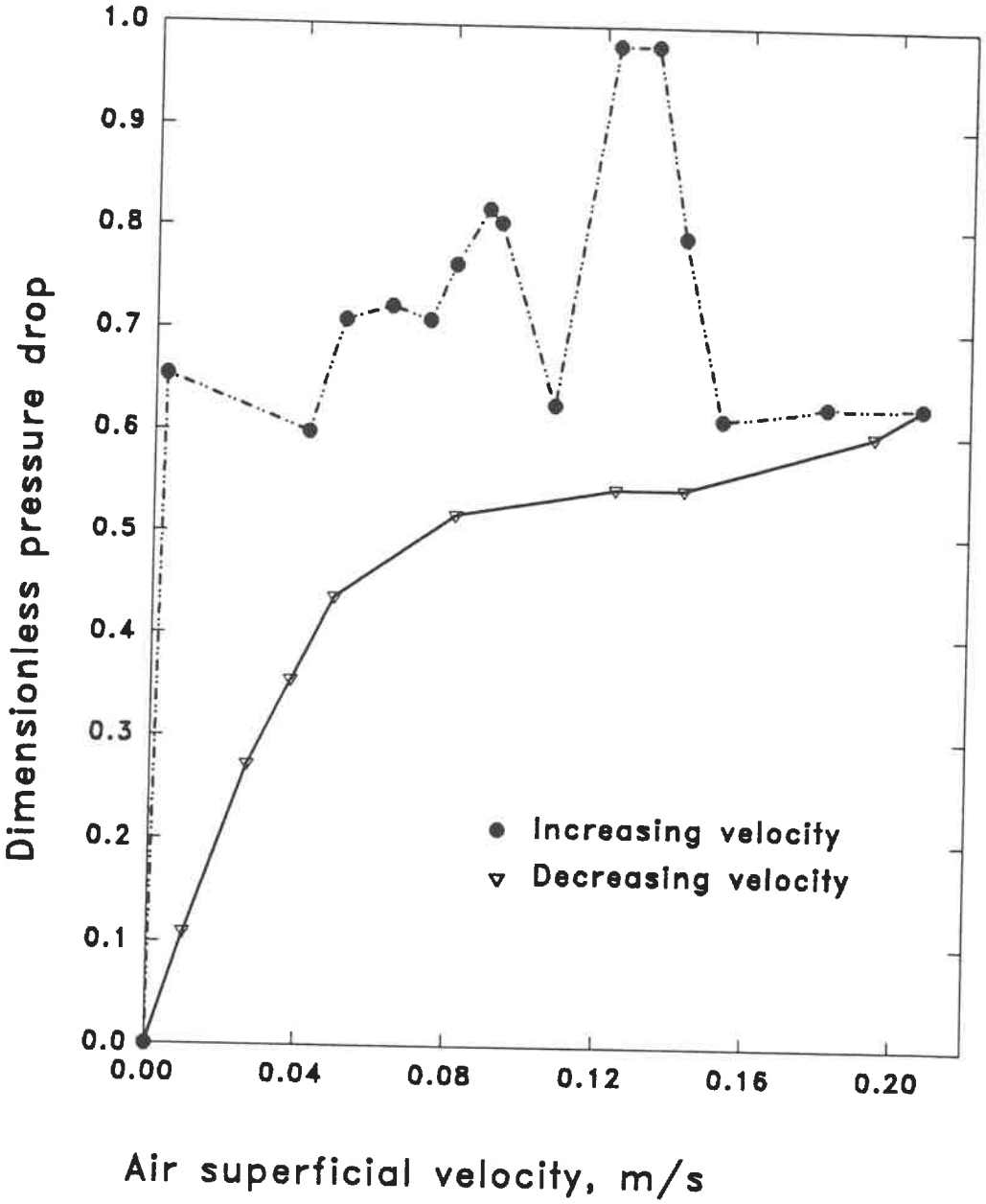

Figure 3.2 Fluidization of 9.13% Ni cryogel

C) Fluidization of 14% Ni cryogel

Case 1: Normal (unaided) fluidization

The fluidizability of this cryogel was different than that of the previous sample. Here, there was no observable bed expansion. Though only 48% of the bed was fluidized, the U_{mf} value both while increasing and decreasing gas flow were clearly identified as 0.23 m/s and 0.26 m/s respectively. It is clear that the fixed bed region is even longer than in the other cases (refer Appendix III). Stagnant zones of unfluidized particles and agglomerates were the cause of the partial fluidization. The fluidizing air was observed to pass through channels in these zones while fluidizing the rest of the bed above.

In this case, the observations of the bed rearrangement during the fluidizability test is explained as follows:

0.05 m/s : Channelling both at the centre and at the bed periphery.

0.09 m/s : Bed-cracking and the resultant channelling. Particle entrainment from channels.

0.19 m/s : Bed loosening to yield fluidization of small clusters. The stagnant parts act as a gas distributor.

>0.23 m/s: Partial fluidization of the bed consisting of agglomerates and stagnant zones.

Size measurements of the agglomerates in the dense bed and the entrained clusters

were measured from video images and the corresponding real values of dimensions were found out using the column diameter as the reference. They are listed as follows:

Agglomerate in dense bed:

Maximum diameter = 4.8 mm

Minimum diameter = 1 mm

Clusters (20 cm above the distributor):

Length = 1.4 mm

Diameter = 0.36 mm

Case 2: Manually-aided fluidization

An attempt was made to study the influence of manual vibration of the column on the fluidizability of this particular cryogel. This was done by manually tapping the bed region of the column. It was interesting to note that the whole structure of the bed changed dramatically. The agglomerate size was reduced to 1 mm and nearly 90% of the bed was fluidized with a thin layer of stagnant mass (Figure 3.3). Also, exceptionally the agglomerate bed was mono-sized. In this case, the U_{mf} was reduced to one-fourth. Note that in figure 3.3, the plot of the dimensionless pressure drop while reducing the velocity of air is a curve at the transition of the bed from the fluidized state to the fixed state and hence U_{mf} is not well-defined. In the light of recent studies by Ham (1994), the curvature is explained by the bed compaction

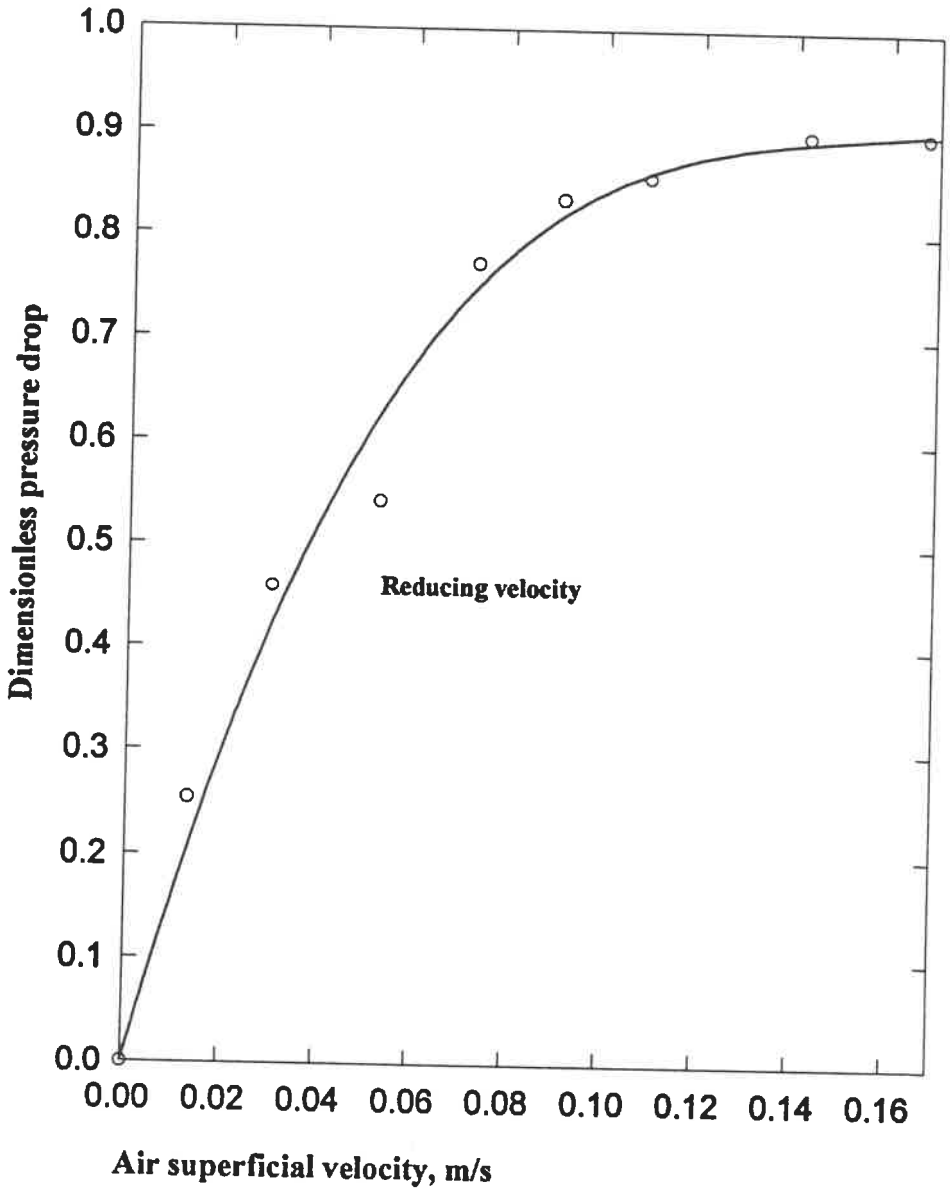

Figure 3.3 AIDED-FLUIDIZATION OF 14% Ni CRYOGEL

(Manual vibration of column)

caused by the applied vibration. For all practical purposes, the value of U_{mf} is taken to be 0.065 m/s.

D) Fluidization of 20% Ni cryogel

Similar to the 14% Ni cryogel sample, the degree of fluidization of cryogel 20% Ni was limited due to the existence of stagnant bed portions and particle agglomeration (Appendix III). A summary of the bed characteristics of all four samples in the fluidized condition is presented here:

Table 3.1 Fluidized bed characteristics of cryogel samples

% Ni / Bed characteristics	0	9.13	14	20
Fraction fluidized	0.66	0.55	0.48	0.5
Agglomerate size(mm)* Minimum	0.56	0.69	1.0	0.86
Agglomerate size(mm)* Maximum	3.38	2.88	4.8	1.85
U_{mf} (m/s)# Increasing velocity	0.17	0.12	0.23	-
U_{mf} (m/s)# Decreasing velocity	0.15	0.07	0.26	0.24
Cluster dimensions(mm)* Length	0.88	-	1.4	0.51
Cluster dimensions(mm)* Diameter	0.63	-	0.36	1.01

* data from video recordings; # partial fluidization

From the above studies one may conclude that the presence of nickel in the cryogel mars its fluidizability. Channelling, agglomeration and partial fluidization of the cryogel bed due to stagnant zones were the causes of the poor fluidization.

3.3 Choice of nickel composition in the catalyst

Putting both the activity and fluidizability studies into perspective, the presence of nickel increases the activity of the catalyst (conclusions of section 2.3) whereas it diminishes the fluidizability (conclusions of section 3.2). The cryogel having 14% Ni composition was chosen based on the activity tests. Due to the equally poor fluidization of both the catalysts containing 14% and 20% Ni respectively, the final nickel composition suitable for the hydrogenation process is 14%. This catalyst alone was used for further studies, namely, experiments to improve the fluidizability and hydrogenation in the fluidized bed reactor.

3.4 Improvement of the fluidizability of cryogels

The poor fluidization of the nickel-supported on-alumina cryogels as seen in the previous section is due to the prevalent interparticle forces. This section explains the efforts put forth in order to develop a simple technique to minimize particle-particle interaction and produce an improved fluidizability of the cryogels. Before dealing with the actual methods of improvement of the fluidizability of cryogels, an overview of the relevant techniques tested by some researchers with Group-C particles has been made in the following sub-section.

3.4.1 Methods used to improve the fluidizability of Group-C particles

The general principle in all these methods available in the literature is to introduce an external source of energy capable of overcoming the particle-particle forces.

A list of the techniques used in the recent past is given below:

1. Mechanical vibration or Vibro-fluidization (Mori *et al*, 1990; Eccles *et al* (1989)).
2. Stirring at the bottom of the bed (Kozulin & Kulyamin, 1965)
3. Utilization of an acoustic source at the bottom of the bed (Morse, 1955) and at the top of the disengagement zone (Chirone *et al*, 1993).
4. Reduction of interparticle forces (Lauga *et al*, 1991).
5. Pulsating gas supply (Alfredson *et al*, 1970).

Morse (1955) had developed the technique of aiding the fluidization of fine powders by acoustic fields using loudspeakers located at the bottom of the bed. Low frequencies ranging from 50-500 Hz with high intensity ($>$ 110 dB) could cause fine particles to fluidize easily under otherwise non-fluent conditions.

Massimilla *et al* (1972) had tried to improve the fluidizability of cohesive powders using pulsation of gas feed.

Brekken *et al* (1970) explain the anti-agglomeration of a highly agglomerative flour, 10 to 39 μm diameter, by the addition of 1% of a precipitated hydrated silica. Also, the use of a mechanical stirrer at the bed bottom was advocated to break down the channels spontaneously.

Alfredson *et al* (1970) have emphasized the destruction of channels in a bed of fine particles by pulsating the fluidizing gas supply.

Chaouki *et al* (1985) clearly describe the smooth fluidizability of aerogel powder beds by self-agglomeration above a minimum superficial velocity of 0.04 m/s at ambiant and high temperatures. An hydrodynamic model which describes the system as clusters of the elementary grains originally present in the bed. As a result, the bed behaviour shifted from the typical Group-C behaviour to that of particulate

fluidization.

Eccles *et al* (1989) introduce the phenomenon of resonance in an aerated vibrated bed of fine particles (particle size $< 200\mu m$) both in cylindrical as well as rectangular beds. The model is based on the agreement that the aerated vibrated bed is a single-mass system. Particles ranging from Group-C to Group-D were tested, while only in the case of the $6\mu m$ and $100\mu m$ alumina, resonance was observed.

Lauga *et al* (1991) studied the factors which influence the interparticle forces and in turn the fluidizability of a Ni/SiO_2 aerogel. The conclusions pointed out that increase in the initial bed porosity, nickel composition, fluidizing gas humidity and aerogel mixtures with alumina particles reduced the interparticle forces whereas reduction of the nickel oxide to metallic Ni as necessitated by the hydrogenation process reduces the fluidizability.

Reports on cryogel fluidization by Perras (1992) have established the formation of channels at lower velocities and also the existence of dead zones. In this respect, the performance of the cryogel prepared from inorganic precursors was better than that of the 'organic cryogel', but is nevertheless inferior to that of an aerogel in terms of U_{mf} and bed expansion. The same study also showed that a 50% mixture by volume of the 'inorganic cryogel' mixed with alumina particles improved the fluidization of

the cryogel, though at a higher value of U_{mf}. The bed expansion was said to be unaffected in this case.

Chirone *et al* (1993) have experimented with the bubble-free fluidization of a cohesive powder in an acoustic field. A catalyst bed (1-45 μm) was fluidized homogeneously by a gas with the aid of a loud-speaker generating sound waves. The freeboard acted as the wave-guide. Varying the sound pressure level (SPL) could break the initially present large clusters into easily fluidizable sub-clusters alone and not to individual particles. The effectiveness of the technique is explained by the overcoming of the van der Waals' forces.

Some have also worked on the acoustic excitation of flow. Acoustic energy was found to decrease the U_{mf} value and increase heat transfer rates at particular frequency levels. At low frequency, the quality of fluidization was considerably improved. Elutriation of fines was said to be controlled and acoustic resonance helped in high mixing even at very low gas flow rates.

Recent simulations at the chemical engineering department by Bloise (1995) throw light on the possibility of destroying agglomerates by providing sufficient energy of mechanical agitation (vertical direction) to a trapezoidal bed of particles. The behaviour of Group C particles was reproduced by the molecular dynamics method.

The kinetics of the particle size distribution was related to Smoluchowski's model of fast coagulation.

3.4.2 Effect of UltraSonic sound on a cryogel bed

The influence of an ultrasonic sound field produced at the distributor surface of a 5 cm diameter column containing a Ni/Al_2O_3 cryogel sample was studied. The ultrasonic source was a Sonic Dismembrator 2000 (Artek Systems) generating an UHF (20 kHz) signal causing a microtip (1 cm in diameter) protruding just above a distributor of lead shots (412 μm) to produce ultrasonic waves. Amplitudes over the entire allowable range (0-300 W) of the dismembrator at various gas velocities had no observable effect on the fluidization or the agglomerate size of the catalyst. The observations were made at each gas velocity (0-20 cm/s) for a period of about 30 minutes.

It was concluded that the intensity of the produced ultrasonic energy was insufficient to overcome the cohesive forces.

3.4.3 Choice of a suitable technique

The inference of the previous section demands the involvement of a stronger applied force to counteract the interparticle forces. However, acoustic methods involving the use of loud-speakers cannot be adopted since the final application of the technique

would be in a hydrogenation reactor. Also, techniques like bed-stirring and mechanical vibration introduce the role of an external force in the hydrodynamics of the powder bed. Such methods are highly disadvantageous since they may not be feasible for large scale fluidized beds. *The objective of choosing a technique was to achieve total bed fluidization, i.e., to fluidize both the largest agglomerate situated at the bed bottom (Photo 3.1) as well as the smallest cluster found at the bed surface (Photo 3.1), at the same gas flow rate. In this case, the velocity at the bottom has to be higher than the velocity at the top. This implies that the flow area has to increase along the bed height, calling for a Conical Fluidized Bed with expanding cross-section.* This choice would also allow intense particle circulation (Toyohara & Kawamura, 1993; Bloise, 1995) and might aid in destroying the stagnant zones near the distributor. The literature was consulted to study the hydrodynamics of conical fluidized beds.

3.4.4 Advantages and disadvantages of a conical fluidizer

The general advantages of a conical fluidizer found in the literature are listed here:

1. Shi Yan-Fu *et al* (1984) has treated the advantages of a conical fluid bed operation over that of cylindrical beds:

a) Fluidization of cylindrical beds having large particle size distributions may result in fine particles being entrained and large particles remaining defluidized at the distributor. In the case of tapered beds this situation is avoided since the cross-

Photo 3.1 PARTIALLY FLUIDIZED AGGLOMERATE BED

(14% Ni/Al_2O_3 cryogel)

sectional area of the bed increases with the bed height. Tapered fluidized beds are therefore ideal for fluidization processes such as coal combustion, crystallization, microbial growth, etc.,. where the particle size varies.

b) In deep gas-solid cylindrical beds, the pressure drop across the bed is large and this accelerates the up-flowing gas. Such a gas leaving the bed surface is said to agitate it violently and cause instability in the bed and in addition increases elutriation (Sutherland, 1961).

c) Tapered fluidized beds can be operated in the case where the fluid velocity at the bottom of the bed is greater than the particle terminal velocity (Golubkovich *et al*, 1970).

2. In the atomic energy industry, the gas expansion problem mentioned above in 1(a) is reported to have been dealt with by using a tapered fluidized bed (expanding flow area) designed so as to maintain the gas velocity constant (Sutherland, 1961).

3. Certain tapered beds have the advantage of a better particle circulation and are also useful when using multi-component particle mixtures (Toyohara & Kawamura, 1993).

4. Tapered lift reaction vessels (ascending solid stream) are employed in large-scale catalytic cracking and coal gasification processes. Process intensification and parameter distribution in such vessels are achieved by the choice of the taper angle (Zhorov *et al*, 1986).

5. Kwauk (1992) presents the following advantages of conical fluidizers:

a) Satisfactory fluidization of the coarse particles at the bottom of a bed of polydisperse solids can be achieved while simultaneously having lower velocities at the top end.

b) Due to the high inlet gas velocity, the hyperfluidized coarse particles below act as a distributor of the gas before it reaches the upper zone of fines.

c) Bed segregation leads to the confinement of larger particles at the bottom. As mentioned earlier, for highly exothermic reactions, the lower specific surface area of the coarse particles and the high gas velocity near the distributor enhances rapidity of heat release.

d) Incineration of waste materials is performed well in conical vessels.

e) Conical fluidized beds have been used in drying of cement due to their 'balling action' which is not produced in rotary kilns.

Some of the disadvantages of the use of a conical fluidizer are mentioned below:

1. In the case of a bed of mono-sized particles, fluidization in a tapered bed resulted in two distinct zones of fluidization; a highly fluidized core surrounded by a peripheral region with increased solid circulation (Toyohara & Kawamura, 1993).

2. The design of a conical fluidizer is specific only to the given design criteri(on)a such as bed height or constant gas velocity.

3. Care should be taken in order to ensure that the design of a conical fluidizer does

not lead to spouting effects. The disadvantages of having such a situation are low bed-to-wall or bed-to-surface heat transfer rates, limited gas throughput and non-viability for scaling-up (Hetsroni, 1982). In the case of catalytic reactions, the conversions would be very low due to poor gas-solid contact.

4. Due to axial variations in the cross-section, the hydrodynamic or reaction modelling in tapered beds is supposedly complicated.

Based on the above comparitive study, the following conclusions were drawn to employ a conical fluidized bed reactor for the hydrogenation of toluene on Ni/Al_2O_3 cryogels:

1. Elutriation of fines, a major industrial problem, especially in the case of fine and light cryogels could be considerably reduced by the axial reduction in the gas velocity due to the expanding flow area in the conical bed.

2. High solids-mixing characteristics of conical beds would enable temperature homogeneity of the catalyst bed.

3. At certain design values of the cone angle and the height of the fluidized bed, gas velocities high enough to destroy the agglomerate structure was expected to be attainable at the bed bottom while still avoiding high solids entrainment on top.

4. The presence of dead zones which is inevitable in columnar fluidized beds was also expected to be avoided in the conical fluidizer.

5. The formation of channels and the stagnant regions in a cylindrical bed would lead

to ineffective heat transfer and poor gas-solid contact. In the case of a conical fluidizer this limitation could possibly be eliminated as stated by Singh *et al* (1992).

3.5 Conical fluidized bed

3.5.1 Design of the conical bed

The principal objective of the design is to have a homogeneously fluidized cryogel bed without stagnant zones. Other aims are to reduce particle entrainment, discovering the possibility of destroying the agglomerate structures at high gas velocities and thereby reduce agglomeration.

The design parameters involved in the design of a conical fluidizer are given hereunder:

1. The inlet diameter of the bed
2. The diameter at the top of the fixed bed
3. The diameter at the outlet of the fluidizer
4. Cone angle
5. Height of the fixed bed
6. Height of the fluidizer

Some of these parameters are coupled. For instance, given the cone angle and the

bed height, the inlet diameter and the diameter at the bed surface can be trigonometrically found out and vice versa. The following are the assumptions posited to evaluate the design parameters:

1. The inlet diameter of the bed is 50 mm. This assumption was made in order to minimize the total quantity of catalyst to be prepared knowing that a conical bed has a greater capacity than that of a cylindrical bed of the same height.

2. The fixed bed height should be at least twice the inlet diameter in a fluidized bed in order to avoid a shallow bed design. The initial bed height was therefore taken as 100 mm.

The only design criteria in this case (uniformly fluidized bed with no stagnant zones) is derived as follows:

In section 3.2, for the 14% Ni catalyst, the U_{mf} values under normal conditions as well as manually-aided conditions was experimentally found to be 0.26 m/s and 0.07 m/s respectively. An ordered segregation of agglomerates (size range of 1-5 mm) were observed during fluidization in the former case (Photo 3.1). The fluidization of the surface of the catalyst bed occurred at ease and at a low U_{mf} of 0.065 m/s. This may be termed as 'free fluidization', where interparticle forces are small compared to those of the larger agglomerates at the bottom. Considering the identical size of these clusters with those found in the latter case (manually-aided fluidization), this U_{mf} value is accorded to the minimum-sized clusters at the surface of the bed. Now, the

fluidization of the largest agglomerate found at the bottom of the bed (Photo 3.1) where interparticle forces are maximum is termed to be 'restrained fluidization' occuring at 0.259 m/s.

In order that these two velocities 0.07 m/s and 0.26 m/s at the top and bottom of the bed respectively, appear at the same gas volumetric flow rate, the ratio of the flow areas is given by:

$$\frac{A_H}{A_0} = \frac{0.259}{0.065}$$

From this, the diameter at the bed surface is calculated as 100 mm. The cone angle is:

$$\Theta = \tan^{-1}\left(\frac{D_H - D_0}{2H}\right)$$

A value of 28 degrees was found out to be the cone angle. The criteria for the determination of the height of the fluidizer had been the axial velocity profile. In figure 3.4, the height of the fluidization column corresponding to 10% of the entrance velocity is found to be 212 mm.

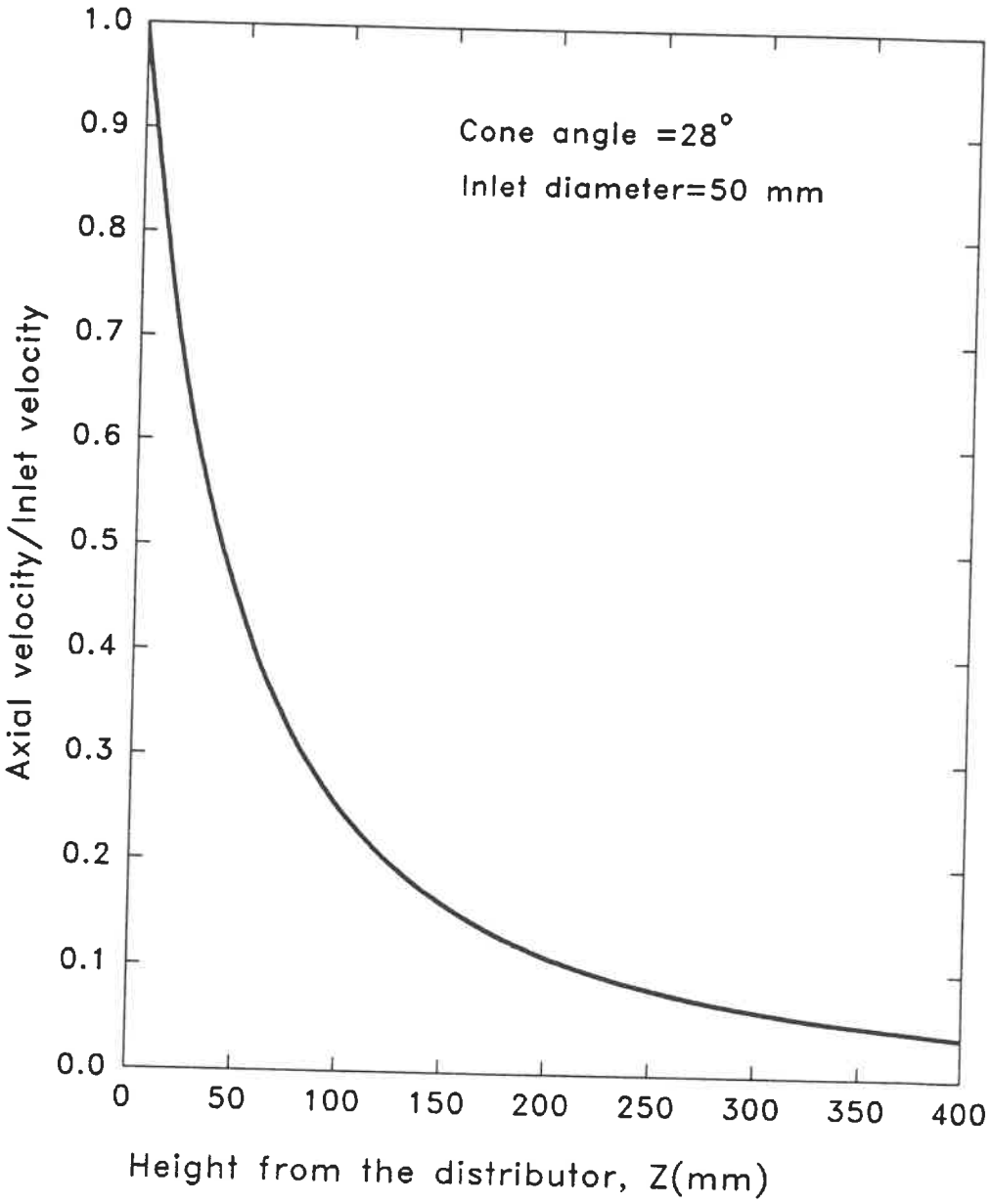

Figure 3.4 Axial velocity profile in the conical bed

Care should be taken in such designs to avoid spouting. The design parameters were tested for the maximum spoutable bed height and inlet diameter (Mathur & Epstein, 1974) which generally decide bed spoutability for a given particle size distribution. The correlations best suitable for the case of cryogels were chosen for this verification since others were not applicable to powders of very low densities.

The maximum spoutable height for fine particles was calculated using the Lefroy & Davidson correlation taking the inlet diameter too into account (Mathur & Epstein, 1974):

$$H_m = \frac{0.168 d_p^{1/3} D_H^{8/3}}{D_0^2}$$

The following table compares the current design values with the critical values required for spouting.

Table 3.2 Comparison of conical bed characteristics

Parameters	Design values	Critical values required for spouting
D_0/D_H	0.5	< 0.1 (Becker)
Cone angle, Θ (degrees)	28	40
D_0/d_p	50-10	< 30 (Ghosh)
Bed height, H (mm)	100	< 20 (Lefroy & Davidson)
Particle size distribution	1-5 mm	Mono-size

The maximum spoutable height H_m is said to decrease with increasing orifice diameter until a critical value beyond which spouting is impossible (Mathur & Epstein, 1974). This critical value is 0.1 for finer particles having diameter less than 1 mm.

Spouting becomes unstable in the case of beds with cone angles smaller than 40° both for conical as well as conico-cylindrical beds. In the case of cryogels the size distribution of the agglomerate bed is fairly wide. This is not in favour of spoutability. Even the addition of small portions of fines to a mono-sized spouted bed is reported to be detrimental to its stability (Mathur & Epstein, 1974).

3.5.2 Conical fluidizer and cyclone separator

Besides the conical bed region and the cylindrical, the fluidizer (figure 3.5) consisted of the following:

(a) A glass cylinder (ID=212 mm; height=400 mm) forming the freeboard to ensure sufficient reduction in particle entrainment.

(b) Porous plate gas distributor

For the purpose of testing the hydrodynamics of the 14% Ni/Al_2O_3 cryogel in the conical fluidizer, the distributor employed was a classical porous plate distributor with a conical gas entry (as sketched in figure 3.6), 5 cm in diameter with the cone below packed with glass spheres (3 mm diameter). A sufficient distributor to bed pressure drop ratio ($\Delta P_d / \Delta P_b$) is required for efficient gas distribution. For gas

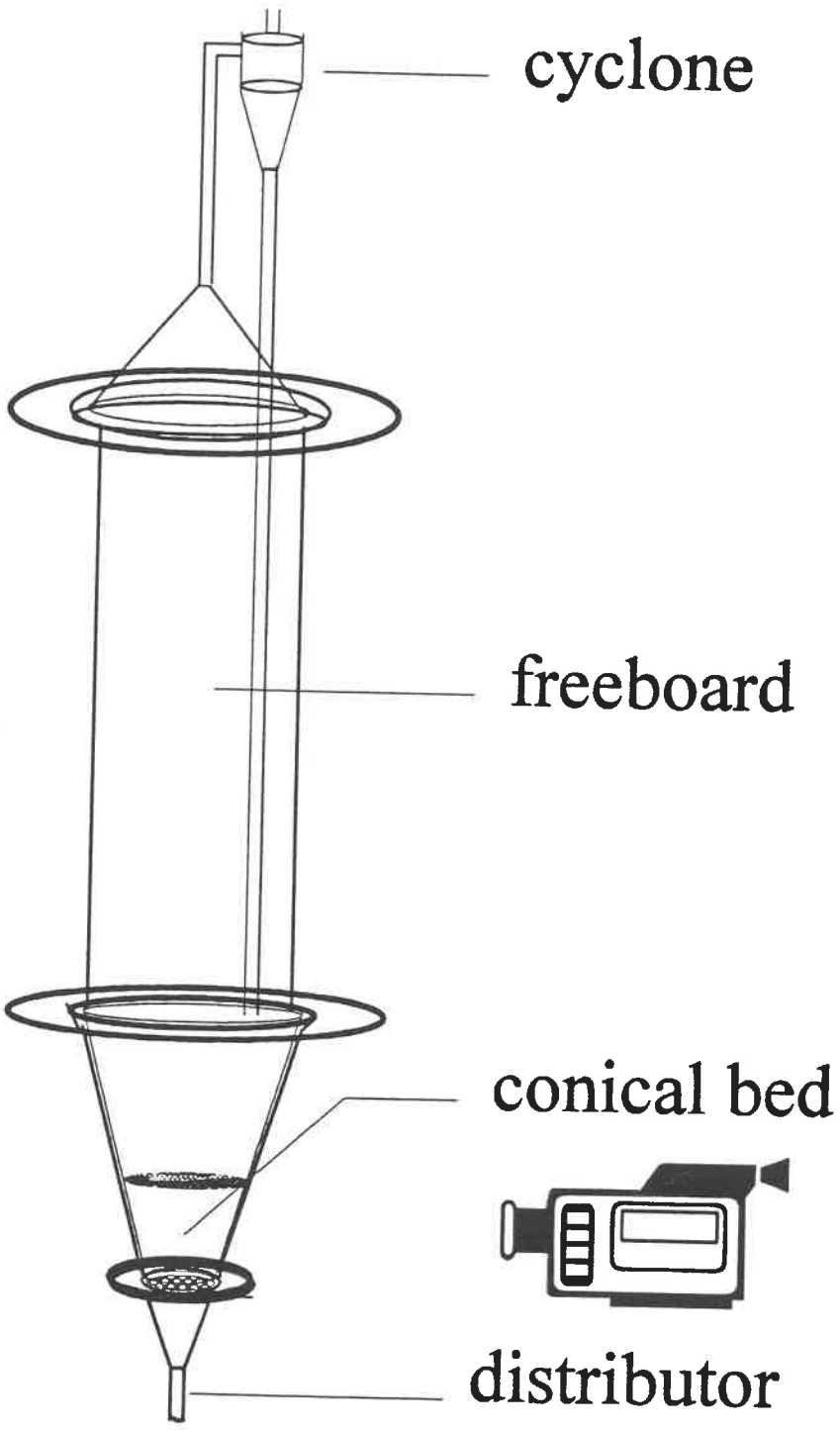

Fig. 3.5 Conical fluidizer

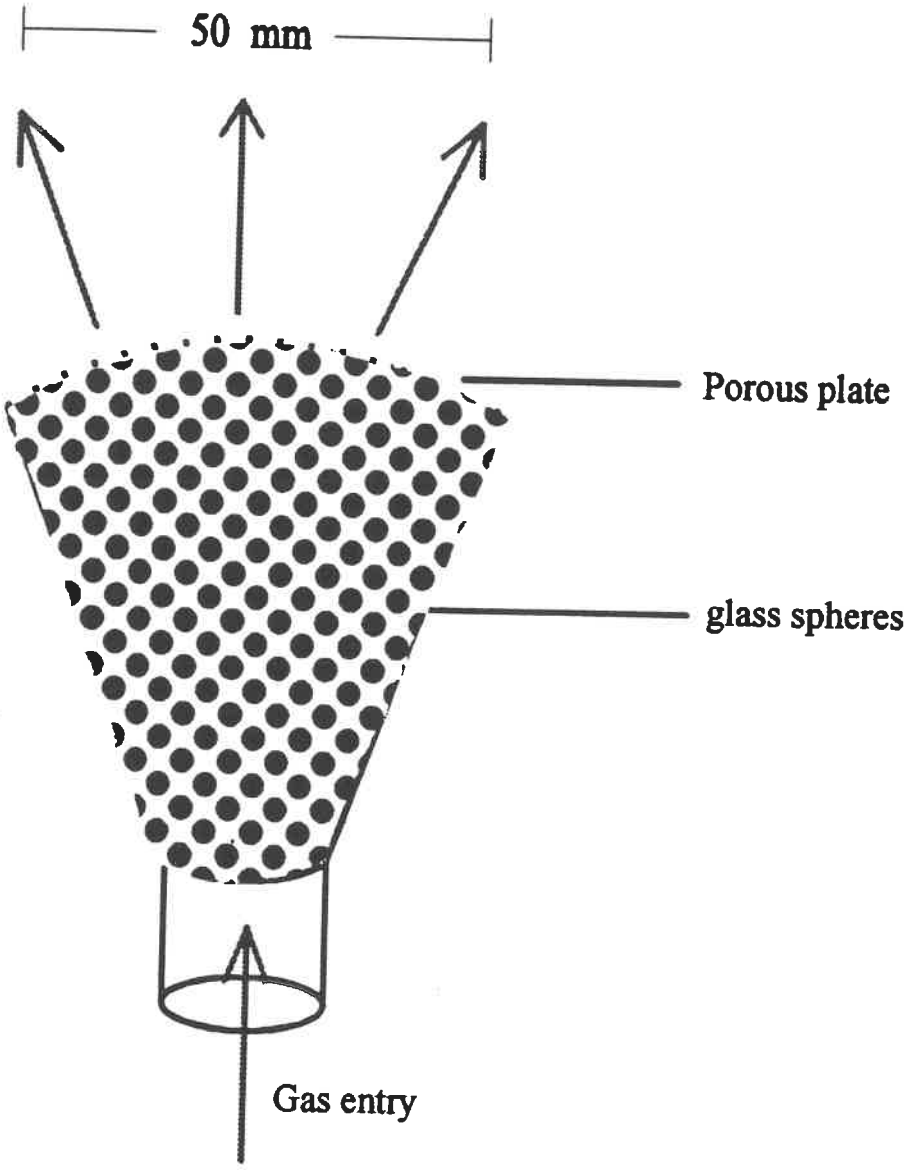

Figure 3.6 Classical distributor

distributors with porous plates, a minimum ratio of 0.3 is suggested in the literature (Sathiyamoorthy & Rao, 1981; Hiby, 1964). This condition was met by the above design for the given bed mass. The porous plate distributor also avoids spout formation.

(c) Cyclone separator

A cyclone was used to collect entrained fines, the recovered solids being conveyed back to the fluidized bed.

3.6 Hydrodynamic studies of 14% Ni/Al_2O_3 cryogel in the conical fluidizer

This particular section deals with the hydrodynamic influence of the geometry of the column on the fluidization of a cohesive powder. The fluidizing apparatus used was exactly the same as that seen in figure 3.1, the cylindrical fluidizer replaced by the conical one.

3.6.1 Experimental results

25 grams of the catalyst containing 14% nickel was required to be carefully fed into the column to reach an initial bed height of 10 cm, the design height of the bed.

Figure 3.7 shows the pressure drop characteristics of the conical bed while reducing the inlet air velocity (U_0). The models representing the different states of fluidization (A, B & C) of the cryogel bed indicated in this figure are shown in the subsequent figure 3.8.

The following is the description of these fluidization states:

(A) U_0=44 cm/s: Perfectly mixed fluidization

At the initial velocity of 44 cm/s, the bed attained a state of intense solids mixing. There was no observable agglomeration in the homogeneous fluidized bed. Ultra fine particles of sub-micron size were heavily entrained by the gas. A slight bed

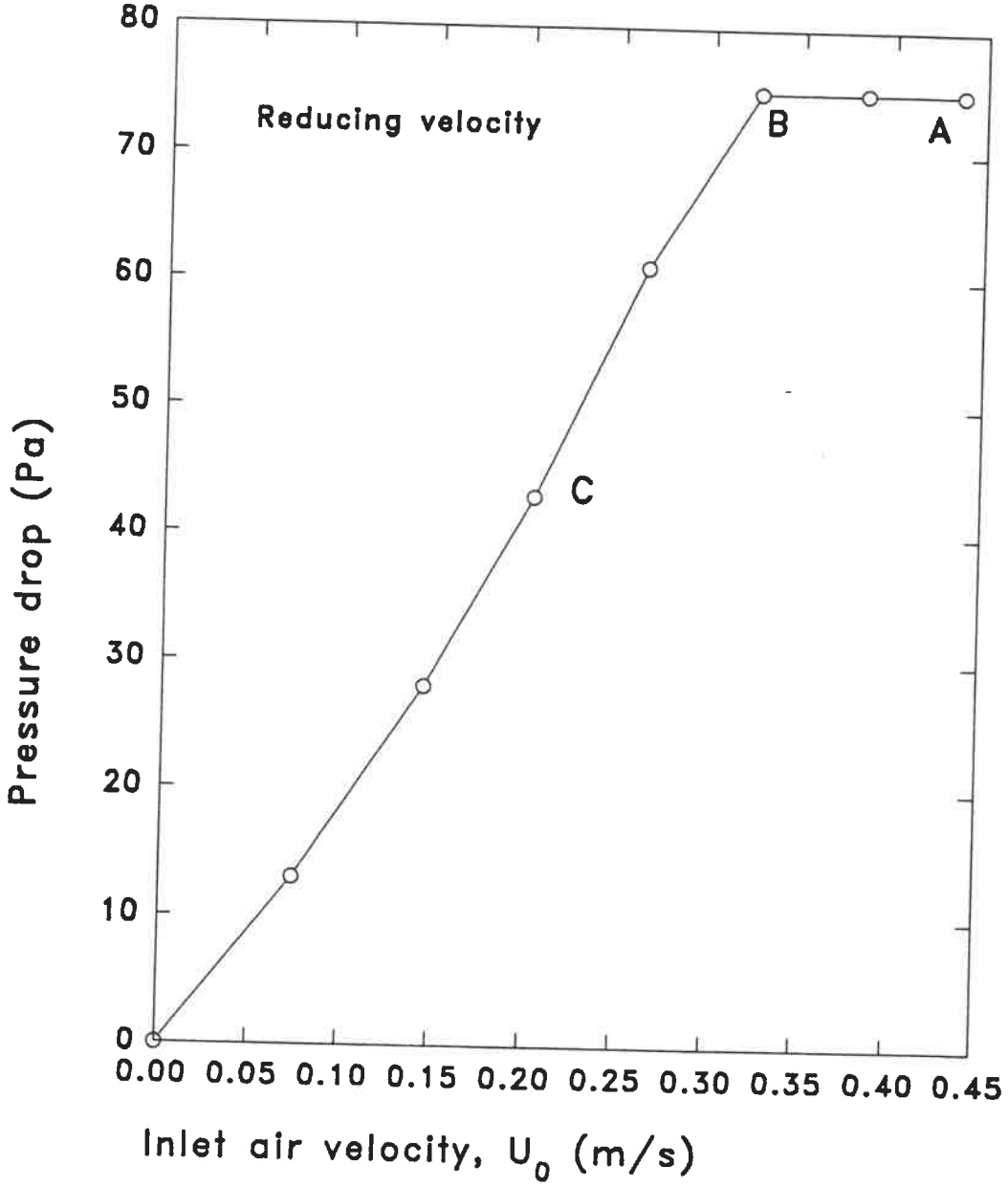

Figure 3.7 Pressure drop
Vs
Inlet air velocity

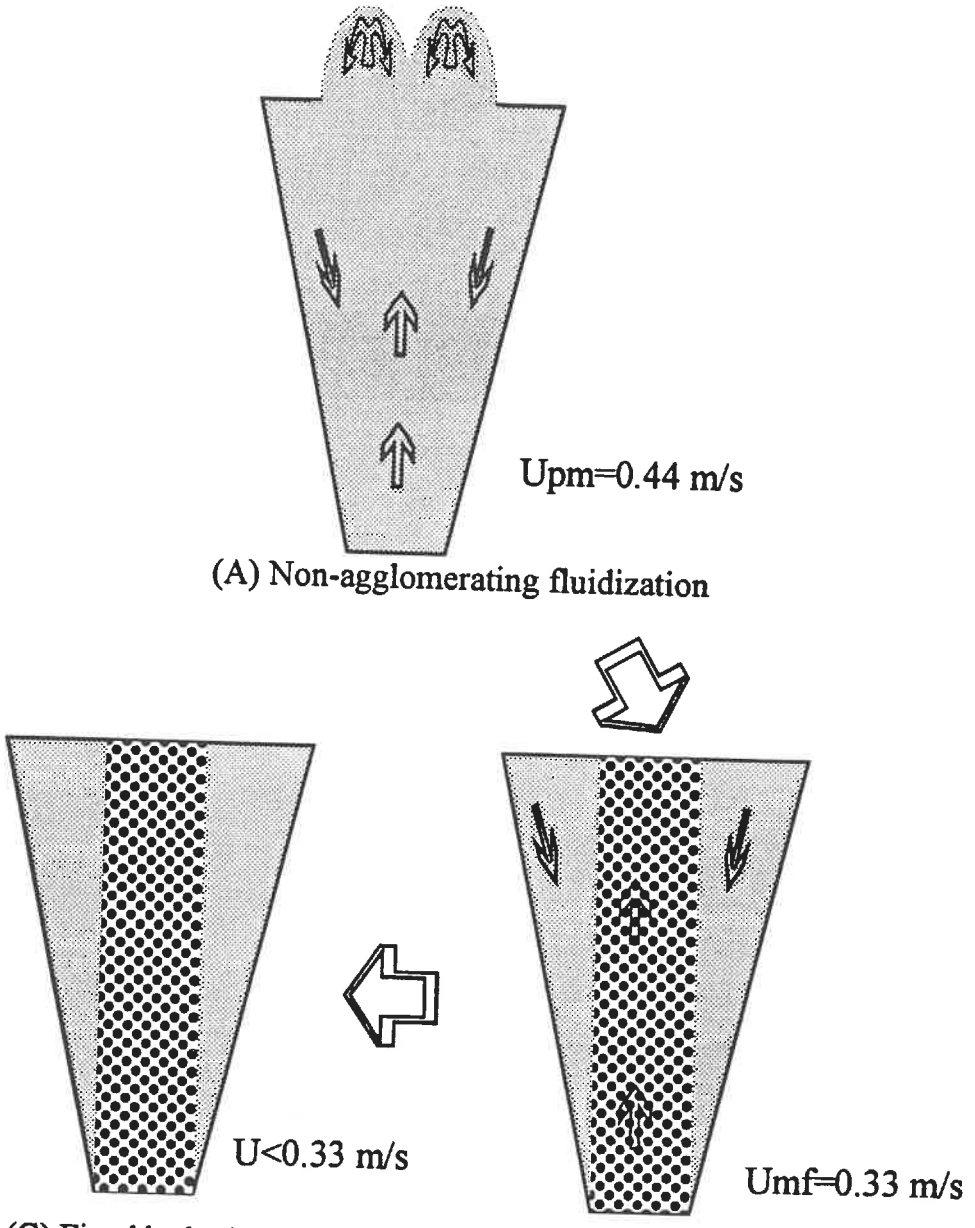

Figure 3.8 Fluidization states of 14% Ni cryogel in the conical fluidizer

expansion was also observed (Figure 3.9). Surrounding the agglomerate core was the annulus which comprised of clusters which constituted the initial fixed bed. The annular solids near the wall underwent a downward motion. This downflow of solids near the wall is characteristic of conical or tapered fluidized beds (Toyohara & Kawamura, 1993).

(B) $33 \leq U_0 \leq 44$ cm/s: Core-annulus type segregative fluidization

Perfectly-mixed fluidization ceased to exist below 44 cm/s giving place to agglomeration of a fraction of the bed. Visual observations show the spontaneous formation of a fluidized agglomerate core. The diameter of the agglomerates was roughly 2 mm. For this velocity range, the bed pressure drop remained virtually constant.

(C) $U_0 \leq 33$ cm/s: Fixed bed condition

On further reduction of the air velocity, the segregated bed entered the packed condition. The dimensions of the constituent particles were apparently the same as in case (B). The bed pressure drop decreased with decrease in the fluid velocity.

From figures 3.7 and 3.9, the experimental value of U_{0mf} is taken to be 0.33 m/s.

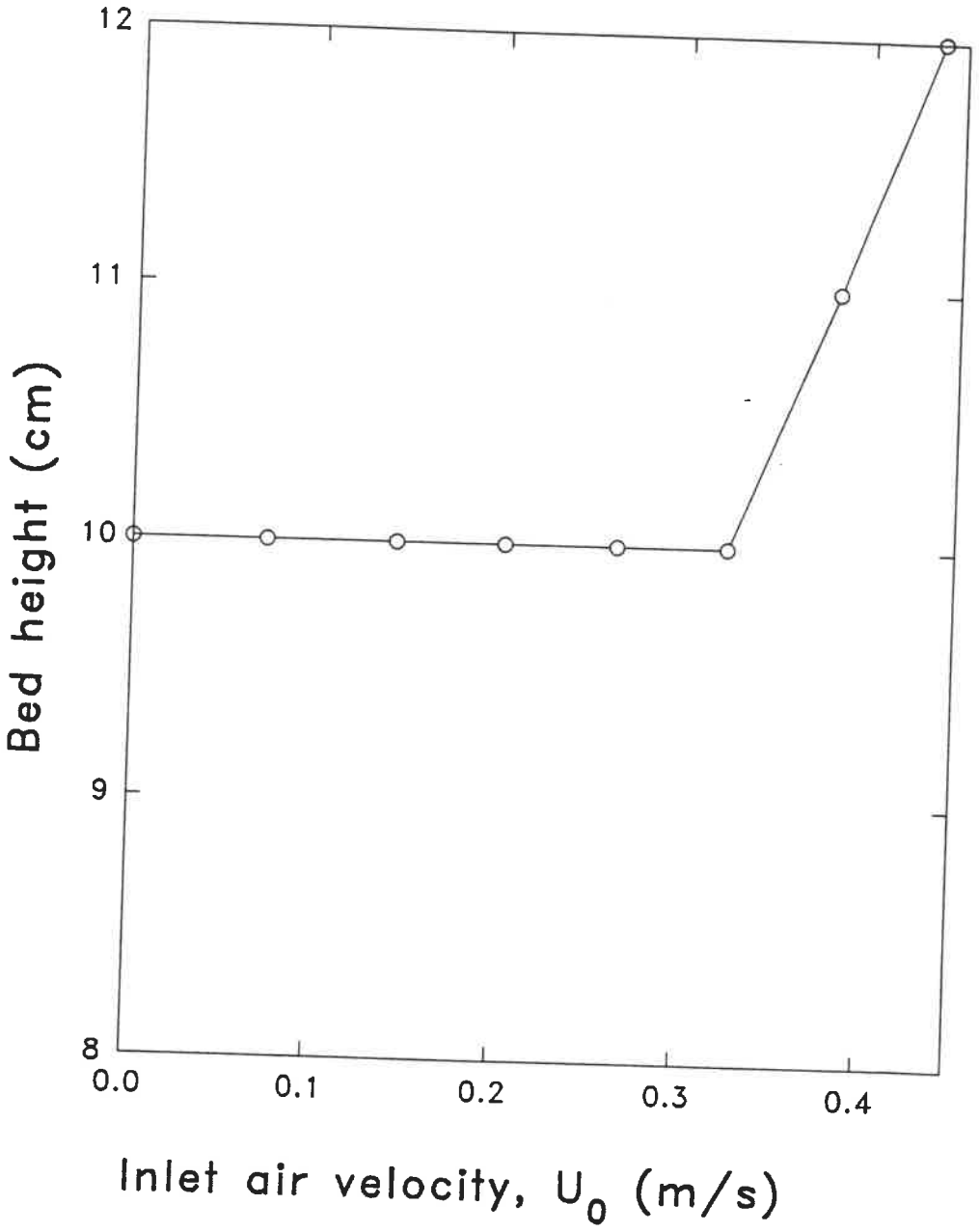

Figure 3.9 Bed expansion

3.6.2 Predictions of pressure drop and U_{0mf}

Modelling of a conical packed bed of uniform particle size

In order to derive an equation for the pressure drop characteristics with decreasing velocity in the conical fixed bed, an elemental volume of height dz at a distance z from the distributor was considered. It can be readily concluded that the Ergun equation (Ergun, 1952) applies for this cylindrical volume. The Ergun equation can be written as:

$$-dP=(AU+BU^2)\,dz \qquad \ldots\ldots \quad (1)$$

where,

$$A=150\frac{(1-\epsilon)^2}{\epsilon^3}\frac{\mu_f}{d_s^2} \qquad \ldots\ldots\ldots \quad (2)$$

and

$$B=1.75\frac{(1-\epsilon)}{\epsilon^3}\frac{\rho_f}{d_s} \qquad \ldots\ldots\ldots \quad (3)$$

The overall pressure drop across the entire bed height H is obtained by integrating the above equation. Hence, the general form of the modified Ergun equation for the conical packed beds is obtained as follows:

$$\frac{(-\Delta P)}{H} = \frac{AD_0}{D_0+2H\alpha} U_0 + \frac{BD_0}{3} \frac{(4H^2\alpha^2+3D_0^2+6D_0H\alpha)}{(D_0+2H\alpha)^3} U_0^2 \quad . \quad . \quad (4)$$

When $\alpha=0$, the equation reduces to the cylindrical bed characteristics. The derivation of this equation is detailed in Appendix IV.

The modified Ergun equation is applicable at the velocity of minimum fluidization as well. But due to the axial variation of the flow area, the force exerted by the fluid in the solid particles is not directly proportional to the pressure drop (Shi *et al*, 1984). This force in the differential bed height introduced above is

$$dF = \frac{\pi}{4} D^2 (AU+BU^2)\, dz \quad . \quad . \quad . \quad . \quad . \quad . \quad . \quad (5)$$

The overall force exerted by the fluid is obtained by integrating this equation for the entire bed height (Appendix 5). The following expression is obtained.

$$F = \frac{\pi}{4} D_0^2 H [AU_0 + B(\frac{2\alpha D_0}{D_0+2H\alpha}) U_0^2] \quad . \quad . \quad . \quad . \quad . \quad . \quad (6)$$

On the other hand, the effective weight of the powder bed in the elemental volume is

$$dF_s = g(1-\epsilon)(\rho_s-\rho_f)\frac{\pi}{4}D^2 dz \quad \ldots\ldots \quad (7)$$

and for the entire bed,

$$F_s = \frac{\pi}{4}(1-\epsilon)(\rho_s-\rho_f)gH\left[\frac{4H^2\alpha^2+3D_0^2+6D_0H\alpha}{3}\right] \quad \ldots \quad (8)$$

At U_{mf}, $F=F_s$, whence the following equation

$$B'U_{0_{mf}}{}^2+A'U_{0_{mf}}-C'=0 \quad \ldots\ldots\ldots \quad (9)$$

where

$$B' = BH\left(\frac{2\alpha D_0^3}{D_0+2H\alpha}\right) \quad \ldots\ldots\ldots \quad (10)$$

$$A' = AHD_0^2 \quad \ldots\ldots\ldots \quad (11)$$

$$C' = (1-\epsilon)(\rho_s-\rho_f)gH\left[\frac{4H^2\alpha^2+3D_0^2+6D_0H\alpha}{3}\right] \quad \ldots \quad (12)$$

U_{0mf} is the solution of the above quadratic equation. It is interesting to note that U_{0mf} is a function of the bed height (H) unlike in the case of a cylindrical fluidized bed. Given that the cryogel fixed bed is composed of a binary particle mixture, the above correlation cannot be used directly. The Sauter mean diameter and the external

porosity of the bed have to be calculated. In order to find out the mean diameter, the size and mass fractions of both agglomerates as well as the clusters are required. A model explained by figure 3.10 has been developed to predict the pressure drop characteristics and the U_{mf} value of the mixed-sized bed.

Modelling of the conical packed bed of binary particle mixture

The segregated packed bed is considered to be composed of two distinct zones, viz., the central core (C) and the surrounding annular region (A).

Assumptions:

(i) The core consists of the agglomerates alone whereas the clusters are restricted to the annulus.

(ii) It is supposed that the bulk density of the annular zone is the same as that of the mono-sized fixed bed at the start of the experiment (55 kg/m^3).

(iii) The agglomerates as well as the clusters in their respective regions are of uniform size and have apparent densities equal to the tap bulk density of the cryogel bed (Table 2.3). This assumptions explains the compacted condition caused by the interparticular forces.

(iv) The agglomerate diameter is assumed to be 2 mm and the approximate size of the cluster to be 0.33 mm based on experimental measurements. These values are comparable with the size distributions of the agglomerates specified in Table 3.1.

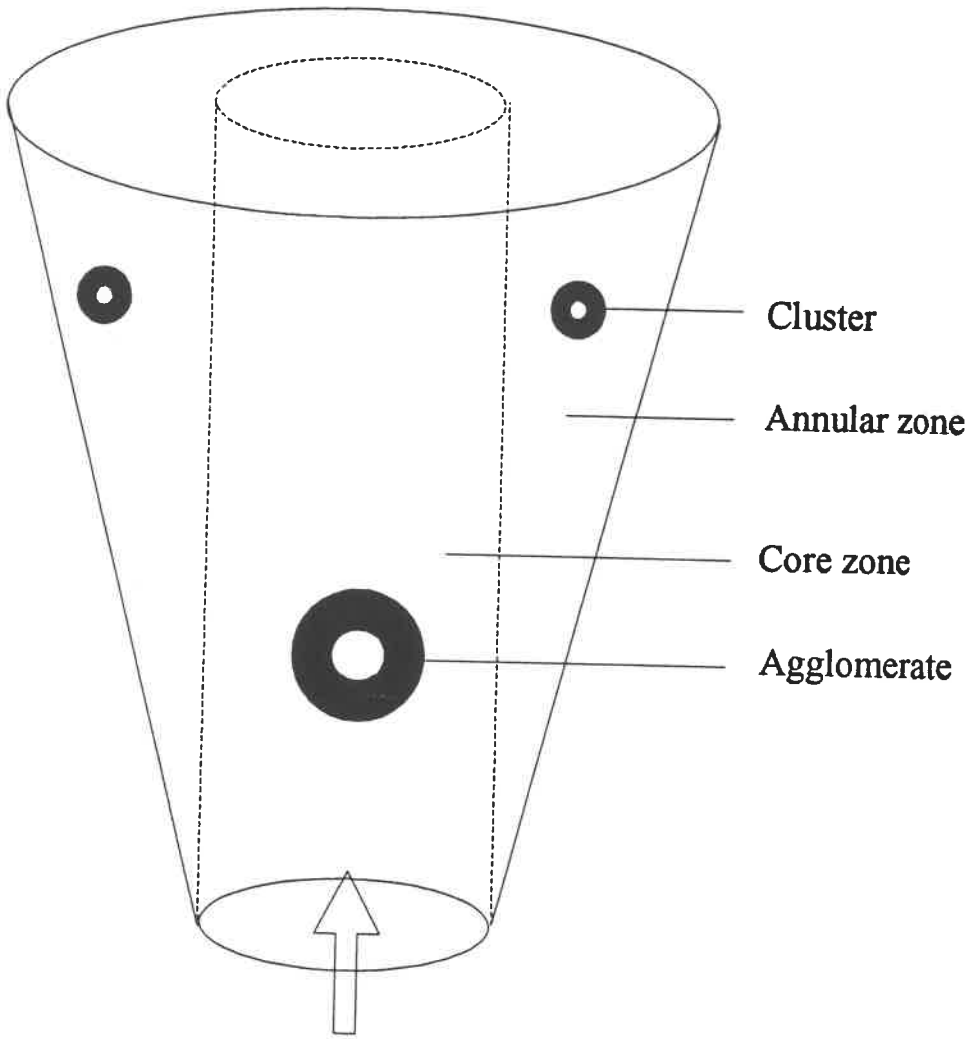

Figure 3.10 Conical fixed bed model

Preliminary calculations

The mass fractions of the agglomerates and in the core and annular zone respectively have been calculated as follows:

(i) For the purpose of utilizing the model under discussion, the bed porosity ϵ in the expressions for U_{mf} and pressure drop was replaced using the relation,

$$(1-\epsilon)\,\rho_s = (1-\epsilon_{be})\,\rho_{bt} \quad \ldots\ldots\ldots \quad (13)$$

ϵ_{be} the external bed porosity excludes the interstitial void space within the agglomerates and clusters.

ϵ_{bt} is the tapped bulk density of the 14% Ni cryogel (Table 2.3).

(ii) The mass of solids in the core (m_{sc}) can be found out by determining the external porosity of the core zone from the following balance:

$$\epsilon_{bc}\, V = \epsilon_c\, V_c + \epsilon_a\, V_a$$

(iii) The relation between ϵ_c and m_{sc} is

$$\epsilon_c = 1 - \frac{V_{sc}}{V_c} = 1 - \frac{m_{sc}/\rho_{bt}}{V_c} \quad \ldots\ldots\ldots \quad (14)$$

The value of m_{sc} is found to be 10 g. Similarly, the mass of the clusters (m_{sa}) is calculated as 13 g. That is to say, nearly 40% of the cryogel had agglomerated.

(iv) From the values of the diameters (assumption iv) and the mass fractions of solids (calculation iii) in each of the zones, the Sauter mean diameter for the entire bed is

calculated as 0.5 mm.

The results are summarized in the following table:

Table 3.3 Characterization of the segregated fixed bed

	Parameter	Value
C O R E	Diameter of the agglomerate Density of the agglomerate External porosity Solids fraction	2 mm 169 kg/m^3 0.7 0.4
A N N U L U S	Diameter of the cluster Density of the cluster External porosity=Initial porosity Solids fraction	0.33 mm 169 kg/m^3 0.67 0.6
B E D	Overall initial bed porosity External bed porosity Sauter mean diameter Total mass	0.91 0.68 0.5 mm 23 g

The ϵ_{be} and the Sauter mean diameter are used to obtain the pressure drop across the fixed bed (equation 4) as well as the developed correlation for U_{mf} (equation 9). Figure 3.11 shows a good fit of the modified Ergun equation. The minimum fluidizing velocity was also estimated with sufficient accuracy (refer to table 3.4).

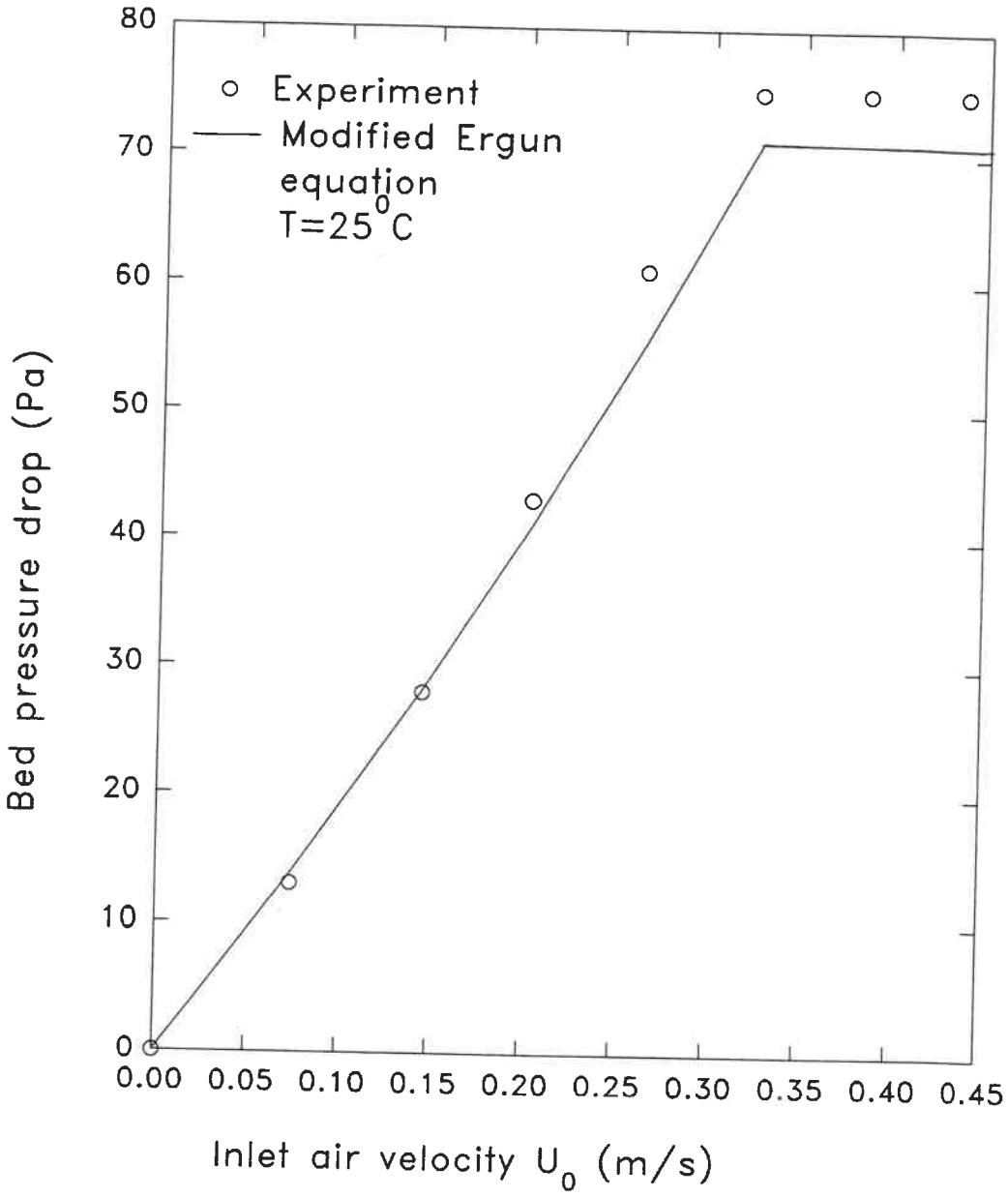

Figure 3.11 Predictions of the modified Ergun equation

Table 3.4 Prediction of U_{mf} by the conical fixed bed model

Experimental U_{0mf} (m/s)	0.33
Calculated U_{0mf} (m/s)	0.32

From the above table, it is evident that for the packed bed region, the derived equations are reliable and the U_{mf} value can be very well estimated using the appropriate correlation (equation 9) for a known Sauter mean diameter.

To compare the U_{mf} values in the cylindrical and conical fluidized beds, the following points have to kept in mind.

(a) The U_{0mf} calculated using equation 4 is a reference velocity. Due to the existence of an axial velocity profile, the U_{mf} representing the conical fluidized bed has to be the z-averaged velocity given by

$$\overline{U} = \frac{\int_0^H U dz}{\int_0^H dz} \quad \ldots\ldots\ldots \quad (15)$$

Its calculated value is 0.165 m/s.

(b) The U_{mf} of the agglomerates in the cylindrical fluidized bed is found to be 0.6. From this, according to the core-annulus model, for a given bed height the minimum fluidization velocity obtained in the conical fluidized bed is found to be lower than

that of the cylindrical bed.

Synopsis of the hydrodynamic studies in the conical column

Recollecting the main points of the hydrodynamic studies of the 14% Ni/Al_2O_3 cryogel in the conical column, it can be concluded that satisfactory fluidization of the catalyst was achieved in the apparatus. Results clearly indicate that above a critical gas inlet velocity (U_{pm}=44 cm/s) the following points are observable:

1. Homogeneous fluidization
2. Intense bed agitation
3. No bed segregation

Toyohara and Kawamura (1992) have observed similar solids mixing in a conical liquid-fluidized bed of a binary particle mixture. Also in their case, the bed was termed to have been 'perfectly mixed' above a certain gas flow rate. There was also a bed segregation below a critical velocity, the large-sized population restricting themselves to the core and the finer particles to the annulus.

The U_{0mf} was found to be 0.33 m/s. A core-annulus type segregation model has been developed to describe the conical fixed bed and the pressure drop and U_{0mf} predictions are quite satisfactory. The experimental and estimated values of U_{mf} of the agglomerates in cylindrical and conical fluidizers were compared. The value in the conical bed was slightly lower than the other.

Formation and destruction of agglomerates

Observation of the hydrodynamic behaviour of cryogels in a cylindrical and a conical column allows to state certain inferences regarding the agglomeration phenomenon. Visually, agglomeration appears to be a sudden process. However, the fine particles agglomerate neither at very low nor at very high velocities. For typical group-C powders at very low velocities, the particle-particle contact area is not highly pronounced, while at very high gas velocities, the agglomerate-agglomerate attrition causes their destruction or size reduction. This invariably leads to the conclusion that there exists a range of gas velocities where alone agglomeration is substantiated.

In a cylindrical column, it is a fact that the largest agglomerate remains always at the bottom (due to bed segregation). In an expanding conical column, if the fluid momentum at the bed bottom is large enough to cause attrition, the result would be the destruction of the agglomerates. Thus the conical fluidized bed plays the dual role of a particle separator at incipient fluidization conditions as well as a 'deagglomerator' at high fluid velocities.

Overview of the fluidizability of fine particles

The present work on fluidization of fine particles in the conical fluidizer has thrown more light on the nature of interparticular forces, their reaction against the fluid force and their reduced effect at high velocities of the fluidizing medium. This introductory study opens the door for further understanding of 'finer' concepts such as the role of

fluid velocity in increasing the particle-particle contact area and time which may be ultimately used to model the effect of interparticular forces and hence the phenomenon of agglomeration due to them. However, agglomeration seems to take place only within a certain range of gas velocity(the simulation results of Bloise (1995) are coherent with this conceptualization from the point of view of energy of agitation). It is supposed that below this range the particle-particle contact area is not sufficient enough to cause agglomeration whereas above that range, the contact time is below the value required to cause the undesirable effect.

Hence, before embarking on a particular method of elimination/reduction of interparticular forces, simulation studies of the aforementioned variables could be extremely interesting and significant.

3.7 Hydrogenation of toluene in the conical fluidized bed reactor

The ultimate objective of this work was the hydrogenation of toluene on Ni/Al_2O_3 cryogel catalyst in a fluidized bed reactor. For this purpose, the conical column which was described in section 3.5.2 replaced the tubular integral reactor of the reaction system. The reaction system used for the reaction in the fluidized bed is described in the following sub-section. About 500 ml of the 14% Ni/Al_2O_3 cryogel (Batch 2) was prepared for the hydrogenation reaction. The characterization of this sample has been provided in section 2.2.3.

3.7.1 Experimental set-up and procedure

The fluidized bed reaction system (figure 3.12) mainly consists of the parts mentioned below:

1. Reactant feed system
2. Conical fluidized bed reactor and cyclone
3. Reactor for catalyst activation
4. Sampling system and Gas chromatograph
5. Particle separator

1. Reactant feed

Pure hydrogen necessary for both the activation of the catalyst in A and the subsequent reaction in R issues from three interconnected gas cylinders. Toluene feed

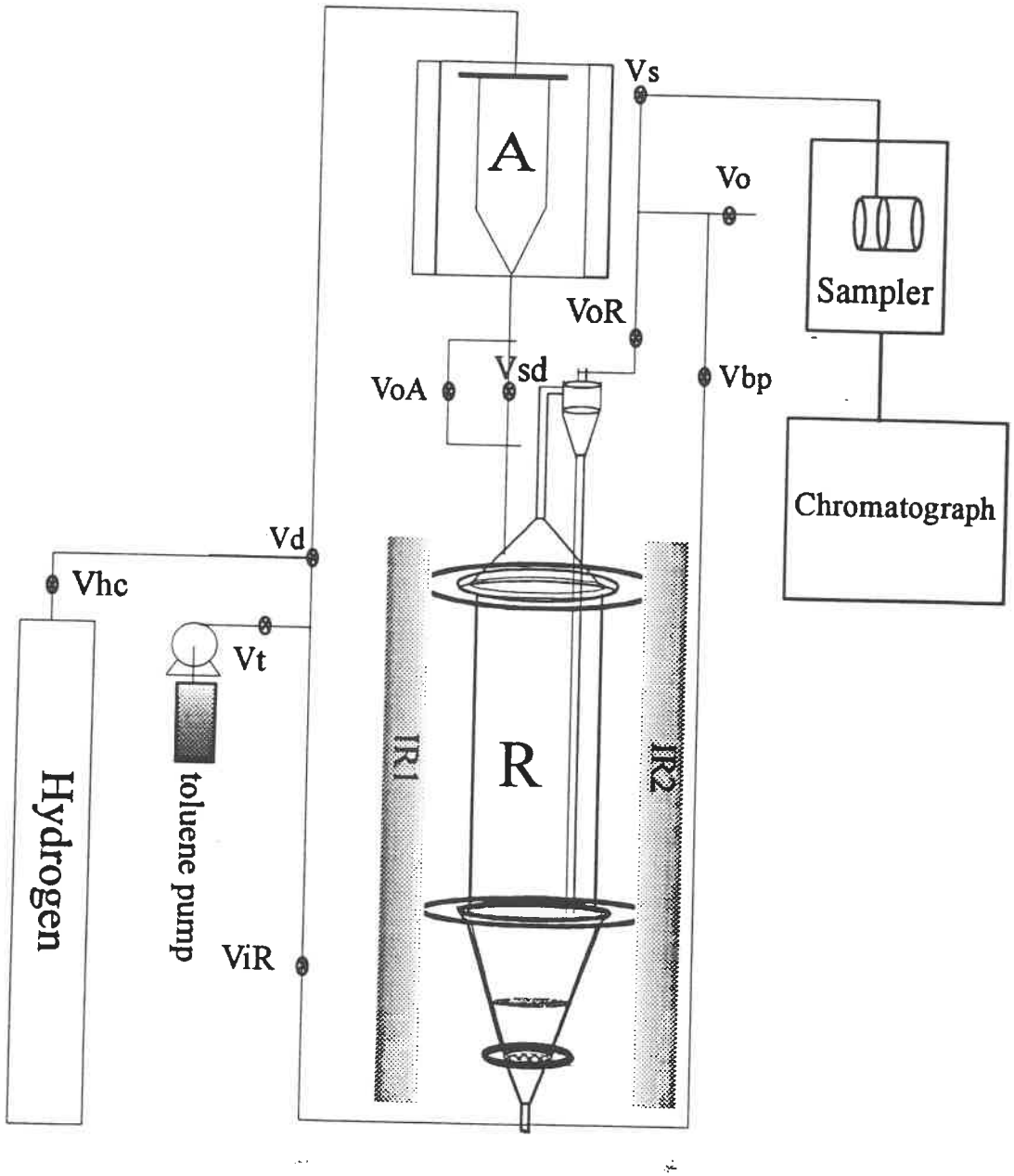

Figure 3.12 Reaction system for hydrogenation of toluene
(Conical fluidized bed reactor studies)

is available by means of a dosage pump at constant flow rates ranging from 0.1 to 9.9 cm^3/min. The tube conveying the toluene feed to the gas inlet pipe of the reactor R is heated externally by a series of electric coils connected to a dimmerstat, in order to vaporize the reactant. Valve V_t connects the toluene flow with the gas mainstream.

2. Conical fluidized bed reactor and cyclone

The conical fluidizer discussed in section 3.5 together with the cyclone separator was used as the reactor (R) for the fluidized bed hydrogenation of toluene. The mercury manometer ΔP_R is used to note the pressure inside the reactor and the thermocouple T_R for the temperature. It should be noted that T_R can be slided vertically to determine the axial temperature profile. The reactant mixture enters R through valve V_{iR} and leaves the cyclone through V_{oR}.

3. Reactor for catalyst activation

Since the reactor (R) consisted of a glass cone for the dense bed region and a glass cylinder for the freeboard height, it could not be used for the activation process which requires heating up to 500°C. Therefore, yet another reactor (A) was used for the activation process. This reactor consists of a steel cylinder 7.5 cm in diameter and 25 cm in length with a conical bottom to facilitate downflow of solids. Both reactors A and R are well-aligned so that a straight pipe connects the hopper in A directly to the top of the freeboard in R though a ball valve (V_{sd}). The gas inlet for this reactor

is on top (through valve V_{iA}) and the downflowing gas by-passes the ball valve through a tube and a gate valve (V_{oA}). This by-pass tube is filled with steel wool to avoid solids carry-over by the gas. The reactor is heated by two pairs of electric coils in series, the temperature in the reactor being measured by the thermocouple T_A and controlled by a controller operating at 240 V input. The whole arrangement is insulated and enclosed in a metallic box situated above reactor R. The gas pressure in the reactor A is measured by the mercury manometer ΔP_A.

4. Sampling system and chromatograph

This part of the reaction system is exactly the same as that used for the activity tests described in section 2.3.1.

5. Particle separator

Fine particles entrained from the fluidized bed and yet not recirculated by the cyclone separator escape through the outlet tube of reactor R. The outlet tube is connected to the top of an Erlenmeyer flask where the particles are released and the gas alone escapes through the side-tube, out of the laboratory.

Besides the above described major components of the fluidized bed reaction system, there is a separate tube bypassing the reactor R before V_{iR} and after V_{oR}.

The entire hydrogenation process is conducted in four different modes of operation viz., (a) Initial purging (b) Activation mode (c) Reaction mode and (d) Final purging. The procedures for the modes of operation are described in detail in Appendix VI.

3.7.2 Experimental results

The following table 3.3 shows the operating conditions and the experimental results during the hydrogenation reaction on the activated 14% Ni/Al_2O_3 cryogel in the conical fluidized bed reactor. The reaction temperature (T) was fixed at 150°C, the hydrogen molar flow rate (F_{H2}) at 0.04 moles/s corresponding to an inlet velocity of 50 cm/s and the toluene feed flow rate (Q_{tol}) at 1 ml/min. The only variable was the mass of the catalyst (W) which was varied by the particle entrainment.

Table 3.5 Experimental observations for the hydrogenation of toluene in the fluidized bed

#	H (cm)	W (g)	Conversion
1	10	23	0.82
2	9.8	21	0.77
3	9.6	20	0.73
4	9.2	17	0.63
5	8.9	16	0.57

P_{atm} = 747.3 mm Hg ΔP_R = 80 mm Hg

T_{atm} = 23°C T=150°C

F_{H_2} = 0.04 moles/s Q_{tol}=1 cm^3/min

3.8 Reactor modelling

In order to model the toluene hydrogenation reaction in the conical fluidized bed of the 14% Ni/Al_2O_3 cryogel, the reactor was first considered to be a plug flow reactor (PFR), whose characteristic equation is :

$$\frac{dX}{d\left(\frac{W}{F^0_{tol}}\right)} = r$$

Integration of the above equation (using POLYMATH) employing the kinetic model mentioned in section 2.5 for the experimental conditions of the hydrogen and toluene flow rates at the specified reaction temperature enables to find the theoretical conversion in the fluidized bed reactor.

Secondly, the reactor was considered to be a completely stirred tank reactor (CSTR). The theoretical conversion in this case was calculated using its characteristic equation:

$$\frac{X}{\left(\frac{W}{F^0_{tol}}\right)} = r$$

Figure 3.13 is a simulation of the homogeneous models for various W/F^0_{tol} values for conversions ranging from 0 to 1. It is seen that the predictions of both models are

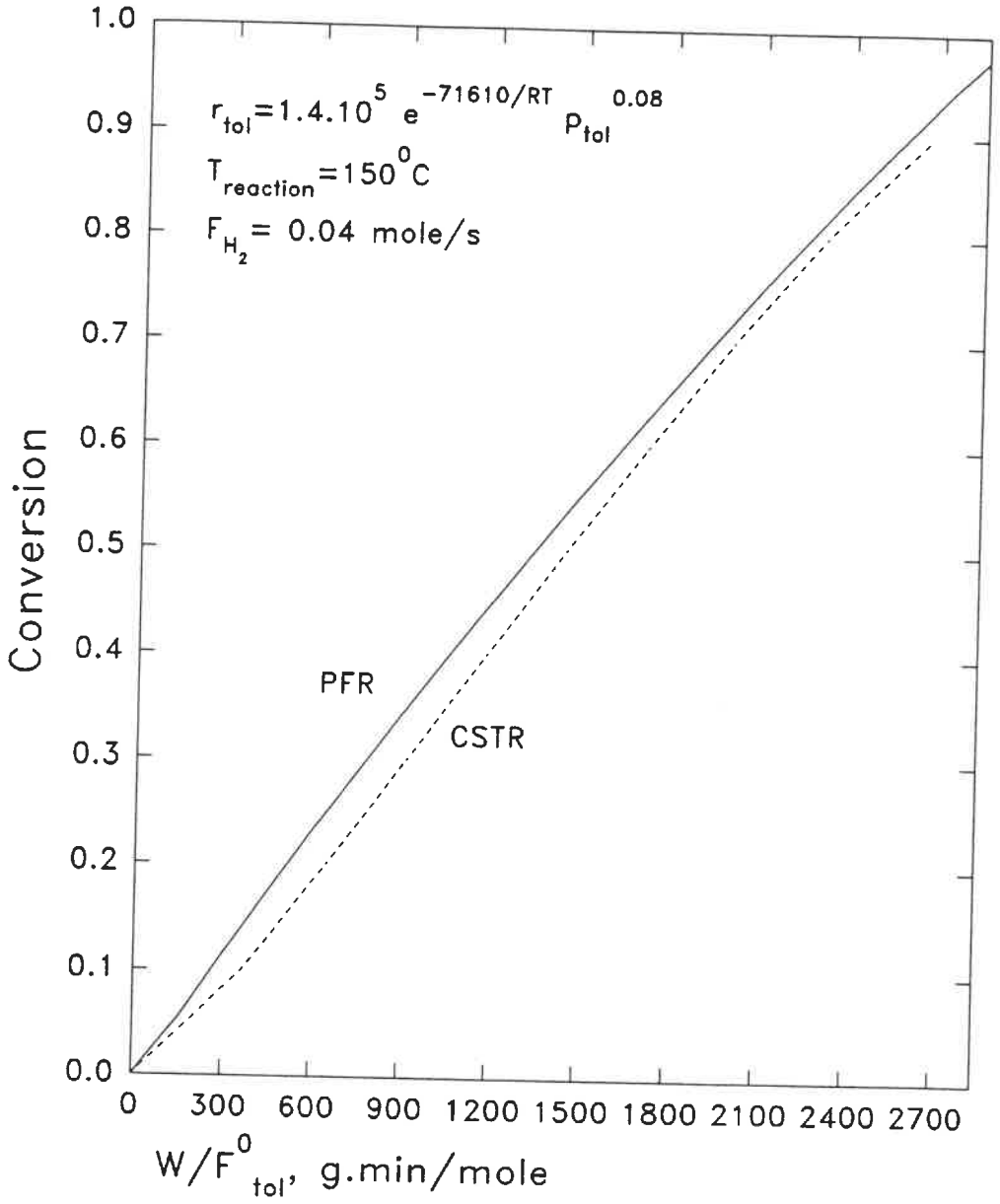

Figure 3.13 PFR and CSTR simulation

nearly identical. This is attributed to the low rate of reaction (slow reaction) which is the limiting factor.

The conversions predicted by the above two models for the W/F^0_{tol} values used in the hydrogenation reaction were compared with the corresponding experimental conversions. The analysis is shown in figure 3.14. From this figure, it can be stated that the kinetics of the hydrogenation reaction is limiting and the experimental conversions for the given operating conditions can be predicted by the homogeneous models.

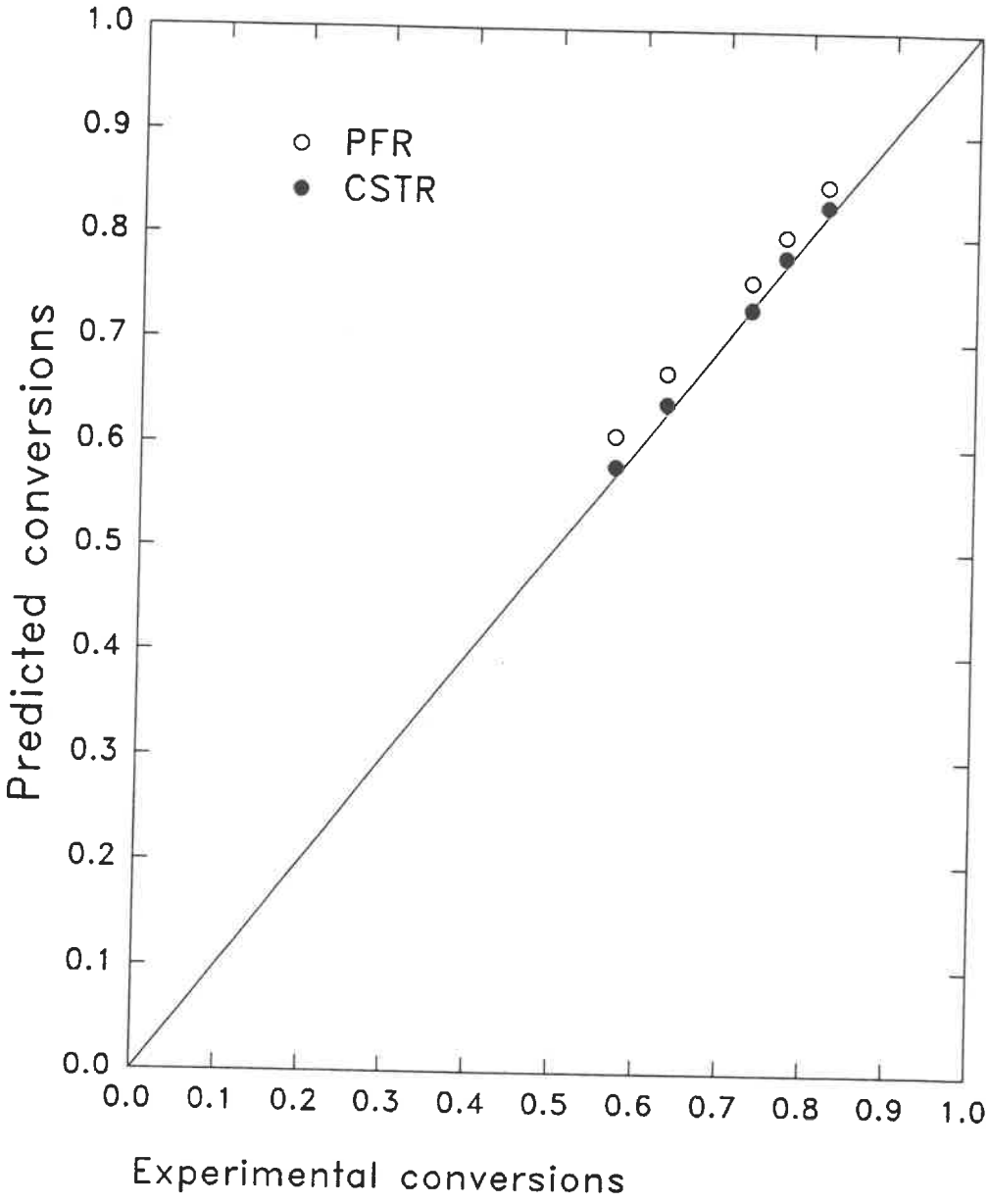

Figure 3.14 Experimental and model conversions

CHAPTER 4

CONCLUSIONS AND RECOMMENDATIONS

Based on the results of studies discussed in Chapters 2 and 3, certain conclusions have been enlisted in the following section. The shortcomings of this work have been taken into consideration while detailing the recommendations for future work in the area.

4.1 Conclusions

1. The physical characterization studies such as laser particle size measurement, BET surface area measurement, mercury and gas porosimetry studies of the prepared cryogels containing 0, 9.13, 14 and 20% Ni showed no appreciable differences between the properties of these samples. The total surface area of cryogels was found to be nearly 400 m^2/g, macropore volumes of 5-6 cm^3/g.

2. Activity tests on the Ni/Al_2O_3 cryogels at two different reaction temperatures of 130°C and 150°C respectively, indicated negligible catalytic activity for catalysts containing nickel compositions less than 4.5%, the activity increases proportional to the nickel content in the range 4.5-14%. Above 14% Ni, addition of nickel unaffects the activity. From the activity point of view, the cryogel containing 14% Ni is best suited for the process.

3. Activation studies on the 20% Ni catalyst (which has the same activity as that the 14% Ni cryogel) showed the influence of the maximum temperature of activation, rate of heating, activation time period and hydrogen flow rate during activation, on the activity of the catalyst. Activation was not possible when the sample was heated to a maximum of 200°C. Then on, the maximum temperature of activation was fixed as 500°C. During a fast activation process from 200°C till the maximum temperature, i.e., with a 10°C/10 min rate of increase of the catalyst temperature, the activity deteriorated compared to the conversions in the case of the normal activation rate (10°C/20 min). The rate of heating in the range 25-200°C does not influence conversions. One important factor governing the activity of the cryogels is the flow rate of hydrogen used for the activation process. Increase in the flow rate from 90 to 380 ml/min showed remarkable increase in the activity. This is due to the dependence of the gas adsorption rate of the activation process (reduction of NiO to metallic Ni) on the flow rate of hydrogen. The activation period which is the time during which the catalyst is maintained at the maximum temperature (500°C) under hydrogen flow was varied from 14 h to 28 h which did not produce any considerable variation in activity.

4. Air fluidization of cryogels in a cylindrical fluidizer having 5 cm diameter led to the phenomena of plug-rise at very low velocities, channelling in the fixed bed and fluidized states, partial fluidization due to dead zones, particle agglomeration and

segregation of the agglomerate bed. This behaviour is typical of cohesive powders belonging to Group-C of Geldart's classification. Characterization studies of cryogels produced values of the Hausner ratio (ratio of the tapped to the loose bulk densities) higher than 1.4, the lower limit of Group-C particles. The dimensions of the dense bed agglomerates and the clusters in the freeboard were measured from video pictures. Based on points 2 and 4, the cryogel containing 14% Ni was considered best suited for the process.

5. Satisfactory fluidization of the chosen cryogel was achieved in a conical fluidizer specifically designed for the purpose along with a conical distributor and porous plate. Above a critical air inlet velocity (U_{pm} = 44 cm/s), the bed fluidizes in a state of perfect-mixing in the absence of agglomerates. Reduction of the air velocity led to agglomeration of a bed core having diameter equal to that of the distributor surrounded by an annular zone of solids downflow comprised of the original bed particles. The minimum fluidization velocity (U_{0mf}) was found to be 33 cm/s. A slight bed expansion was observed beyond U_{0mf}.

Regarding the theoretical analysis, a core-annulus type segregated model was proposed to describe the conical fixed bed. A modified Ergun equation was derived to estimate the pressure drop across the bed. Using this equation, a correlation to predict the velocity at the inlet of the fluidizer at the minimum fluidization condition

(U_{0mf}) was also developed. Experimental data validate the accuracy of the pressure drop and U_{0mf} predictions. The bizonal fixed bed was characterized by measurement of the agglomerate size and estimations of the solid mass fractions in each zone. The agglomerate size in the core was found to be 2 mm whereas the clusters in the annulus had a mean size of 0.33 mm. Nearly 40% of the bed mass was agglomerated.

6. Hydrogenation of toluene in the conical fluidized bed reactor was conducted on the 14% Ni/Al_2O_3 cryogel, operating at the critical gas velocity at 150°C. Conversions were recorded where bed height was varied simultaneously. Hydrogenation of toluene was found to be a slow reaction, i.e., the conversion is limited by the reaction. Conversions in the fluidized bed could be predicted using the homogeneous models.

4.2 Recommendations

1. Multi-point surface area measurement by the BET method for total pore area measurement and mercury porosimetry method for total pore volume measurement are recommended for the characterization of cryogels.

2. It would be interesting to study the change in both activity and fluidizability of the 14% Ni cryogel by altering the support to pure SiO_2 or Al_2O_3-SiO_2.

3. Detailed studies on the conditions favourable for agglomeration of fine cohesive

powders could lead to the root of the problem. The effect of particle-particle contact time under fluidized conditions would be interesting to start with.

4. The effect of the initial bed height, inlet diameter and cone angle on the hydrodynamics of cryogels in the conical fluidizer can be studied. For a given solid and fluidizing gas, there seems to be an optimum cone angle for which the solids downflow is minimum while the intensity of particle circulation is sufficient enough to maintain agglomerate-free fluidization.

5. The application of conical fluidizers for Group-C particles can be tested by conducting further hydrodynamic experiments with other cohesive powders.

6. The possibility of working at lower gas velocities (to minimize entrainment and increase gas residence time for higher conversions) by the use of a mechanically vibrated conical bed is worth exploring.

7. Axial and radial profiles for gas velocity/pressure drop and bed temperature during the reaction would lead to a more profound understanding of the hydrodynamics of conical fluidized beds.

8. For conical fluidizers of small inlet diameter ($>$ 5 cm), solids (of any type)

downflow may be reduced or even eliminated by employing a special type of distributor which is comprised of a conical fixed bed of particles (glass or steel spheres, for instance), the bed being placed in the windbox. The radial distribution of the resistance to flow of gas can be controlled by varying the angle of the cone. In the case of large diameter fluidized beds, a distributor consisting of nozzles with the peripheral ones inclined and more in number so as to streamline gas flow towards the neighbourhood of the bed wall.

REFERENCES

ALDERSON J.E.A., HAMMERLI M., MURPHY J.R.B. and TAYLOR J.B. (1985). Hydrogen and Energy Storage Status Report.

ALFREDSON P.G. and DOIG I.D. (1970). In "Chemica 70", Session 1, Butterworths and Institution of Chemical Engineers.

BLOISE Y. (1995). Applications de la dynamique moléculaire à la fluidisation de particules par vibration, M.Sc.A. thesis, Department of chemical engineering, Ecole Polytechnique de Montreal, Canada.

BOTTERILL J. M. (1975). Fluid-bed heat transfer, Academic Press, New York.

BREKKEN R.A., LANCASTER E.B. and WHEELOCK T.D. (1970). Fluididization of flour in a stirred aerated bed, Chem. Eng. Prog. Symp. Series, 66, 277.

CHAOUKI J. (1984). Hydrogénation sélective du cyclopentadiène sur l'aérogel Cu/Al_2O_3 fluidisé, Doctoral thesis, Chemical Engineering department, Ecole Polytechnique de Montreal, Canada.

CHAOUKI J., CHAVARIE C. KLVANA D. and PAJONK G. (1985) Effect of Interparticle Forces on the Hydrodynamic Behaviour of Fluidized Aerogels, Powder Technology, 43, 117-125.

CHAOUKI J., MAHFOUD R.B. & KLVANA D. (1994). Expansion Prediction of Fine Particles Using Interparticle Forces, First International Particle Technology Forum, American Institute of Chemical Engineers, 421-427.

CHAUVEL A. et LEFEBVRE L. (1985) Procédés de pétrochimie, caractéristiques techniques et économiques, Editions Technip, Paris.

CHAVARIE C. (1969). Déshydrogénation du cyclohexane en phase vapeur sur un catalyseur de palladium dans un réacteur continu, type réservoir avec agitation, M.Sc.A. thesis, Chemical Engineering Department, Ecole Polytechnique de Montreal, Canada.

CHEREMISINOFF N. P. and CHEREMISINOFF P. N. (1984). Hydrodynamics of Gas-Solids Fluidization, Gulf Publishing Company.

CHIRONE R., MASSIMILLA L. and RUSSO S. (1993). Bubble-free fluidization of a cohesive powder in an acoustic field, Chemical engineering Science, 48, 41-52.

CLAUSE O., REBOURS B. MERLEN E., TRIFIRO F. and VACCARI A. (1992). Preparation and Characterization of Nickel-Aluminium Oxides obtained by Thermal Decomposition of Hydrotalcite-Type Precursors, Journal of Catalysis, 133, 231-246.

ECCLES E.R.A., ERDESZ K. and MUJUMDAR A.S. (1989). Resonance Phenomenon in Aerated Vibrated Beds of Particles, Fluidization VI, 219-228.

ERGUN S. (1952). Fluid Flow Through Packed Columns, Chemical Engineering Progress, 48, 89-94.

GACHES S. (1993). Contribution au développement d'un réacteur à membrane pour la séparation in situ de l'hydrogène, M.Sc.A. thesis, Chemical Engineering Department, Ecole Polytechnique de Montréal, Canada.

GELDART D. (1973). Types of gas fluidisation, Powder Technology, 7, 285-292.

GELDART D., WONG A.C. and HARNBY N. (1987). Fluidization of Cohesive Powders, Powder Technology, 37, 25.

GOLUBKOVICH A. V., KONDUKOV N. B. and VOROB'EV KH. S. (1970). Some hydrodynamic features of spouting-pulsating fluidization of granular material

in conical apparatus, Technical translation 1395, National Research Council, Canada.

GUY C. (1992). Les réacteurs à membrane: Possibilités d'application dans l'industrie pétrolière et pétrochimique, Revue de l'Institut Français du Pétrole, 47, 133-149.

HAM R. (1994). Effect of Relative Humidity and Electrostatics on Fluidized Bed Characteristics of Cracking Catalyst, Doctoral thesis, Chemical Engineering department, University of Western-Ontario, Canada.

HETSRONI G. (1982). Handbook of Multiphase systems, McGraw-Hill.

HIBY J.W. (1964). Critical minimum pressure drop of the gas distribution plate in fluidized bed units, Chem. Ingr. Tech., 36, 228-229.

KLVANA D., CHAOUKI J., REPELLIN-LACROIX M. and PAJONK G. M.(1989). A new method of preparation of Aerogel-like materials using a Freeze-drying process, Revue de Physique appliquée, Colloque C4, supplément au No. 4, Tome 24, (C4-29) - (C4-32).

KLVANA D., CHAOUKI J. et PERRAS L. (1992). Powder catalyst for a New Hydrogenation Process for Aromatic Hydrocarbons, Progress in Catalysis, 239-246.

KOZULIN N.A. and KULYAMIN A.F. (1965). Mixing of powdered materials in a fluidized bed, International Chemical Engineering, 5, 157-161.

KUSOHORSKY D. (Feb. 1989). Cinétique de l'hydrogénation du toluène sur l'aérogel Ni/SiO_2, M.Sc.A. thesis, Chemical Engineering Department, Ecole Polytechnique de Montreal, Canada.

KWAUK M. (1992). FLUIDIZATION Homogeneous and Bubble-less, Conical Fluidized Beds (Chapter 6), 91-100.

LAKSHMANAN R. (1970). Kinetic study of the vapor-phase hydrogenation of benzene in a continuous stirred reactor, Doctoral thesis, Chemical Engineering Department, Ecole Polytechnique de Montreal.

LAUGA C. (Sept. 1989). Modélisation de l'hydrogénation du toluène sur l'aérogel Ni/SiO_2 en lit fluidisé, M.Sc.A., Chemical Engineering Department, Ecole Polytechnique de Montreal, Canada.

LAUGA C., CHAOUKI J., KLVANA D., CHAVARIE C. (1991). Improvement of the fluidisability of Ni/SiO_2 aerogels by reducing interparticle forces, Powder Technology, 65, 461-468.

LEPAGE J.F. (1978). Catalyse de Contact, IFP Editions Technip, Paris.

MAHFOUD R. (May 1993). Modélisation des lits fluidisés gaz-particules en présence de forces interparticulaires, M.Sc.A. thesis, Chemical Engineering Department, Ecole Polytechnique de Montréal, Canada.

MASSIMILLA L., DONSI G. & ZUCCHINI C. (1972). The structure of bubble-free gas fluidized beds of fine fluid cracking catalyst particles, Chemical Engineering Science, 27, 2005.

MATHUR K.B. and EPSTEIN N. (1974). Spouted beds, Academic Press.

MORI S., YAMAMOTO A., IWATA S., HARUTA T., YAMADA I. and MIZUTANI E. (1990). Vibro-fluidization of Group-C particles and its Industrial Application, Advances in Fluidization Engineering, AIChE Symposium Series, 88-93.

MORSE R.D. (1955). Sonic Energy in Granular Solid Fluidization, Industrial Engineering and Chemistry, 47, 1170.

ORR Jr. C & DALLA VALLE, J.M. (1959). Fine Particle Measurement, MacMillan, New York.

PAJONK G. M. (1989). Drying methods preserving the textural properties of Gels, Revue de Physique appliquée, Colloque C4, Supplément au No. 4, Tome 24, (C4-13) (C4-22).

PAJONK G. M. (1991). Aerogel Catalysts, Review, Applied Catalysis, Elsevier Science Publishers, 72, 217-266.

PÉPIN G. (1986). Etude Cinétique de l'hydrogénation du toluène, Projet de fin d'études, Chemical Engineering Department, Ecole Polytechnique de Montreal, Canada.

PERRAS L. (1992). Hydrogénation du toluène, Projet de fin d'études, Chemical Engineering department, Ecole Polytechnique de Montreal, Canada.

PONTIER T. (1991). Modélisation et simulation de la désactivation du catalyseur utilisé pour la déshydrogénation du méthylcyclohexane, M.Sc.A. thesis, Chemical Engineering Department, Ecole Polytechnique de Montréal, Canada.

SATHIYAMOORTHY D., RAO S. (1981). The Choice of Distributor to Bed Pressure Drop Ratio in Gas Fluidized Beds, Powder Technology, 139-143.

SHI YAN-FU, YU Y. S. and FAN L. T. (1984). Incipient Fluidization Condition for a Tapered Fluidized Bed, Ind. Eng. Chem. Fundam., 23, 484-489.

SINGH R. K., SURYANARAYANA A. and ROY G. K. (1992). Prediction of Minimum Velocity and Minimum Bed Pressure Drop for Gas-Solid Fluidization in Conical Conduits, The Canadian Journal of Chemical Engineering, 70, 185-189.

SUTHERLAND K.S. (1961). Solids Mixing Studies in Gas Fluidised Beds, Part I A Preliminary Comparison of Tapered and Non-Tapered Beds, Trans. Instn. Chem. Engrs., 39, 188-194.

TERNAN M. & MYSAK L.P. (1987). Hysteresis Caused by Dimensional Changes of Porous Solids During Mercury Porosimetry, Powder Technology, 52, 29-34.

TOUZANI A., KLVANA D. and BELANGER G. (1984). Dehydrogenation of Methylcyclohexane on the Industrial Catalyst: Kinetic study, Catalysis on the Energy Scene, Elsevier Science Publishers B.V., Amsterdam.

TOYOHARA H., KAWAMURA Y. (1993). Circulation of particles in the side regions of a tapered fluidized bed, International Chemical Engineering, 33, 525-530.

ZIELINSKI J. (1982). Morphology of Nickel-Alumina Catalysts, Jounal of Catalysis, 76, 157-163.

ZHOROV Y.M., MARON V.I., OSTRER L.A., GATSOLAEV O.S. (1986). Mathematical Modeling of Chemical Processes in a Tapered Reaction Vessel, Theoretical foundations of Chemical Engineering, 20, 116-120.

APPENDIX I

Model calculations for activity test on Ni/Al_2O_3 cryogels

The following is the list of experimental data necessary for the calculation of the conversion as well as the W/F^0_{tol}:

Catalyst weight (W)	g
Atmospheric temperature (T_{atm})	°C
Atmospheric pressure (P_{atm})	mm Hg
Saturator temperature (T_{sat})	°C
Hydrogen flow rate (Q_{H2})	ml/min
Reaction temperature (T)	°C
Saturator exit pressure (P_{sat})	mm Hg
Reactor exit pressure (P_R)	mm Hg
Sampler exit pressure (P_S)	mm H_2O
Chromatographic readings:	
Methylcyclohexane (N_{mch})	-
Toluene (N_{tol})	-

From the above experimental observations, the variables are calculated as below:

Since the flow rate of hydrogen leaving the system is measured using a bubble

flowmeter, the true flow rate of hydrogen is the mole fraction of hydrogen in the downstream times the total flow rate, thus taking in to account the water content in the stream.

$$F^0_{H_2} = \frac{(\frac{Patm}{760} * 10^5) * Q_{H_2} * 10^{-6}}{8.314 * (T+273)} moles/\min$$

The Antoine equation for the evaluation of the toluene partial pressure is:

$$\ln P_{tol} = 6.95 - \frac{1344}{T_{sat} + 219.4}$$

where P_{tol} is expressed in mm Hg.

The molar flux of toluene at the reactor entrance is given by:

$$F^0_{tol} = F^0_{H_2} * \frac{P_{tol}}{P_{atm} - P_{tol}}$$

Thus the ratio W/F^0_{tol} is calculated.

The conversion is calculated from N_{tol} and N_{mch} as follows:

$$X = \frac{V_{mch} \frac{\rho_{mch}}{M_{mch}}}{V_{mch} \frac{\rho_{mch}}{M_{mch}} + V_{tol} \frac{\rho_{tol}}{M_{tol}}}$$

(a) From the chromatographic calibration, the volume in ml corresponding to each of the analyzed components are interpolated. Let V_{tol} and V_{mch} be the respective volumes.

Subsequently, the partial pressures of hydrogen and toluene can be calculated.

$$P_{H_2} = P_{tot} \frac{(F^0_{H_2} - 3F^0_{tol})}{F^0_{H_2} + F^0_{tol}(1-3X)}$$

$$P_{tol} = P_{tot} \frac{F^0_{tol}(1-X)}{F^0_{H_2} + F^0_{tol}(1-3X)}$$

APPENDIX II

Fluidizability test results

Model results of the fluidizability test conducted on the 9.13% Ni cryogel:

R	cycles	V m3	t s	P_{in} psi	U m/s	dP_b mmH_2O	ratio	H_1 cm	H_2 cm
2	0.1	.001	170	0	.003	2.4	.6	-	-
15	1	.01	122	0	.042	2.2	.71	8	8
20	3	.03	299	0	.051	2.6	.72	8	8
25	4	.04	321	0	.063	2.65	.71	8	8
28	9	.09	621	0	.074	2.6	.76	8	8
30	8	.08	505	0	.081	2.8	.82	8	8
33	9	.09	514	0	.089	3	.80	8	8
35	8	.08	441	0	.092	2.95	.63	8	8
40	17	.17	805	0	.107	2.3	.98	8	8
43	8	.08	330	0	.123	3.6	.98	6	8.5
45	14	.14	532	0	.134	3.6	.79	6	9
47	15	.15	537	0	.142	2.9	.61	5.5	7.5
49	6	.06	200	0	.153	2.25	.63	5.5	7.5
51	6	.06	192	2	.181	2.3	.63	5.5	7.5
55	4	.04	119	3	.207	2.3	.6	5	8
50	3	.03	95	3	.194	2.2	.54	5	7.5
45	3	.03	122	2	.143	2	.54	5	6.5
40	4	.04	186	2	.124	2	.52	4.5	5.5
30	3	.03	188	0	.081	1.9	.44	4	4.5
20	2	.02	207	0	.049	1.6	.35	3.8	4.2
15	1	.01	135	0	.038	1.3	.27	3.8	3.8
10	1	.01	193	0	.026	1	.11	3.8	3.8
5	1	.01	521	0	.009	0.4	0	3.8	3.8

Note: H_1 and H_2 are the bed height fluctuations

APPENDIX III

Hydrodynamic studies of cryogels

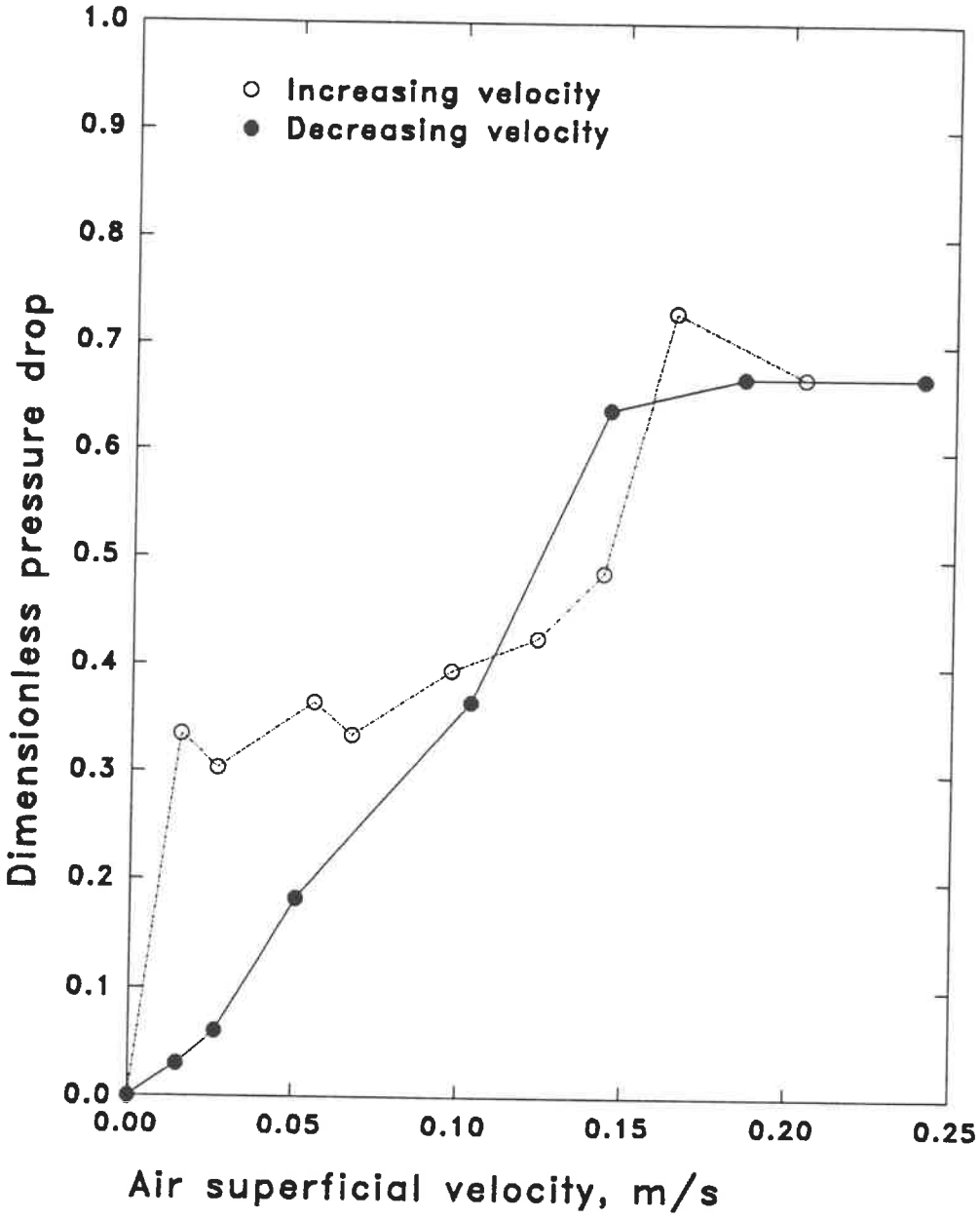

FLUIDIZATION OF ALUMINA CRYOGEL

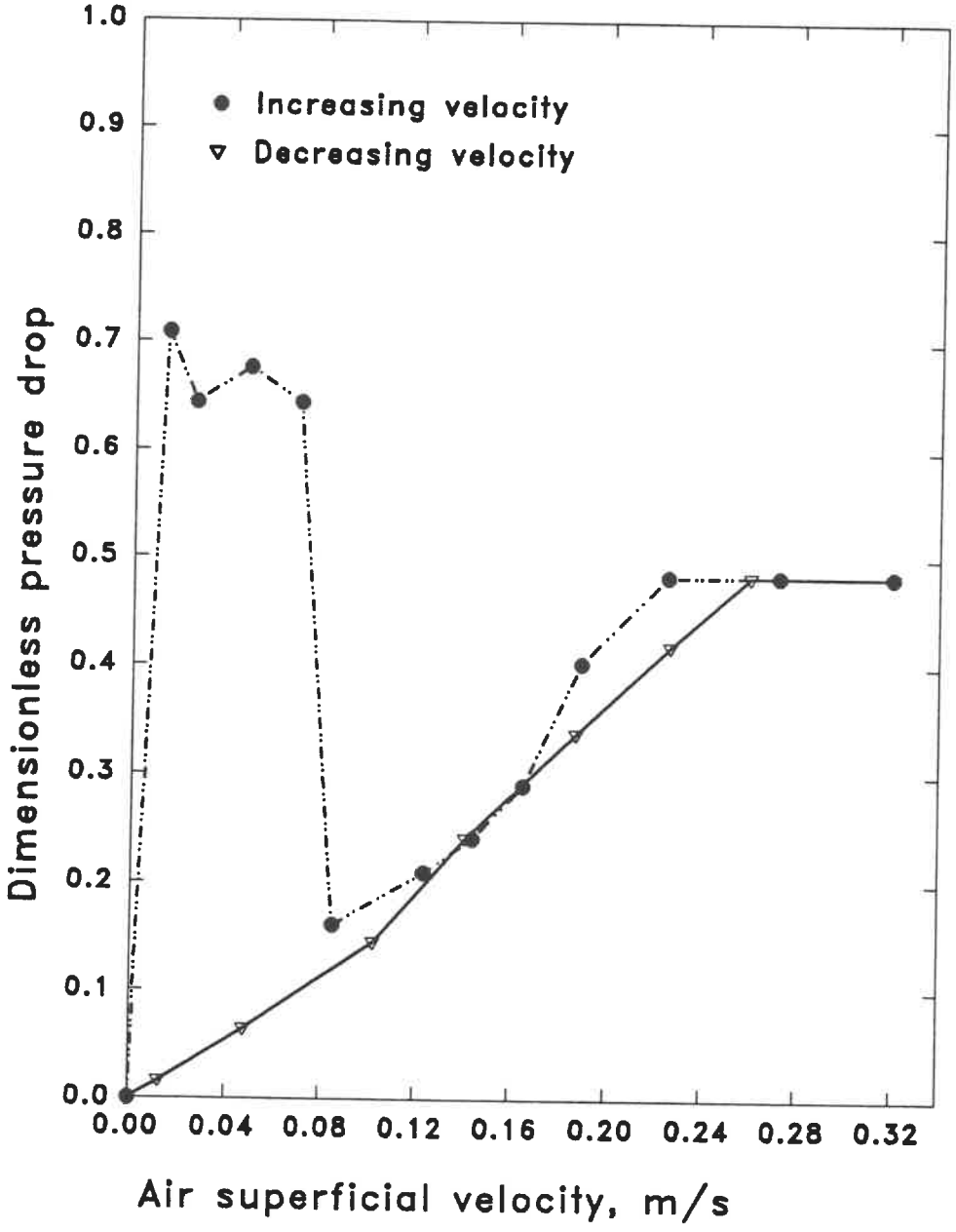

FLUIDIZATION OF 14% Ni CRYOGEL

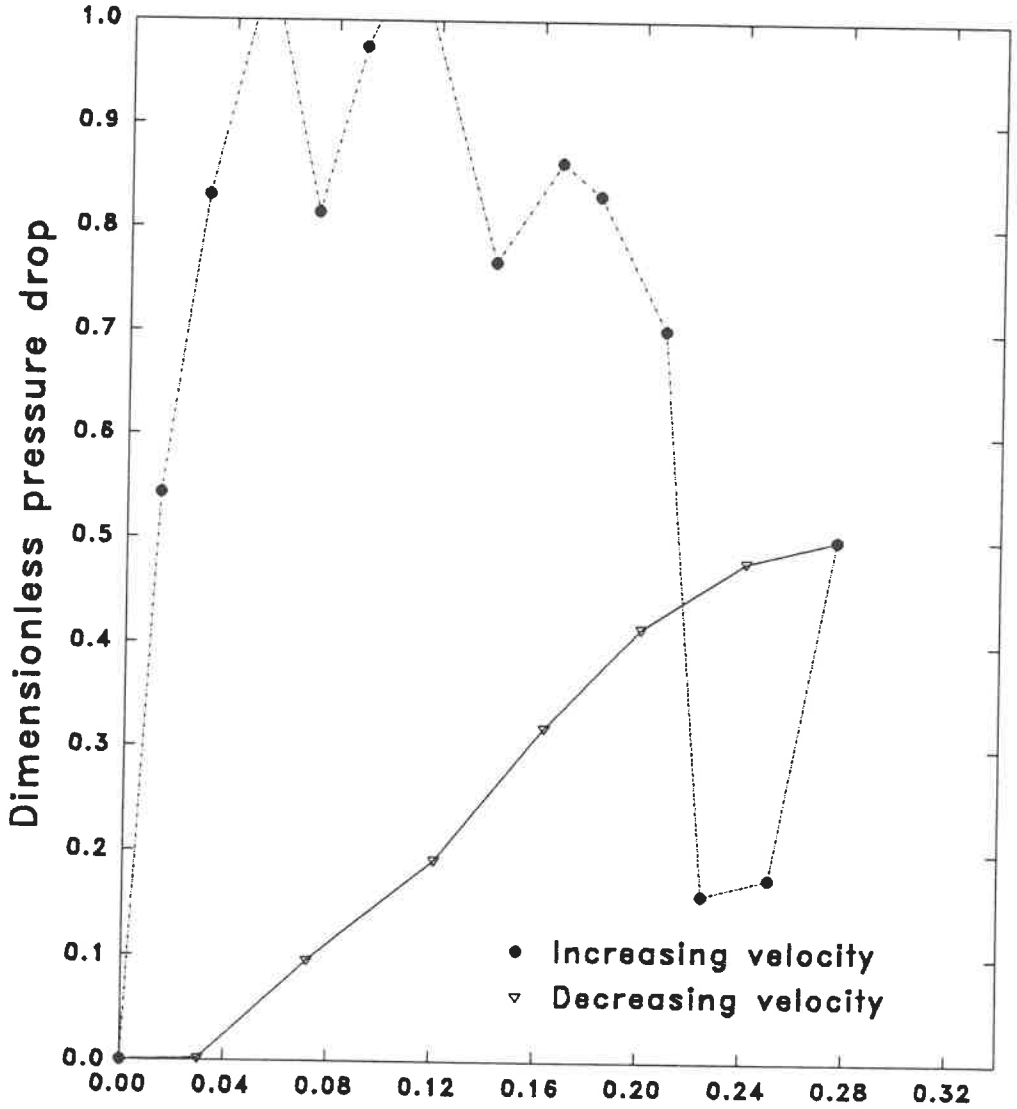

FLUIDIZATION OF 20% Ni CRYOGEL

APPENDIX IV

Derivation of the Modified Ergun equation for conical fixed beds

The Ergun equation can be written as:

$$-dP = (AU + BU^2)\, dz$$

where,

$$A = 150 \frac{(1-\epsilon)^2}{\epsilon^3} \frac{\mu_f}{d_s^2}$$

and

$$B = 1.75 \frac{(1-\epsilon)}{\epsilon^3} \frac{\rho_f}{d_s}$$

The overall pressure drop across the entire bed height H is obtained by integrating the above equation.

$$(-\Delta P) = \int_{P_0}^{P_H} (-dP) = \int_0^H (AU + BU^2)\, dz \quad . \; . \; . \; . \qquad \textbf{(10)}$$

Cone geometry provides the following relationships:

$D = D_0 + 2z\alpha$ and $U = U_0 . D_0^2 / (D_0 + 2z\alpha)^2$

Substituting these expressions in Equation 10 and effecting a change of variable, the following is obtained:

$$(-\Delta P) = AU_0 D_0^2 \int_{D_0}^{D_0+2H\alpha} \frac{dD}{2\alpha D^2} + BU_0^2 D_0^4 \int_{D_0}^{D_0+2H\alpha} \frac{dD}{2\alpha D^4} \quad . \; . \qquad \textbf{(11)}$$

The integration yields the final expression of the modified Ergun equation for conical fixed beds:

$$(-\Delta P) = \frac{AU_0 D_0 H}{D_0 + 2H\alpha} + \frac{BU_0^2 D_0}{3}\left[\frac{4H^3\alpha^2 + 3D_0^2 H + 6D_0 H^2\alpha}{(D_0 + 2H\alpha)^3}\right] \quad \cdots \quad (12)$$

APPENDIX V

Derivation of fluid force and the effective bed weight at minimum fluidization conditions

Consider an elemental height dz of the bed at a distance z from the distributor. The force exerted by the fluid in this elemental volume is

$$dF=\frac{\pi}{4}D^2\,(AU+BU^2)\,dz \quad . \quad . \quad . \quad . \quad . \quad . \quad . \quad (13)$$

Integrating over the entire bed height H,

$$F=\int_0^H \frac{\pi}{4}D^2\,[\frac{AU_0D_0^2}{D^2}+\frac{BU_0^2D_0^4}{D^4}]\,dz \quad . \quad . \quad . \quad . \quad . \quad (14)$$

Changing the variables and the limits of integration,

$$F=\frac{\pi}{4}D_0^2AU_0H+\frac{\pi}{4}D_0^2BU_0^2D_0^2\int_{D_0}^{D}\frac{dD}{D^2} \quad . \quad . \quad . \quad . \quad . \quad (15)$$

The overall force exerted by the fluid is obtained as:

$$F=\frac{\pi}{4}D_0^2H\,[AU_0+B(\frac{2\alpha D_0}{D_0+2H\alpha})\,U_0^2] \quad . \quad . \quad . \quad . \quad . \quad (16)$$

The effective weight of the powder bed in the same elemental volume is

$$dF_s = g(1-\epsilon)(\rho_s-\rho_f)\frac{\pi}{4}D^2dz$$

Upon integration for the total bed height H,

$$F_s = (1-\epsilon)(\rho_s-\rho_f)g\int_0^H \frac{\pi}{4}D^2dz \quad . \quad . \quad . \quad . \quad . \qquad (18)$$

With change of variable and limits,

$$F_s = (1-\epsilon)(\rho_s-\rho_f)g\int_{D_0}^{D} \frac{\pi}{4}D^2\frac{dD}{2\alpha} \quad . \quad . \quad . \quad . \quad . \qquad (19)$$

Finally, the integration enables to calculate the overall effective weight of the particles in the bed. The expression is given below:

$$F_s = \frac{\pi}{4}(1-\epsilon)(\rho_s-\rho_f)g\left[\frac{4H^3\alpha^2+3D_0^2H+6D_0H^2\alpha}{3}\right] \quad . \quad . \qquad (20)$$

APPENDIX VI

Procedure for the hydrogenation of toluene in the fluidized bed reactor

The initial conditions of each valve should be ascertained to be in the following manner (see nomenclature):

- V_{hc1}, V_{hc2}, V_{hc3} and V_{nc} are CLOSED
- V_i is CLOSED
- Positions of V_{d1} and V_{d2} are UP
- Valves V_{sd} and V_{oR} are CLOSED
- Valves V_{oA}, V_{iR}, V_{bp} and V_o remain OPEN

1. At first, the required quantity (25 gms) of the 14% Ni/Al_2O_3 cryogel is weighed and placed inside the reactor A with the lid tightened.

(a) Initial purging

2. Since a considerable flow rate of pure hydrogen is to be used for the activation process, it is safe to purge all air present inside the reactors A and R simultaneously using pure nitrogen by opening the valve V_{nc} of the nitrogen cylinder. Under the initial valve positions described above, nitrogen flows from the top of reactor A down through the distributor in R and out of the system through the gas by-pass tube.

3. After nearly 20 mins. of purging, temporarily change V_{oR} to OPEN and V_{d2} to DOWN positions to purge the stagnant air pockets.

4. Power the controller, with its output connected to the heater circuit in reactor A.

5. Now, V_{nc} is CLOSED and valves V_{hc1}, V_{hc2} and V_{hc3} are to be OPEN.

(b) Activation mode

6. The rotameter is fixed at the required position for the hydrogen flow rate necessary for activation.

7. Step 3 is repeated for hydrogen.

8. The controller set-point is increased rapidly from lab temperature to 250°C and slowed down to the rate of 10°C/20 min from 250°C to 500°C.

9. After attaining the maximum activation temperature, the sample is retained under the existing conditions for nearly 14 hours before heating is stopped.

(c) Reaction mode

10. Initially the sampling box and pumped ethylene glycol are heated to 100°C. The chromatograph and the toluene preheaters are also powered.

11. The Infra-Red lamps are heated in order to record a temperature of 100°C by T_R.

12. Valve V_{sd} is OPENED and V_{oA} are CLOSED.

13. Stir the solids in reactor A by rotating the stirrer S.

14. When all solids are transported to R, OPEN V_{oR}, CLOSE V_{oA} and V_{bp} then switch V_{d2} to the DOWN position.

15. When the system is stable, fix the hydrogen flow rate for fluidizing conditions.

16. Fix the toluene flow rate and OPEN V_t.

17. Slightly OPEN the smapling valve V_s so as to have only about 10 cm H_2O in ΔP_s and sampling is commenced.

18. Note down P_{atm}, T_{atm}, P_{in} (meter), Q_{H2}, ΔP_R, T_R vs Z, T_{tol} and H.

19. Repeat step 18 for different heights of the catalyst bed which is varied by particle entrainment. The mass of the bed is taken to be the average of those values before and after the chromatographic analysis. The effective bed mass is calculated from the mass collected by the particle collector C.

(d) Final purging

20. To eliminate the possibility of hydrogen-air contact at the end of the reaction, simultaneous to the CLOSE of valves V_{hc1}, V_{hc2} and V_{hc3}, OPEN V_{nc} to purge off the hydrogen present in reactor A for a few minutes.